Analysis of signal transduction pathways and the cytoskeleton in VASP-deficient cell lines and mouse models

Dissertation zur Erlangung des
naturwissenschaftlichen Doktorgrades
der Bayerischen Julius-Maximilians-Universität Würzburg

Vorgelegt von

Maísa Inés García Arguinzonis

aus
Buenos Aires

Würzburg 2003

Eingereicht am: ……..

Mitglieder der Promotionskommission:

Vorsitzender:	……
1. Gutachter	Prof. Dr. Ulrich Walter
2. Gutachter	Prof. Dr. Ricardo Benavente

Tag des Promotionskolloquiums …….

Doktorurkunde ausgehändigt am …….

Declaration:

I hereby declare that the submitted dissertation was completed by myself and no other; and I have not used any sources or materials other than those enclosed.

Moreover, I declare that the following dissertation has not been submitted further in this form or any other form and has not been used for obtaining any other equivalent qualification in any other organization.

Additionally, other than this degree I have not applied or will attempt to apply for any other degree or qualification in relation to this work.

Würzburg,

(Maísa I. García Arguinzonis)

A las personas que más quiero en el mundo, que, a veces sin saberlo, me ayudaron a llevar a cabo mi trabajo:

Mis padres,
que me incentivaron desde siempre
a hacer lo que me gusta y me
enseñaron a ser independiente

Juan,
donde siempre encuentro fuerza para
seguir adelante, con quien me siento
orgullosa de compartir mi vida

Y "el Porotín",
que todavía es muy chiquito pero
espero que algún día esté orgulloso
de sus papás

Esta tesis también es suya

Acknowledgements

I would like to express all my gratitude to Prof. Ulrich Walter for giving me the possibility to do my PhD work in his group. Thank you for your trust on the scientific level as well as on the personal level. Thank you for having always time to listen to me.

I would like also to acknowledge Prof. Ricardo Benavente for his time and his kind advices (¡y por hablar un castellano tan rioplatense, que tanto se extraña!).

I would like to thank Dr. Andreas Simm for his engagement. This work would not be possible without his help, advices and optimism.

A special thank to Dr. Matthias Reinhard who has coordinated most of my work. Thank you for the long discussions and excellent ideas.

I also acknowledge the Deutsche Forschungsgemeinschaft (DFG) for financial support.

Very special thanks to Birgitta Schinke and Inge Klier for taking care of the mice. Inge, you have always been a great, great help.

I am also thankful to those who have helped me and have participated on my work: the group of Dr. Friedl, specially Katharina Wolf with whom I made the Time-Lapse Video Microscopy; Dr. Suzanne Kneitz and the microarray facility and the group of Dr. Massberg in Munich for the in vivo adhesion assay. Thank you very much for your collaboration.

Thanks to everybody in the Institut für Klinische Biochemie und Pathobiochemie, that made the everyday-life pleasant and amusing: Gunnar (thanks for the wine and the music!!), Lilo, Elfi, Petra (I will never forget Berlin!), Jörg, Lino, Petra T., Ingvild, Albert, Michael, Thomas, Monika, Laura, Mario, Silke, Marga, Renne, Elke, Stepan, Suzanne, Achim, Thomas R., Martin… and, of course, Gisela, Sylvia and Martina.

Thanks to my “würzburger” friends: Karin, Nora, Naresh, Mani, Annette and, specially to Catherine (merci d’être là à me relever le moral et à me donner du courage!), Jochen (The one and only “Young Investigator”! I am really missing our long talks!) and my “Sorello” Barsom (Thanks for letting me be your G_i-protein! I think I have never told you how important you are for me!).

Gracias a Fer, Antonia, Pablo, Flavio y Ana que me ayudaron a tener un buen comienzo en Würzburg. Gracias a Silvia, a Eva y a Lupe, que llegaron justo al final para acompañarme en los últimos meses de la tesis. Y a la “mafia colombiana” (con cabecilla argentino) que alegraron más de una cena con la picardía de sus comentarios.

Y Gracias a los amigos de siempre: “Los Constipados” que aunque desparramados por el mundo nos seguimos el rastro; Isa, que ahora la tengo mucho más cerca; e Irene que siempre estuvo a mi lado, orgullosa de su “hermanita” (y yo de ella), aunque no entienda un pito de lo que hago.

1. SUMMARY (ZUSAMMENFASSUNG) 5

1.1. English 5
1.2. Deutsch 7

2. INTRODUCTION 9

2.1. The Vasodilator-Stimulated Phosphoprotein: VASP 9
2.1.1. Structure 9
2.1.1.1. The EVH 1 domain 11
2.1.1.2. The Proline Rich Region (PRR) 12
2.1.1.3. The EVH 2 domain 12
2.1.2. Subcellular localization 13
2.2 Platelets 13
2.2.1 Platelet Activation 13
2.2.2 Platelet Inhibition 15
2.2.3 VASP in Platelets 16
2.3 Cytoskeletal Remodelling 18
2.3.1 Actin Polymerization 18
2.3.2 The Actin Cytoskeleton 19
2.3.3 Integrins 20
2.3.4 The Rho GTPase family 22
2.3.4.1 Rho 22
2.3.4.2 Cdc42 23
2.3.4.3 Rac 23
2.3.4.3.1 The Rac/Pak pathway 23
2.3.5. VASP and the actin cytoskeleton. 24
a. The Listeria model 24
b. Axon Guidance 25
2.3.6 The small GTPases and the Ena/VASP family 25
2.3.6.1 Ena and the Rho-GEF Trio 26
2.3.6.2 Mena-IRSp53-Cdc42 26
2.3.6.3 WASP and Cdc42 26
2.4 The "Knock-Out" approach 27
Ena-deficient Drosophila melanogaster 27
VASP$^{-/-}$ mouse model 27
Mena$^{-/-}$ mouse model 27
Caenorhabditis elegans deficient in unc34 gene product 27
2.5 Aim of the Work 28

3. MATERIALS 29

3.1.1 Primary Antibodies 29
3.1.2 Secondary Antibodies 29
3.1.3 Fluorescent Labels 30
3.1.4 Bacteria 30
3.1.5 Plasmids 30
3.1.6 Oligonucleotide 30
3.1.7 Antibiotics 31
3.1.8 Chemicals 31
3.1.9 Protein Markers 31
3.1.10 DNA Markers 32

3.1.11 Materials for Microarrays 32
3.2 Equipment and Software 32
3.2.1 Equipment 32
3.2.2 Software 33

4. METHODS 34

4.1 Cell Culture 34
4.1.1 Isolation of mouse cardiac fibroblast. 34
Phosphate-buffer saline (PBS) 34
Earl's buffer 34
4.1.2 Cell Passage 34
4.1.3 Cell Counting 35
4.1.4 Cell Cloning 35
4.1.5 Cell Freezing and Storage 35
Freezing Medium 35
4.1.6 Immunofluorescence 35
4.1.7 Wound-Healing assay 35
4.1.8 Cell adhesion assay 36
4.1.9 Detachment 36
4.1.10 Flow Cytometry analysis of β_1 and β_3 integrins 36
4.2 DNA Manipulation 36
4.2.1 DNA Isolation. 36
Proteinase K buffer: 37
4.2.2 DNA precipitation 37
4.2.3 Genotyping. 37
4.2.4 DNA Electrophoresis 41
TAE Buffer 41
4.2.5 Stable transfection of mouse cardiac fibroblasts 41
4.3 RNA Manipulation 41
4.3.1 RNA isolation from Mouse Cardiac Fibroblasts (MCFB) 41
4.3.2 Northern Blotting. 42
SSC Buffer (2x) 42
4.3.3 RT-PCR 43
4.3.4 Microarrays 43
4.3.4.1 Labelling first-strand cDNA with Cy3- or Cy5-nucleotides: 44
4.3.4.2 Purification of labeled cDNA 45
4.3.4.2.1 Preparation of the AutoSeq G-50 columns 45
4.3.4.2.2 Purification of the labeled cDNA 45
4.3.4.3 Microarray hybridization 45
Prehybridization Solution 45
4.3.4.4 Hybridization 46
4.3.4.5. Scanning 46
4.4 Protein Manipulation 46
4.4.1 Determination Protein Concentration 46
4.4.2 SDS-Polyacrylamide Gel Electrophoresis (PAGE) and Immunoblotting (Western Blot) 46
Separating Gels 47
Stacking gel 47
Sample Loading buffer (3x) 47
Electrophoresis buffer 48
Transfer buffer 48
TBS-T 48
4.4.3 Two-Dimensional Gel Electrophoresis 48
Solubilization buffer 48
Equilibration Buffer 49

4.4.4 Preparation of GST-PBD Sepharose Beads for Rac Pull Down assay 49
LB-medium 49
4.4.5 Determination of Rac activation (Rac Pull Down Assay) 49
MCFB Lysis buffer (2x) 50
Platelet Lysis buffer (2x) 50
Washing buffer 50
4.4.6 Pak In-Gel Kinase Assay 51
Buffer 1 51
Buffer 2 51
Buffer 3 51
Buffer 4 51
Buffer 5 or Kinase Buffer 51
Wash Buffer 52
Coomasie Blue Staining Solution 52
Coomasie Destaining Solution 52
4.5. Blood Manipulation 52
4.5.1 Blood sampling (mice) 52
CCD Buffer 52
4.5.2 Preparation of Washed Mouse Platelets. 53
Hepes-Tyrode Buffer (without Ca^{2+}) pH 6,3 53
Hepes-Tyrode Buffer (with Ca^{2+}) pH 7,3 53
4.5.3 Preparation of Washed Human Platelets. 53
Resuspension Buffer pH 7,4 54
4.5.4 Stimulation of Washed platelets 54
4.5.5 *In vivo* fluorescence microscopy 54
4.5.6 Assessment of platelet adhesion following vascular injury – inhibition of platelet adhesion by nitric oxide 55

5. RESULTS 56

5.1 Mouse Cardiac Fibroblast (MCFB) 56
5.1.1 Establishment of a mouse cardiac fibroblast cell line 56
5.1.2 Mena and Evl expression are not up- or down- regulated in $VASP^{-/-}$ cells 58
5.1.3 $VASP^{+/+}$ and $VASP^{-/-}$ cell lines have similar growth rates 59
5.1.4 $VASP^{-/-}$ cells are more spread 60
5.1.5 $VASP^{-/-}$ cells have thicker stress fibers 65
5.1.6 $VASP^{-/-}$ stress fibers are also more stable 67
5.1.7 $VASP^{-/-}$ cells have prominent focal adhesion sites 68
5.1.8 Adhesion and detachment rates decrease in $VASP^{-/-}$ cells. 70
5.1.9 The cGMP analog 8p-CPT-cGMP accelerates attachment of MCFB cells 72
5.1.10 Reorientation and motility of $VASP^{-/-}$ cells are impaired in a wound healing assay 73
5.1.11 Prolonged Rac activation in the absence of VASP 76
5.1.12 Pak is activated in $VASP^{-/-}$ cells 77
5.1.13 Differences in the expression pattern of $VASP^{+/+}$ and VASP-deficient MCFB analyzed by Microarrays. 79
5.2 Platelets 84
5.2.1 Rac activity regulation by VASP 84
5.2.2 Enhanced Platelet adhesion in VASP deficient mice: An *in vivo* approach. 85
5.2.2.1 VASP regulation of platelet adhesion in vivo 85
5.2.2.2 VASP deficient platelets show enhanced adhesion following endothelial denudation. 87
5.2.2.3 VASP deficient platelets are unresponsive to nitric oxide 89

6. DISCUSSION 90

6.1 Function of VASP in the stabilization of stress fibers and its consequence in cell morphology and behavior 91
6.1.1 Function of VASP in stabilization of stress fibers 91
6.1.2 VASP and the regulation of membrane tension 92
6.2. VASP deficient cells show no differences in Mena and Evl expression levels 92
6.3. VASP may modulate the expression pattern of some binding partners 93
6.4. Rac and other small GTPases are good candidates to be involved in VASP dependent regulation of actin cytoskeleton 93
6.4.1 How does VASP regulate the Rac/Pak pathway? 95
6.5. Adhesion: observations in vitro and in vivo point to the importance of VASP in this cellular process 97
6.5.1 Influence of cGMP analogs in cell adhesion 98
6.6 Future perspectives 100

7. REFERENCES 101

8. ABBREVIATIONS 109

9. CURRICULUM VITAE 111

10. LIST OF PUBLICATIONS 112

1. Summary (Zusammenfassung)

1.1. English

The mammalian Vasodilator Stimulated Phosphoprotein (VASP) is a founding member of the Ena/VASP family of proteins that includes Drosophila Enabled (ena), the mammalian Ena homologue (Mena) and the Ena-VASP-like protein (Evl). VASP was initially discovered and characterized as a substrate for cGMP- and cAMP-dependent protein kinases (cGKs and cAKs). Ena/VASP proteins are involved in Actin-filament formation, plasma membrane protrusion, acceleration of Actin-based motility of *Listeria* and the establishment of cell-cell adhesion. Moreover, Ena/VASP proteins have been implicated as inhibitory factors in repulsive axon guidance and inhibition of plasma membrane activity and random motility in fibroblast.

In order to study the physiological function of VASP, VASP-deficient mice had been generated in the laboratory by homologous recombination. $VASP^{-/-}$ mice showed hyperplasia of megakaryocytes in the bone marrow and spleen and a two-fold increase in thrombin- and collagen-induced platelet activation.

To further investigate the cellular function of VASP, I established cardiac fibroblast cell lines derived from both wild type and $VASP^{-/-}$ mice. Both cell lines presented similar growth rates and normal contact dependent-growth inhibition but showed differences in morphology, migration and adhesion. Adherent $VASP^{-/-}$ cells, despite normal Mena and Evl expression levels, were highly spread. $VASP^{-/-}$ cells covered about twice the substrate surface area as wild type cells, while the cell volumes were unchanged. This shape difference suggests that VASP is involved in the regulation of spreading. Since the small GTPases Rac and Cdc 42 and their effector p21-activated kinase (Pak) are key regulators of lamellipodia formation and cell spreading, I analyzed this signalling pathway in $VASP^{-/-}$ cells stimulated with Platelet Derived Growth Factor-BB (PDGF-BB) or fetal calf serum. In wild type cells Rac and Pak were rapidly and transiently activated by PDGF or serum; however, in the absence of VASP both Rac and Pak activation was dramatically prolonged. The Rac/Pak pathway is known to play an essential role in cell motility. VASP deficient cells showed compromised migration and reorientation in a wound healing assay, probably due to enhanced Rac activity. The spreading phenotype, compromised migration and the effect observed on the Rac and Pak activities were reverted in $VASP^{-/-}$ cells stably transfected with full lenght human VASP, indicating a VASP dependent modulation of the Rac/Pak pathway and Rac/Pak regulated processes. Moreover, adhesion and detachment of VASP-deficient cells were significantly slower when compared to wild type cells. Preincubation of $VASP^{+/+}$ cells with a cGMP analog accelerated adhesion. This acceleration did not take place in the $VASP^{-/-}$ cells, suggesting a VASP dependent effect.

The second part of this work focused on VASP function in platelets. On the one hand I investigated the possibility of VASP-dependent Rac regulation in mouse platelets. Murine platelets are a good model for studying Rac regulation since they express high levels of VASP but not Mena/Evl and since VASP-deficient platelets show an increased platelet activation. Rac was activated by platelet agonists which was inhibited by preincubation with cGMP and cAMP analogs. Initial results which need to be extended showed that the cGMP-caused inhibition of Rac activation was VASP-dependent. Finally, in vivo platelet adhesion (platelet-vessel wall interactions) was studied using VASP-deficient mice. These studies demonstrated in-vivo that VASP down regulates platelet adhesion to the vascular wall under both physiological and pathophysiological conditions.

1.2. Deutsch

Das Säugerprotein Vasodilator Stimulated Phosphoprotein (VASP) ist ein Gründungsmitglied der Ena/VASP Proteinfamilie, die das Drosophila Enabled (ena), das homologe Säugerprotein ena (Mena) und das Ena-VASP-like Protein (Evl) einschließt. VASP wurde ursprünglich als ein Substrat von cGMP- und cAMP abhängigen Proteinkinasen (cGKs und cAKs) entdeckt und charakterisiert. Ena/VASP Proteine sind bei der Polymerisation von Aktinfilamenten, bei der Protrusion von Plasmamembranen, der Beschleunigung von Aktin-basierter Beweglichkeit von Listerien und bei der Ausbildung von Zell-Zell-Adhäsionen beteiligt. Außerdem wurde gezeigt, dass Ena/VASP-Proteine hemmende Faktoren bei der repulsiven Axonführung sind und sowohl die Plasmamembranaktivität als auch die ungerichtete Fibroblastenbeweglichkeit hemmen.

Um die physiologische Funktion von VASP zu untersuchen, wurden VASP-defiziente Mäuse im Labor durch homologe Rekombination generiert. $VASP^{-/-}$ Mäuse zeigten eine Hyperplasie der Megakaryozyten im Knochenmark und in der Milz sowie eine zweifache Erhöhung der durch Thrombin und Kollagen induzierten Plättchen-Aktivierung.

Um die zelluläre Funktion von VASP weiter aufzuklären, etablierte ich kardiale Fibroblasten-Zelllinien sowohl von Wildtyp als auch von $VASP^{-/-}$ Mäusen. Beide Zelllinien zeigten gleiche Wachstumsraten und eine normale, kontaktabhängige Wachstumshemmung, hatten aber Unterschiede in ihrer Morphologie, Wanderung und Adhäsion. Adhärente $VASP^{-/-}$ Zellen waren trotz normaler Mena und Evl Expression stark ausgebreitet. $VASP^{-/-}$ Zellen bedeckten eine ungefähr zweimal so große Substratoberfläche wie Wildtyp-Zellen, während das Zellvolumen unverändert war. Diese Formunterschiede lassen vermuten, dass VASP bei der Regulation der Ausbreitung involviert ist. Da die kleinen GTPasen Rac und Cdc 42 und ihr Effektorsystem p21-aktivierte Kinase (Pak) Schlüsselregulatoren der Lamellipodienformierung und der Zellausdehnung sind, untersuchte ich diesen Signalweg in $VASP^{-/-}$ Zellen, die mit Platelet Derived Growth Factor-BB (PDGF-BB) oder fetalem Kälberserum stimuliert wurden. In Wildtypzellen wurden Rac und Pak schnell und transient durch PDGF oder Serum aktiviert, in der Abwesenheit von VASP war die Aktivierung von Rac und Pak jedoch dramatisch verlängert. Der Rac/Pak Signalweg ist dafür bekannt, dass er eine essentielle Rolle bei der Zellbeweglichkeit spielt. VASP defiziente Zellen zeigten, wahrscheinlich wegen der erhöhten Rac Aktivität, eine veränderte Wanderung und Reorientierung in einem Wundheilungs-Versuch. Der ausgebreitete Phänotyp, die veränderte Wanderung und die beobachteten Effekte bei den Rac und Pak Aktivitäten wurden in $VASP^{-/-}$ Zellen, die stabil mit humanem VASP transfiziert wurden, normalisiert, was eine VASP abhängige Steuerung des Rac/Pak Signalwegs und der Rac/Pak regulierten Prozesse vermuten läßt. Weiterhin waren die Adhäsion und die Ablösung von VASP-defizienten Zellen signifikant langsamer als in den Wildtyp-Zellen. Die Vorinkubation von $VASP^{+/+}$ Zellen mit

einem cGMP-Analog beschleunigte die Adhäsion. Diese Beschleunigung fand in VASP$^{-/-}$ Zellen nicht statt, was einen VASP-abhängigen Effekt vermuten läßt.

Der zweite Teil dieser Arbeit konzentrierte sich auf die VASP Funktion in Thrombozyten. Einerseits untersuchte ich die VASP-abhängige Regulation von Rac in murinen Thrombozyten. Diese sind dafür besonderes gut geeignet, da sie VASP aber nicht Mena/Evl exprimieren und da VASP-defiziente Thrombozyten verstärkt aktiviert werden. Rac wurde durch Thrombozyten-Agonisten aktiviert, was durch eine Präinkubation mit cGMP- und cAMP-Analoga gehemmt wurde. Erste Ergebnisse, die noch einer weiteren Bestätigung bedürfen, zeigten, daß die cGMP-vermittelte Hemmung der Rac-Aktivierung VASP-abhängig war. Abschließend wurde auch die in-vivo Plättchen-Adhäsion (Thrombozyten-Gefäßwand-Interaktion) unter Einsatz von VASP-defizienten Mäusen untersucht. Diese Ergebnisse zeigten für in-vivo-Bedingungen, daß VASP die Thrombozyten-Adhäsion an die Gefäßwand sowohl unter physiologischen als auch pathophysiologischen Bedingungen unterdrückt.

2. Introduction

Cells have the capability among others to divide, move, attach or detach, secrete substances in response to specific external signals. These signals trigger a series of reactions within the cell in order to successfully complete the specific task. The process by which a cell converts an extracellular signal into a response is known as *signal transduction*. Some very important players in signal transduction are second messengers: small molecules that are formed (cAMP, cGMP, IP_3) or released (Ca^{2+}) into the cytosol in response to an extracellular signal and that help to relay it to the interior of the cells. Many of these second messengers transduce the signal by activating a protein kinase, that in turn transmits the signal by phosphorylating another protein changing its activity or localization. In platelets, some vasodilator substances elevate cAMP (e.g., Prostaglandin E1 (PGE1), Prostacyclin (PGI2), etc.) or cGMP levels (e.g., sodium nitroprusside (SNP), nitroglycerin, etc.) and inhibit platelet activation at an early step in the activatory cascade [1]. The inhibitory process is not yet completely understood, but it is known that both cyclic nucleotides activate cAMP- and cGMP- dependent protein kinases (cAK and cGK), respectively. In 1989, studying the protein phosphorylation pattern of platelets treated with cAMP- or cGMP- elevating agents, Halbrügge and Walter [2], identified a protein with and apparent molecular mass of 50kDa that was phosphorylated under both conditions. The new protein was named Vasodilator Stimulated Phosphoprotein (VASP) as phosphorylation was induced by vasodilating substances.

2.1. The Vasodilator-Stimulated Phosphoprotein: VASP

2.1.1. Structure

VASP is a 39 kDa protein, running as 46 kDa in SDS-PAGE, that upon phosphorylation by cAMP elevating agents, shifts to an apparent molecular mass of 50kDa [3]. VASP has three phosphorylation sites: Ser 157[1], Ser 239[1] and Thr 278[1] [4], which are phosphorylated *in vitro* and in intact cells by cAK and cGK [4]. Ser 157 is preferentially phosphorylated by cAK while Ser 239 is the preferred site for cGK (Figure 1).

[1] Amino acids are numbered according to the sequence of human VASP

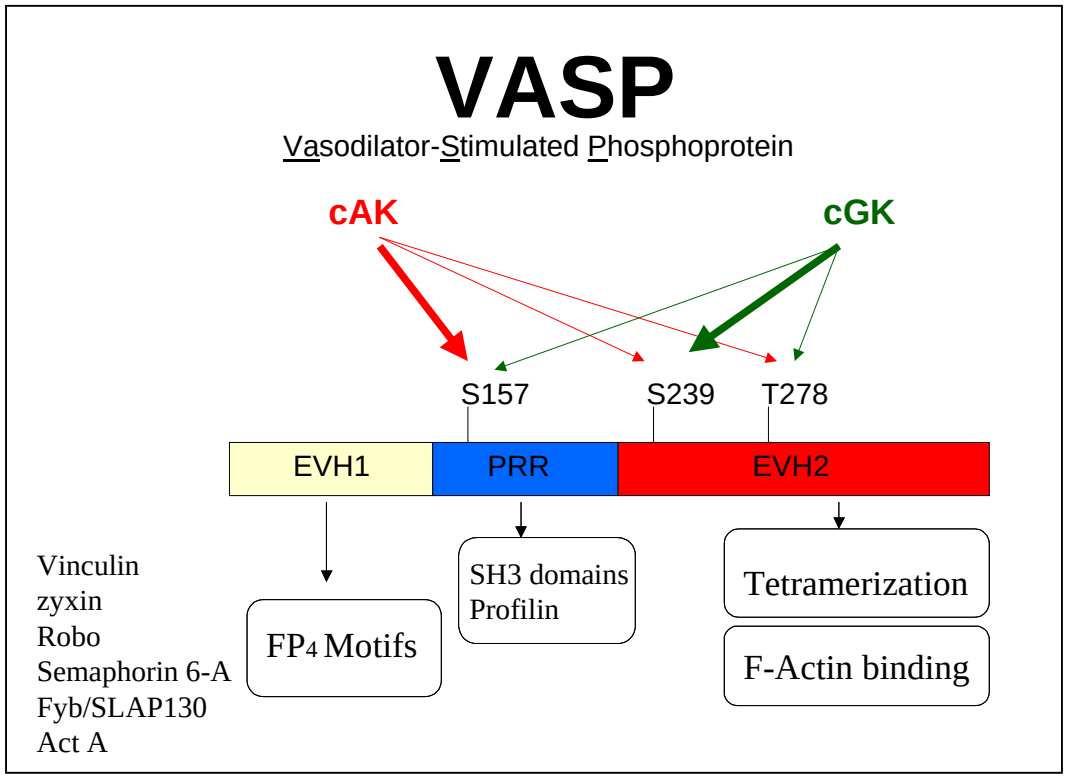

Figure 1: Schematic representation of human VASP structure and phosphorylation sites. EVH1 domains binds FP4 motifs, the proline rich region (PRR) binds SH3 domains and profilin and the EVH2 domain binds to F-actin and is responsible for tetramerization and hetero-oligomerization. VASP is a substrate for both cAK and cGK. cAK preferentially phosphorylates Ser157 and cGK preferentially Ser239. (Modified from [5,6])

VASP is the founding member of the Ena/VASP family [6-8] that includes *Drosophila* Enabled (ena), the mammalian and the avian Ena orthologs (Mena and Avena, respectively [7]) and the Ena-VASP-like protein (Evl) (Figure 2). All the proteins of the Ena/VASP family share the same domain organization that consists of highly conserved N-terminal and C-terminal regions (Ena-VASP homology domain (EVH) 1 and 2, respectively), separated by more variable low complexity (LCR) and proline rich regions (PRR) (Figure 1 and 2).

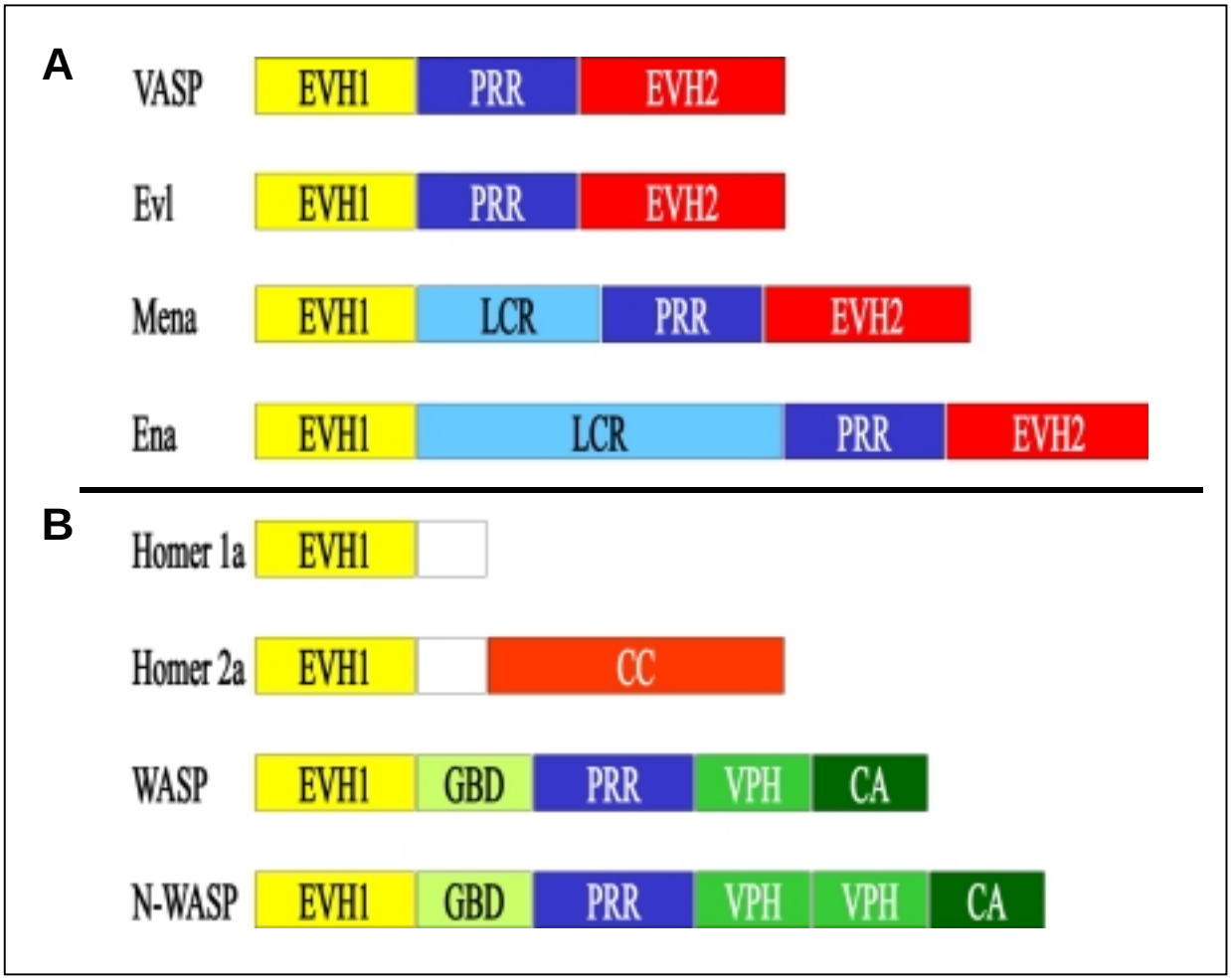

Figure 2: (A) The Ena/VASP family and (B) other EVH1 domain containing proteins such the Homer family (Homer1a and Homer 2a) and the WASP family (WASP and N-WASP). LCR: Low complexity region; PRR: Proline Rich Region; CC: Coiled coil region; GBD: GTPase binding domain; VPH: Verproline homology domain; CA: Cofilin homology and acidic regions. (Modified from [9].)

2.1.1.1. The EVH 1 domain

The EVH1 domain (of about 115 aa) recognizes FP4 motifs (E/DFPPPPXD/E) of the focal adhesion proteins Vinculin [6,10], Zyxin [10] and Lipoma-Preferred Partner (LPP) [11], the axon guidance proteins Roundabout (Robo) [12] and Semaphorine 6A-1 (Sema6A-1) [13], Fyb/SLAP 130 (Fyb/SLP 76 associated Protein)[14] and the *Listeria monocytogenes* surface protein ActA [15] (Table 1).

The structures of the EVH1 domain of Mena, Evl and VASP in complex with their ligands have been recently resolved by X-ray crystallography or nuclear magnetic resonance [16-18] and they show a close structural relationship to the Pleckstrin Homology (PH) and phosphotyrosine-binding (PTB) domains, despite barely detectable sequence similarities.

The EVH1 is also present in proteins of the more distantly related Wiskott-Aldrich syndrome proteins (WASP) and the postsynaptic proteins of the Homer/Vesl family (Figure 2).

2.1.1.2. The Proline Rich Region (PRR)

VASP and the other family members not only bind to proline rich domains but are also proline rich proteins themselves and are able to interact with polyproline binding proteins.

The PRR region binds to the Abl SH3 (Src Homology 3) domain and other SH3 domains [7,19,20] and to the G-actin binding protein Profilin [7,19-22]. Mena PRR also binds to WW domains (such as those of FE65) [23].

2.1.1.3. The EVH 2 domain

EVH2 has been implicated in the tetramerization of VASP [24], in the hetero-oligomerization with other Ena/VASP family members [19] and in the direct binding to F-actin [24].

Ligand	Ena/VASP protein	Comments
EVH1 Domain		
Zyxin	VASP, Mena, Ena	Responsible for Ena/VASP protein localization to focal adhesion[6,7,19,25,26]
LPP	VASP	[11]
Vinculin	VASP, Mena	The interaction with VASP is regulated by PIP_2 [6,7,10] [26,27]
ActA	VASP, Mena, Evl	Ena/VASP binding to ActA accelerates actin based motility of Listeria[10,28,29]
Fyb/SLAP	VASP, Mena	[14,30]
Robo	Ena	Ena strenghens repulsive Robo signaling[12]
Semaphorin 6A-1	Evl	[13]
Proline rich region		
Profilin I and II	VASP, Mena, Evl, Ena	Profilin binding to Ena/VASP proteins is involved in facilitation of actin polymerization [7,20-22,26,31-33]
Abl	VASP, Mena, Evl, Ena	Mutations in ena act as dose-dependent supressor of abl-dependent phenotypes; Ena is a substrate for Abl.; Ena phosphorylation reduces Abl SH3 binding. [19-21,34,35]
Src	VASP, Mena, Ena	Src binds to Ena/ VASP proteins via SH3 domain[7,21]
Drk	Ena	Drk binds to Ena via SH3 domain [21]
Lyn	Evl	Lyn binds to Evl via SH3 domain [20]
FE65	Mena, Evl	FE65 Binds to Mena and Evl via WW domains [20,23]
Yap	Mena	Yap Binds to Mena via WW domain [23]
EVH2 domain		
F-actin	VASP	VASP induces promotion of actin polymerization in vitro, actin filament bundling, stress fiber localization [6,24,26,36]
VASP	VASP	Tetramerization, stabilization and F-actin binding [8,24]
Mena	VASP, Mena, Evl	Homo and hetero oligomerization; stabilization of EVH1 and PRR domains interactions. [37]
Ena	VASP, Ena	Homo and hetero oligomerization; stabilization of EVH1 and PRR domains interactions. [19]

Table 1: Ena/VASP binding partners. Based on [9]

2.1.2. Subcellular localization

VASP is expressed in a wide variety of cell types and tissues, with highest levels in platelets [38]. Subcellularly, high concentrations of VASP are found at focal adhesion [6,7,19,20] and stress fibers, where it colocalizes specifically with α-actinin and Zyxin [6,7]. VASP also localizes at cell-cell contacts [6,39] and is associated with highly dynamic membrane structures such as the leading edge and membrane ruffles. Ena/VASP family proteins are also associated with unipolar actin filaments of some filopodia, especially at the filopodial tips. In focal adhesions, VASP appears to be a peripheral component. Neither the focal adhesion formation, nor the localization of focal adhesion proteins such as Vinculin, Zyxin and LPP, binding partners of VASP, are affected by the lack of Ena/VASP proteins [40].

Listeria monocytogenes is a motile bacterial pathogen. Its virulence and cell-to-cell spreading is dependent on its ability to use the actin-based polymerisation and cytoskeleton of the host cell to support its own motility. A single surface bacterial protein is sufficient to recruit the host actin polymerisation machinery: ActA that binds to the EVH 1 domain of the Ena/VASP proteins. In cells infected with *Listeria monocytogenes*, VASP is found in the interface between the moving bacterium and its actin tail, at the site where actin polymerisation is thought to take place, colocalizing with ActA [15].

2.2 Platelets

Platelets are membrane-bound cellular fragments derived from megakaryocytes. They are circulating in the blood in an unstimulated form, with a discoid-shaped smoth membrane. Any break in the continuity of the vessel wall or a break in the atherosclerotic plaque is followed by an instant response from the platelets: they contact the zone of injury, spread and aggregate forming thrombi [1]. The regulation of the cellular process involved in the activation of platelets has been extensively studied as platelets and endothelial cell, which line the inner wall of blood vessels, also participate in the pathogenesis of atherosclerosis and cardiovascular diseases.

2.2.1 Platelet Activation

Activation of platelets is a complex process that includes stimulation of activating and inhibitory biochemical pathways, reorganization of the cytoskeleton, which lead to shape change and relocation of intracellular secretory granules, secretion of substances and activation of receptors in the plasma membrane. Platelets can be activated by adhesion to proteins of the subendothelial matrix (e.g. collagen) and to von Willebrand factor (vWF) or by

soluble agonists circulating in the blood, such as thrombin, thromboxane A_2 (TxA_2) and ADP [1]. Several of the soluble agonists of platelets act throught G-protein-coupled receptors that transduce signals to the interior of the platelet. Thrombin, TxA_2 and ADP bind to receptors coupled to the $G_{\alpha q}$ protein. $G_{\alpha q}$ activates the phospholipase Cβ (PLCβ) that increases the levels of IP_3 and Diacylglycerol (DAG) by hydrolysis of PIP_2. IP_3 enhances the concentration of intracellular Ca^{2+} by liberating it from the intracellular stocks [41]. Binding of Ca^{2+} to Calmodulin (CaM) activates (among others) the myosin light chain kinase (MLCK), which in turn phosphorylates myosin light chains (MLC) inducing changes in the actin cytoskeleton. Phosphorylation of MLC also occurs through the Rho/ROCK pathway after activation $G_{\alpha 12}$ and $G_{\alpha 13}$ by thrombin and TxA_2 [42,43]. On the other hand, DAG activates protein kinase C (PKC) that is involved in the secretion of substances from intracellular stores: PDGF, Ca^{2+}, ADP, serotonin and Fibrinogen. The $G_{\alpha i}$ inhibits the adenylate cyclase (AC) and reduces the levels of cAMP. The βγ subunit of the G-protein coupled receptor activates both PLC and PI-3-K. Activation of the PI-3-K leads to activation of the Fibrinogen receptor (Figure 3). (for a review on Heterotrimeric G-proteins in platelets see [41])

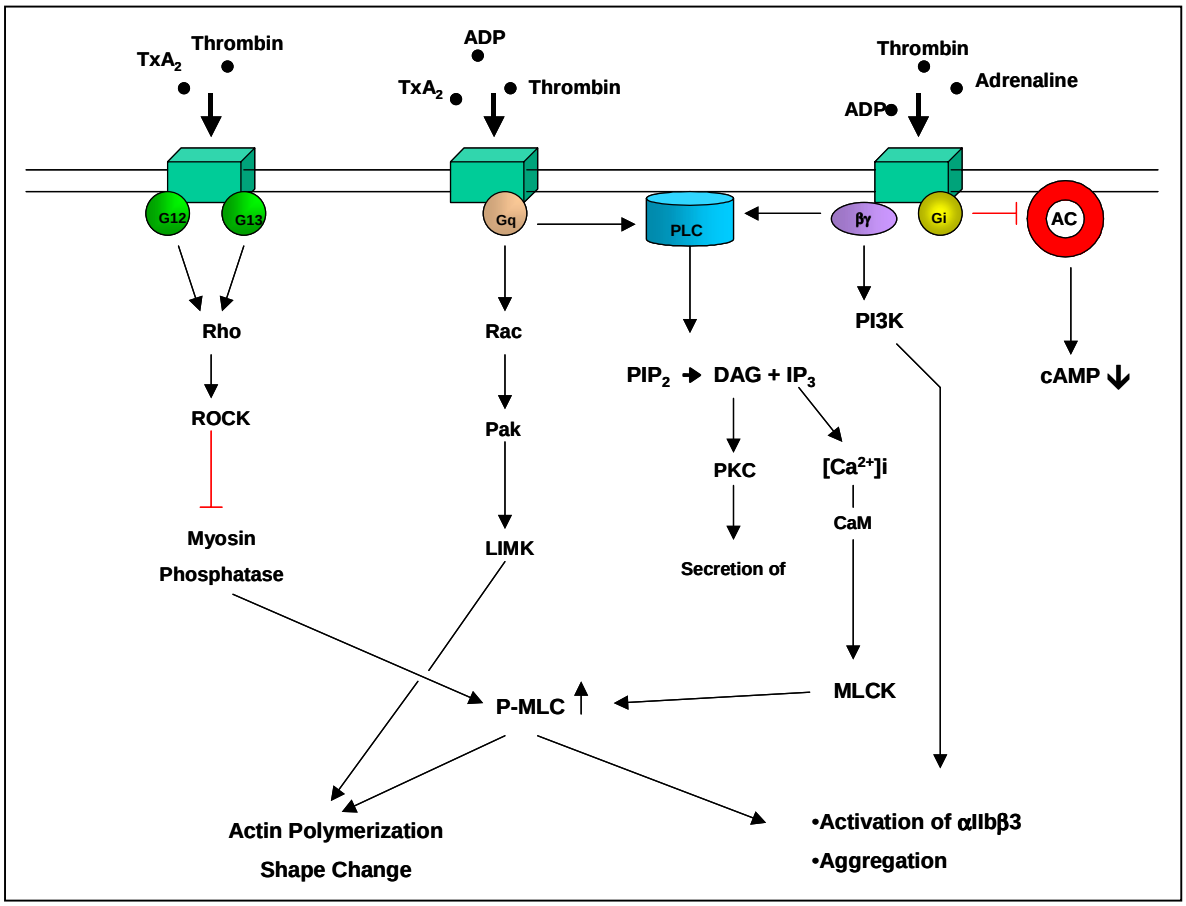

Figure 3: Signalling pathways induced by platelet activation. Black arrows indicate activation, red lines indicate inhibition (Modified from [44])

2.2.2 Platelet Inhibition

Under physiological conditions, platelets are inactive and adhesion and aggregation are tightly regulated. Substances as prostaglandins (PG-E1, PG-I2) and other vasodilators prevent the activation of platelets. These platelet antagonists inhibit aggregation by elevating the intracellular concentration of cyclic nucleotides (cGMP and/or cAMP). PG-E1 and PG-I2 bind to prostaglandin G_s-coupled receptors. The $G_{\alpha s}$ subunit activates the adenylate cyclase (AC) and increases the levels of cAMP in the platelet. Nitric oxide (NO) and other NO-donors stimulate directly the intracellular guanylate cyclase (GC) enhancing the intracellular concentration of cGMP. Cyclic nucleotides induce platelet inhibition via the activation of cAMP- and cGMP- dependent protein kinases (cAK and cGK respectively) [44-46]. It is not yet clear how the substrates of cAK and cGK (see Figure 4) regulate the inhibition of platelets, however several proteins phosphorylated by cAK are involved in the regulation of actin cytoskeleton. Phosphorylation of Caldesmon stabilizes the cytoskeleton of resting platelets [47], phospho-Glycoprotein 1B inhibits actin polymerization [48] and phosphorylation of actin binding protein (ABP) inhibits the reorganization of the cytoskeleton during platelet activation [49]. During platelet activation Rap1b rapidly interacts with the reorganized actin-based cytoskeleton [50]. Moreover, cGMP and cAMP also activate phosphodiesterases (PDE) that control and turn off the inhibitory signal by degradation of cyclic nucleotides (Figure 4). In human platelets three different PDE subtypes were identified: PDE2, which is stimulated by c-GMP and acts on both cGMP and cAMP; PDE3, hydrolyzes cAMP and is activated by cAK and inhibited by cGMP and PDE5, a cGMP stimulated and cGMP specific phosphodiesterase [51] (For a review see [44]).

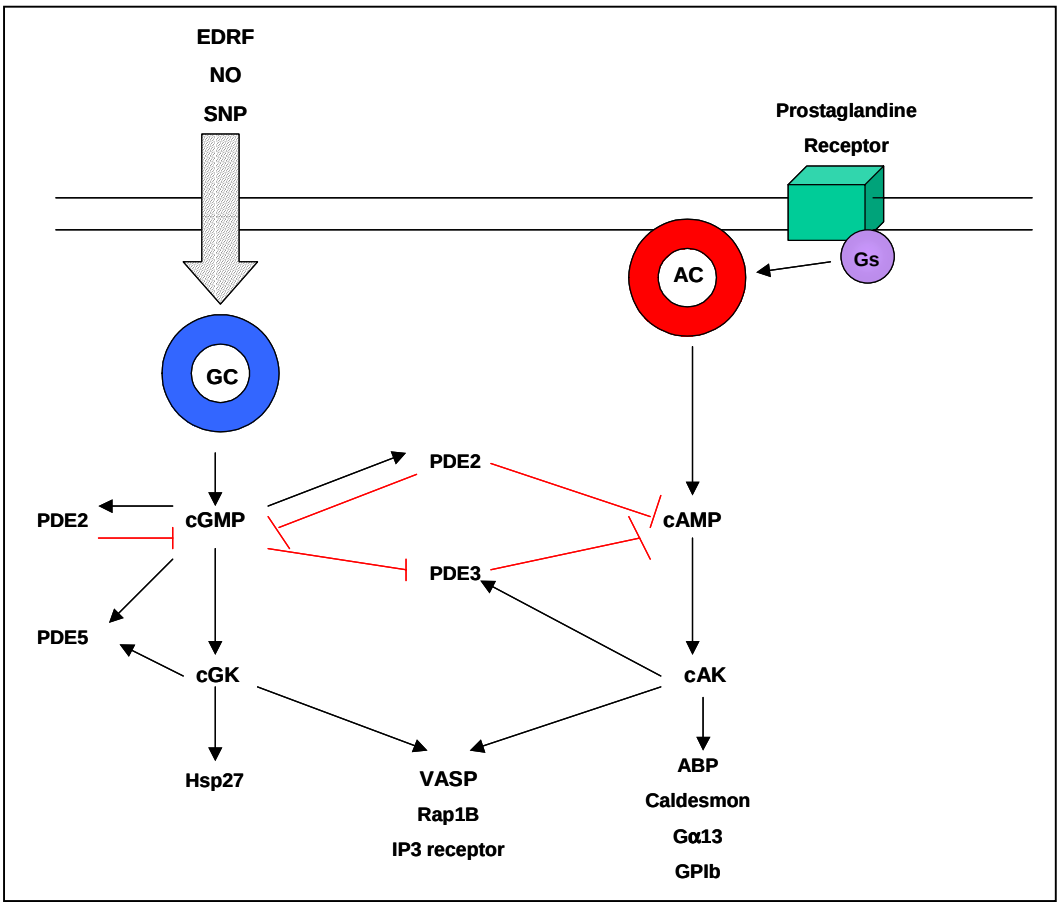

Figure 4: Signalling pathways involved in platelet inhibition. Black arrows indicate activation, red lines indicate inhibition (Based on [44])

2.2.3 VASP in Platelets

VASP is strategically located at the intersection of the major platelet inhibitory pathways described before. In response to the cyclic nucleotide-regulating platelet antagonists NO and PGI_2, VASP is phosphorylated by both cAK and cGK. VASP phosphorylation closely correlates with platelet inhibition and is accompanied by inhibition of the platelet fibrinogen receptor GPIIb-IIIa (also known as $\alpha_{IIb}\beta_3$) activation. The exact role of VASP in the inhibition of platelets is not yet fully understood but importance of the protein during platelet inhibition has been shown in VASP deficient mice that present enhanced collagen and thrombin induced platelet activation and impaired cyclic nucleotide mediated inhibition [52,53] (See ”The Knock-out approach” in this section). The participation of VASP in dynamic cytoskeletal processes (see chapter 2.3) and its phosphorylation induced by platelet antagonists are hints to consider it as an important player in the regulation of platelet inhibition.

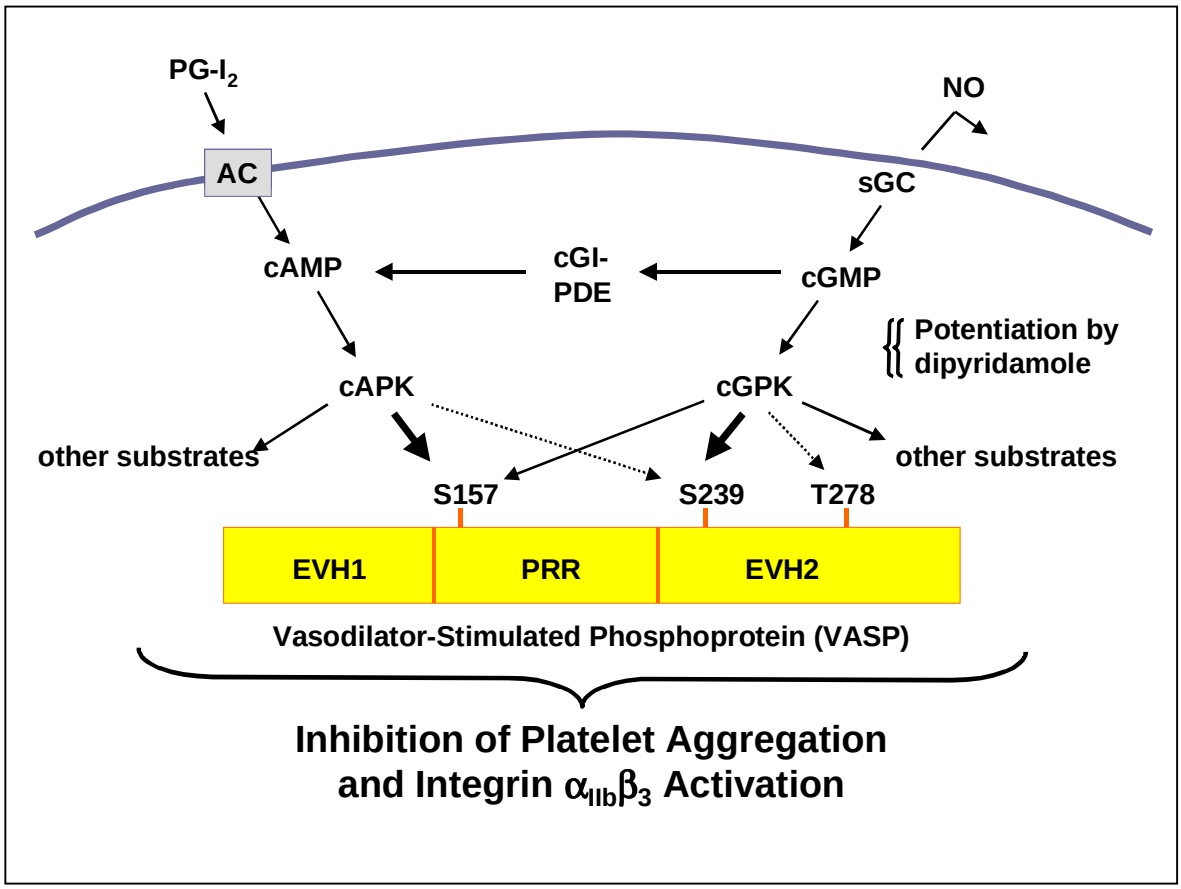

Figure 5: VASP phosphorylation induced by cyclic nucleotides in platelets.

2.3 Cytoskeletal Remodelling

2.3.1 Actin Polymerization

Actin is the most abundant protein in many cell types (± 5% of total cellular proteins) and exist in two forms: monomeric (or G-actin) and filamentous (F-actin). Each actin molecule is a single polypeptide of 42 kDa that has a molecule of ATP tightly associated with it.

F-actin is a thin, flexible and helical homopolymer of actin. Such actin filaments are asymmetric: ATP-bound actin monomers polymerizes onto a fast growing barbed ends (or + ends) of F-actin, while the opposite end of the filament, the pointed end (or – end) is relatively inert and slow growing. Polymerization of actin in vitro requires ATP, K+ and Mg2+. There is initially a lag phase and then a rapid polymerization phase. The lag is due to nucleation of three monomers of actin that are required to initiate the process. Once the nuclei are formed one actin monomer is added at a time. After polymerization ATP bound to actin is hydrolyzed to ADP. The critical concentration for actin polymerization (the free actin monomer concentration at which the proportion of actin as a polymer stops increasing) is about 0.2 μM. However, the concentration of G-actin in the cell is much higher than this, between 50 and 200 μM. To keep the proper amount of free available actin monomers the cell contains actin-binding proteins that sequester the actin monomers. Cofilin (or actin depolymerization factor, ADF) and Thymosinβ4 bind to actin monomers and inhibit the assembly into the filament. On the other hand, another actin-monomer-binding protein that regulates actin polymerization is Profilin, a binding partner for VASP, that accelerates the exchange of ADP for ATP when bound to actin monomers and is thought to stimulate polymerization [54].

Other proteins regulating actin polymerization are the proteins of the Arp2/3 complex. Two of the proteins from this complex, Arp2 and Arp3, present a surface similar to the barbed end of the actin filament suggesting that the Arp2/3 complex serves as a surface were nucleation can be initiated. Indeed, Arp2/3 increases the rate of nucleation of new actin filaments both in vitro [55] and on the surface of *Listeria monocytogenes* [56]. In addition to nucleating new actin filaments, Arp2/3 complex links filaments at 70° angles forming the branching structures observed at the leading edge of motile cells. Branching of the filaments occurs by binding of Arp2/3 to the side of filaments.

In order to stop the extension of the filaments Capping protein binds to the barbed end and inhibits the incorporation of new monomers to the filament.

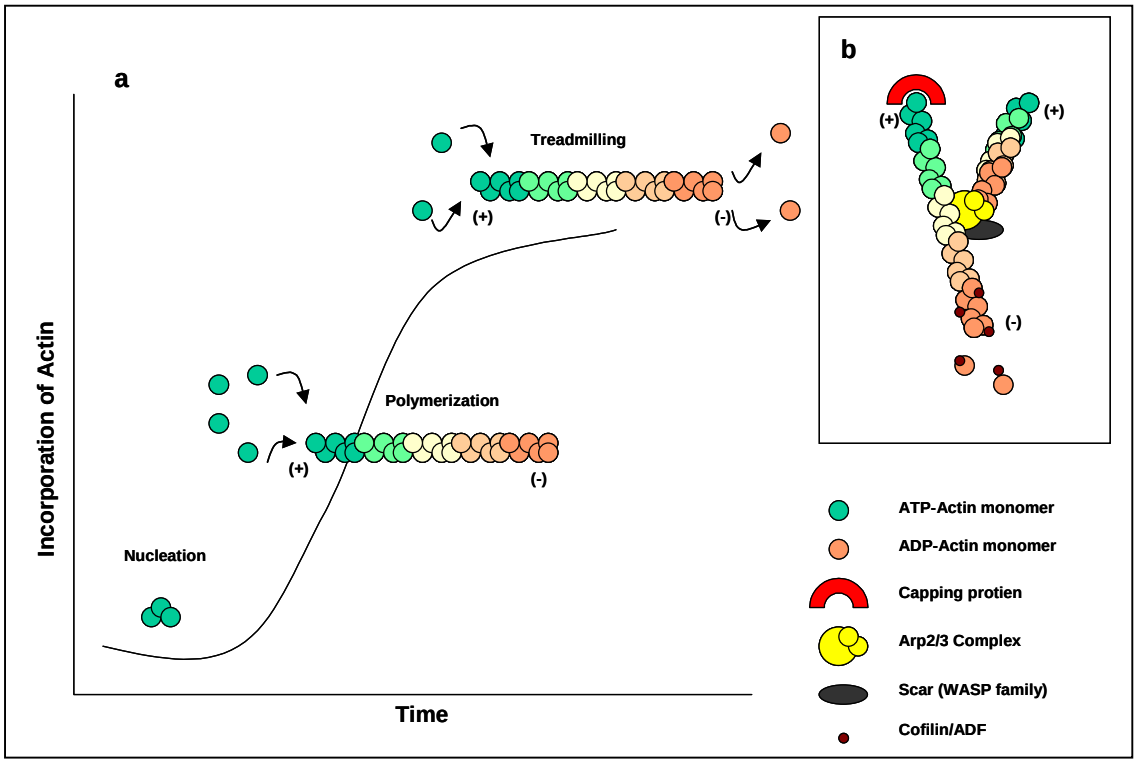

Figure 6: Actin Polymerization. (a) Actin polymerization curve. The lag phase represents the time required for actin nucleation. The rapid polymerization phase represents the time during which short filaments elongate. The steady state at the end of the curve represents an equilibrium between growth of the filaments due to monomer addition and shortening of the filaments due to depolymerization. (+): barbed end; (-) pointed end **(b)** Branching of filaments by Arp2/3 complex. Arp2/3 complex binds to the sides of filaments stimulating actin nucleation so that a new filament is initiated. Binding to WASP/Scar proteins is suggested to be important for activation of Arp2/3 complex. Cofilins are actin-associated proteins that have both actin severing and actin depolymerizing activities. (Modified from [54]).

2.3.2 The Actin Cytoskeleton

Eucaryotic cells can adopt a variety of shapes and can carry out coordinated and directed movements. The cytoskeleton is the complex network that extends throughout the cytoplasm and, despite the idea of rigidity contained in the word “cytoskeleton”, it is a highly dynamic structure that reorganizes continuously as the cell divides, changes its shape and responds to extracellular signals. The cytoskeleton activities depend on three main protein filament structures: actin filaments, microtubules and intermediate filaments. I will concentrate here on the actin filaments or *Actin Cytoskeleton*.

Actin filaments occur as networks or bundles crosslinked by a variety of actin binding proteins. The dynamics of the actin cytoskeleton is determined by new actin polymerisation, nucleation of F-actin at specific subcellular localizations or disassembling of existing filaments. All these processes are tightly regulated by a number of proteins that include, among others, actin binding proteins and also cytoplasmic kinases. In the last 10 years many

proteins have been found to be involved in the regulation of the actin cytoskeleton, however the subject remains complex and a lot of work is needed to fully understand the mechanism.

Often, the remodelling of the actin cytoskeleton is induced by extracellular signals, and more precisely by changes in the extracellular matrix. The main linkers between the extracellular matrix environment and the actin cytoskeleton are the *integrins*.

2.3.3 Integrins

Integrins are members of the large family of transmembrane proteins involved in adhesion of cells to the extracellular matrix (ECM). They bind most of the ECM proteins including collagen, fibronectin and laminin [57]. Integrins bind their ligands with relatively low affinity and are usually present at high concentrations on the cell surface. This arrangement of integrins allows the cell to bind simultaneously but weakly to a large number of matrix molecules so that the cell can explore the environment without loosing completely the attachment to it.

Integrins are composed of two non-covalently associated transmembrane subunits called α and β. Eight types of β subunits and 18 types of α subunits form more 24 different varieties of integrins in human [57]. They function as transmembrane linkers mediating the interactions between the cytoskeleton and the ECM that are required for cells to grip the matrix. Most integrins connect to bundles of actin filaments. After binding to its ligand, the cytoplasmic tail of the β subunit binds to talin, α-actinin, filamin and tensin and initiates the assembly of a complex of intracellular proteins that link the integrins to the actin cytoskeleton [57]. Mutations at the tail of the β chain inhibit the binding to the intracellular proteins but not the binding to their extracellular ligands. However, even though this mutant is able to interact with the ECM, these mutants cannot longer perform a robust cell adhesion and/or cluster of focal contact. But integrins do not only attach the cell to the matrix, they also generate intracellular signals at the attachment sites (focal contacts). They function as signal transducers, activating various intracellular pathways when activated by ECM binding. Some of the pathways activated by integrins are those regulated by the small GTPases of the Rho family.

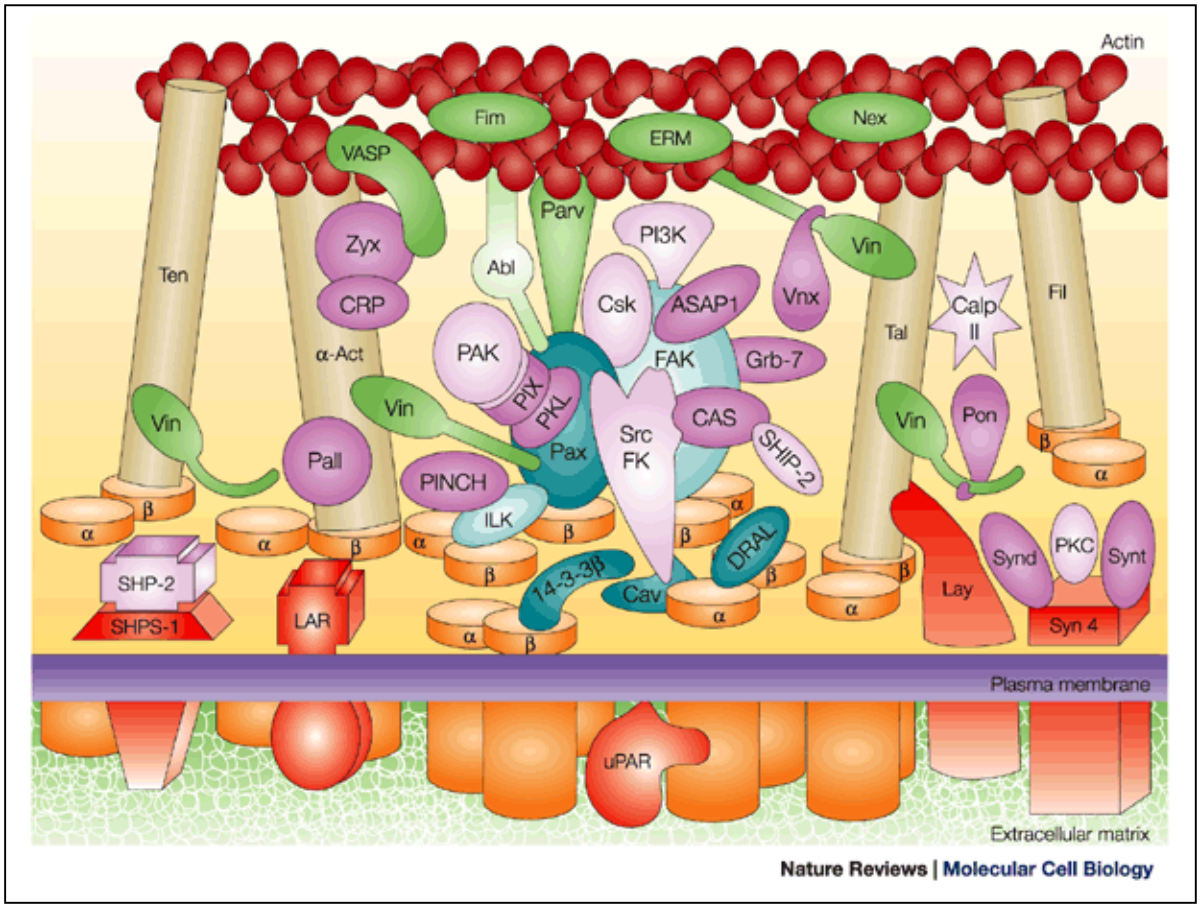

Figure 7: Scheme depicting the complexity of the main molecular domains of cell–matrix adhesions. [Taken from Geiger, Bershadsky, Pankov and Yamada; Transmembrane extracellular matrix-cytoskeleton crosstalk, *Nat. Rev. Mol. Cell Biol.*, **2**, 793-805 (2001)] The primary adhesion receptors are heterodimeric integrins, represented by orange cylinders. Additional membrane-associated molecules enriched in these adhesions (red) include syndecan-4 (Syn4), layilin (Lay), the phosphatase leukocyte common antigen-related receptor (LAR), SHP-2 substrate-1 (SHPS-1) and the urokinase plasminogen activator receptor (uPAR). Proteins that interact with both integrin and actin, and which function as structural scaffolds of focal adhesions, include α-actinin (α-Act), Talin (Tal), Tensin (Ten) and Filamin (Fil), shown as golden rods. Integrin-associated molecules in blue include: focal adhesion kinase (FAK), paxillin (Pax), integrin-linked kinase (ILK), down-regulated in rhabdomyosarcoma LIM-protein (DRAL), 14-3-3 and caveolin (Cav). actin-associated proteins (green) include vasodilator-stimulated phosphoprotein (VASP), Fimbrin (Fim), Ezrin–Radixin–Moesin proteins (ERM), Abl kinase, Nexillin (Nex), Parvin/Actopaxin (Parv) and Vinculin (Vin). Other proteins, many of which might serve as adaptor proteins, are coloured purple and include Zyxin (Zyx), cysteine-rich protein (CRP), Palladin (Pall), PINCH, Paxillin kinase linker (PKL), Pak-interacting exchange factor (PIX), Vinexin (Vnx), Ponsin (Pon), Grb-7, ASAP1, Syntenin (Synt), and Syndesmos (Synd). Among these are several enzymes, such as SH2-containing phosphatase-2 (SHP-2), SH2-containing inositol 5-phosphotase-2 (SHIP-2), p21-activated kinase (Pak), phosphatidyl inositol 3-kinase (PI3K), Src-family kinases (Src FK), carboxy-terminal src kinase (Csk), the protease Calpain II (Calp II) and protein kinase C (PKC). Enzymes are indicated by lighter shades.

2.3.4 The Rho GTPase family

Rho-GTPases are small (≈ 21 kDa) monomeric GTP binding proteins that belong to the Ras Superfamily of GTPases. Like every GTP binding protein, Rho GTPases exist in an inactive form, the GDP bound conformation, and in a GTP bound active form. Their interconversion is mediated by guanine nucleotide exchange factors (GEFs) that favours the binding to GTP, thus activates the protein, and by GTPases activating proteins (GAPs) that enhance the intrinsic GTPase activity. Moreover guanine nucleotide dissociation inhibitors (GDIs) have been identified for the Rho family.

The Rho GTPase family contains: Rho (A, B and C isoforms), Rac (1,2 and 3 isoforms), Cdc42 (G25K, Cdc42Hs isoforms), Rho D, Rho G, TC10, Rnd (Rnd 1, RhoE/Rnd 3 and Rnd6) and TTF. From them Rho, Rac and Cdc42 are the most studied and their function has been examined in great detail. They can be activated by stimulation of growth factor receptors, integrin activation and/or G-protein coupled receptors. Active Rho recognizes RBD domains (Rho binding domains) and Rac and Cdc42 recognize CRIB domains (Cdc42/Rac interacting binding domains) (See [58] for a Review).

2.3.4.1 Rho

Three isoforms haven described: RhoA, RhoB, and RhoC [59,60]. RhoA is ubiquitously expressed and, as RhoC, it is usually present in the cytosol. RhoB is mainly associated with the plasma membrane.

The Major role of Rho is to regulate the assembly of stress fibers and integrin based focal adhesion complexes [61]. The assembly of stress fibers can be induced by transfection of cells with constitutively active mutants (RhoV14 and RhoL63) or by treatment of quiescent cells with several extracellular factors (e.g. serum), in particular lysophosphatidic acid (LPA). Rho activation by LPA is mediated by a G-protein coupled receptor via $G_{12/13}$ and by tyrosine kinase receptor [58,62].

Rho is a substrate for a number of bacterial exoenzymes and toxins. C3 transferase from *Clostridium botulinum* ADP-ribosylates Rho at residue N41 and inhibits Rho activity. Even though Rac and Cdc42 also have the same residue at that position they are no substrates for C3, which therefore is a specific inhibitor for Rho [58].

Rho-GTP can activate a number of downstream protein kinases such us PKN, p160ROCK (also named ROCK or ROK) [63], Rhotekin and PIP5K. ROCK has been shown to induce the phosphorylation of myosin and seems to be in the pathway required for stress fibers formation and stabilization.

2.3.4.2 Cdc42

Cdc42 regulates assembly of adhesion complexes and actin fibers at the cell periphery to form filopodia [64]. Cdc42 is activated by bradikinin and cytokines. Microinjection of constitutively active Cdc42 induces rapid filopodia formation, usual accompanied by subsequent lamellipodia formation. Cdc42 is a potent activator of Rac and both together lead to coordinated filopodia/lamellipodia formation suggesting an important role of these GTPases in cell migration, spreading and growth cone protrusion [64].

Cdc42 activates the Ser/Thr p21-activated kinase (Pak) and binds to WASP.

2.3.4.3 Rac

Rac is activated by growth factors (PDGF; EGF) [62] and insulin in fibroblasts and in platelets by agonist such as thrombin [65], thromboxane [66] and Collagen [65]. The activation is mediated by a tyrosin kinase receptor in the case of PDGF and by a G_q-coupled receptor in the case of thromboxane [66]. Generation of PIP_3 is also a potent Rac activator [62,67]. Moreover, Rac is activated upon adhesion [68,69].

Del Pozo and colleagues showed that growth factors and adhesion to the ECM both contribute independently and approximately equally to Rac activation. In non-adherent cells, activated Rac failed to stimulate its effector Pak. Moreover, V12 Rac or Rac activated by serum translocated to the membrane fraction of adherent cells but remained mainly cytoplasmic in suspended cells [68]. These results showed that ECM regulates the ability of Rac to couple with Pak [68].

Rac regulates the formation of lamellipodia, membrane ruffles and associated integrin adhesion complexes.

GTP-Rac activates Pak and SCAR/WAVE proteins.

2.3.4.3.1 The Rac/Pak pathway

When the GTP form of Rac binds to the CRIB domain of Pak, Pak undergoes a conformational change that liberates the kinase domain from the autoinhibitory domain [70]. Moreover, upon activation Pak is autophosphorylated at several ser/thr residues. Pak regulates myosin light chain phosphorylation via myosin light chain kinase [71] and direct phosphorylation [72]. In addition, Pak activates LIM kinase (LIMK) by phosphorylation of a threonine residue in the activation loop [73-75]. When activated by Pak or Rho-associated protein kinase [75], LIMK phosphorylates and inactivates ADF1/Cofilin, which results in actin filament stabilization (reviewed in Refs. [74,76]).

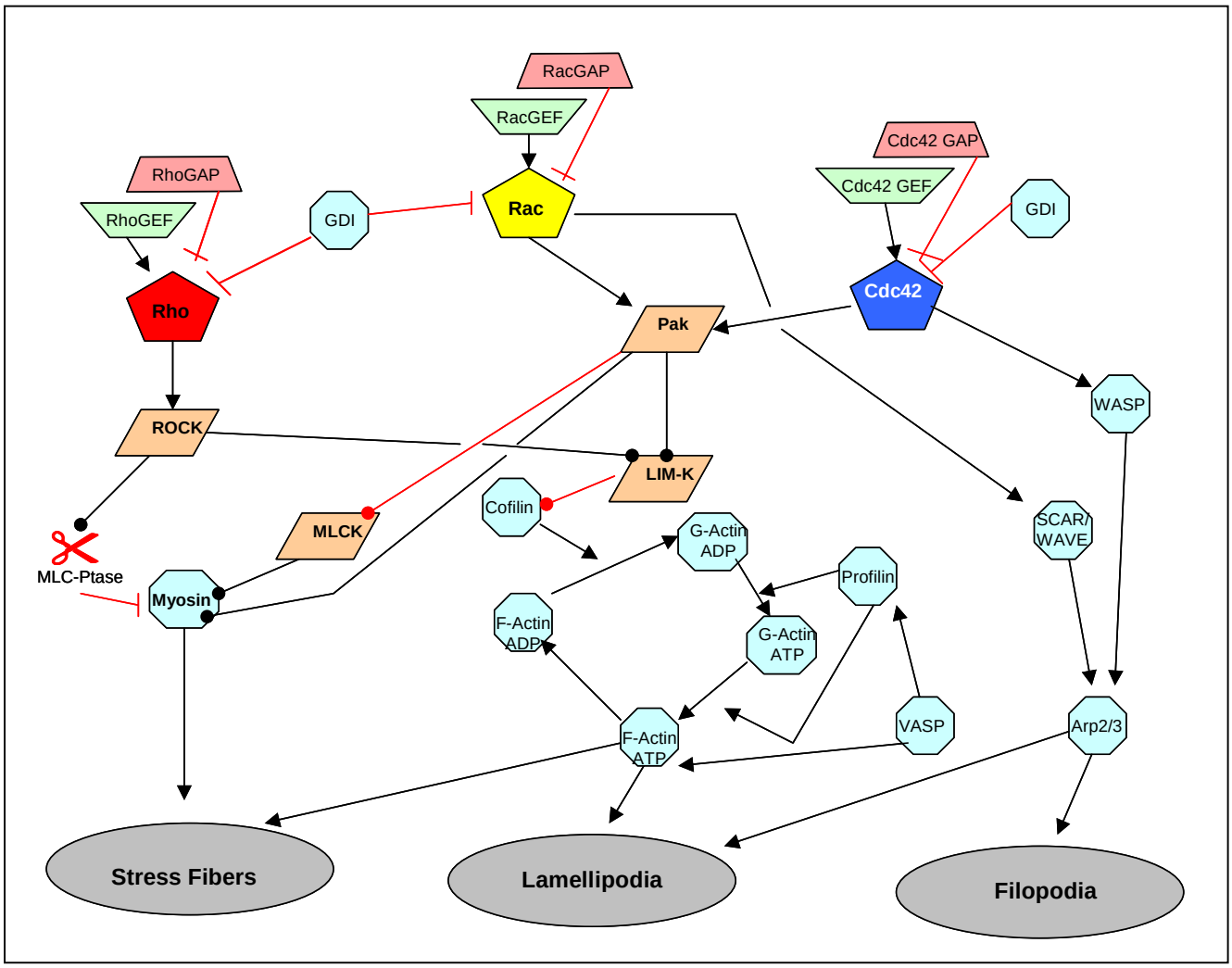

Figure 8: Regulation of the actin cytoskeleton by Rho GTPases (Based on http://cellularsignaling.com/cm2/actin.html) Symbols: ➔ activatory pathways (direct or indirect interaction) ; —| inhibitory pathways; —● activation by phosphorylation; —● inhibition by phosphorylation.

2.3.5. VASP and the actin cytoskeleton.

a. The Listeria model

The motility of the bacterium *Listeria monocytogenes* is an established model system to study actin polymerization processes. Even though the bacterial model is not exactly the same as the situation in an eukaryotic model, parallels have been observed between the mechanism acting at the *Listeria* surface and the leading edge of motile cells, supporting the use of this model. VASP directly binds to the *Listeria* surface molecule ActA [15]. ActA, similar to the WASP family proteins in eukaryotic cells, has the ability to activate the filament nucleation activity of the Arp2/3 complex, a complex comprising seven polypeptides. VASP and profilin are not essential for basal *Listeria* motility in a reconstituted system with purified proteins. However both proteins have been shown to

accelerate *Listeria* motility [28] while in infected cells they appear to be more essential [10,29]. In living cells Mena, Evl and VASP do not induce F-actin assembly or recruitment by themselves (with the exception of one splice variant of Mena: Mena+), indicating that another nucleating activity is required to accomplish F-actin formation. Current thinking favours the idea that Ena/VASP proteins efficiently elongate the actin filaments initiated by ActA or WASP activation of the actin-nucleating activity of Arp2/3 [77,78].

It has also been suggested that Zyxin and ActA can generate new actin structures in a VASP dependent manner and independently of the Arp2/3 complex [79]. Fradelizi et al have shown that although the WA domain of WASP, which is necessary for the Arp2/3 dependent nucleating activity, and the proline-rich domain of ActA (similar to the Zyxin proline-rich domain) were able to nucleate F-actin to coated beads, they use different mechanism. ActA proline rich domain recruits VASP but not Arp2/3 and the opposite has been seen for the WA domain. In a similar way, Zyxin can induce actin nucleation independently of Arp2/3. When the binding site for VASP is abrogated, Zyxin loses its capability to polymerise actin. However, this Zyxin mutant recruits F-actin, indicating that VASP is probably required for proper actin polymerisation. As both, VASP and Zyxin, are focal adhesion proteins, these results suggest a VASP dependent polymerisation activity in Focal Adhesions [79].

b. Axon Guidance

During development, neurons extend axons and dendrites towards their appropriate targets. Extracellular cues indicate the growing axon or growth cone to advance, retract or turn. This process is called *axon guidance*.

Ena/VASP proteins, notably Ena and Mena, appear to mediate axon guidance. Barshaw et al. [12] show that Ena interacts with the repulsive neuronal guidance receptor Robo via the EVH 1 domain and may mediate Robo signaling. Mutations of Ena and/or Robo lead to defective repulsion and consequently defects in neuronal networks. Ena was originally described as a protein having opposite effect of the Ableson tyrosin kinase (Abl). Abl antagonizes Robo signaling, coinciding with the idea that Ena and Abl have opposite effects in the same pathway.

2.3.6 The small GTPases and the Ena/VASP family

Ena/VASP proteins and Rho-GTPases have been shown to be involved in similar processes, such as actin polymerisation, stress fiber structure, filopodia formation and axon guidance. However the relationship between them has not been extensively studied.

2.3.6.1 Ena and the Rho-GEF Trio

In *Drosophila*, genetic mutations of *abl* lead to central nervous system (CNS) defects that are alleviated by Ena deletion. On the other hand, deletion of *Abl* and Drosophila-*trio* (*D-trio*), a GEF for Rac and Rho, lead to severe defects in CNS, while *D-trio* deletion alone shows just subtle defects, similar to the one observed in *abl*$^{-/-}$. These observations suggest that Ena and Trio may play opposite roles in growth cone motility, providing a link between the abl tyrosine kinase, the Ena/VASP proteins and Rho GTPases regulators [80].

2.3.6.2 Mena-IRSp53-Cdc42

IRSp53 (Insulin Receptor Substrate) is a target of Cdc42 and has been involved in filopodia formation. Mena has been identified as a binding partner for IRSp53 and the interaction between Mena and IRSp53 is regulated by Cdc42. GTP-Cdc42 binds to the CRIB domain located in the autoinhibitory region of IRSp53 and liberates the binding site for Mena. Overexpression of Mena or IRSp53 induces the formation of filopodia but when both proteins are overexpressed together the effect is dramatically enhanced. This synergistic action of Mena and IRSp53 is dependent on their interaction as shown in experiments using mutants of IRSp53 that cannot bind to Mena [81].

2.3.6.3 WASP and Cdc42

WASP is an EVH 1 domain-containing protein that also has a CRIB domain able to interact with Cdc42 but not with Rac. Overexpression of WASP induces ectopic actin polymerisation that can be inhibited by dominant negative Cdc42 (N17-Cdc42). In a similar way, SCAR, a relative to WASP, induces actin polymerisation in a Rac dependent manner.

WASP and VASP have always been considered together due to their participation in the regulation of actin dynamics at the leading edge. However, the interaction between WASP and VASP has been demonstrated only recently. The proline rich domain of WASP binds VASP and this interaction enhances the propulsion of WASP coated beads, in a similar way as Listeria motility is accelerated by VASP. WASP is thus bringing together VASP and Cdc42, but the relation between them still needs to be studied [82,83].

2.4 The "Knock-Out" approach

One approach to study the physiological significance of a protein is to create animal models deficient in the protein of interest by targeted gene deletion (gene knock out). That means that the gene encoding for the protein is replaced via homologous recombination with a portion of DNA (usually a short gene encoding for antibiotic resistance) that disrupts the expression of the gen. Here I will summarize the phenotypes of animals deficient in Ena/VASP proteins.

Ena-deficient Drosophila melanogaster

The first Ena/VASP gene to be knocked out was the one encoding for Ena. Ena deficient flies died during embryogenesis with defects in axonal architecture [19]. The lethal phenotype was rescued by wild type *ena*, partially by a mutant of *ena* encoding a protein that lacks the tyrosine phosphorylation sites [35] and by human VASP [19]. Note that despite the high similarities between both proteins, VASP is not phosphorylated by Abl [34].

VASP$^{-/-}$ mouse model

Having the dramatic effect observed in the Ena deficient flies as a precedent, the VASP $^{-/-}$ mice were created one year later by two independent groups (Aszodi et al., Hauser et al.; the latter our group in Würzburg). However, mice deficient in VASP showed only a mild phenotype. Animals were viable and fertile with a mild platelet dysfunction. Both groups agree in that VASP$^{-/-}$ mice present enhanced collagen and thrombin induced platelet activation and impaired cyclic nucleotide mediated inhibition. Moreover, Hauser et al described megakaryocyte hyperplasia. It is important to note that VASP is the only Ena/VASP protein present in platelets [52,53].

Mena$^{-/-}$ mouse model

Mena deficient mice are also viable and fertile with a mild neuronal dysfunction such as some axon misrouting, impaired corpus callosum and hipocampal comisure formation [31].

Caenorhabditis elegans deficient in unc34 gene product

In *C. elegans* ablation of the unc34 gene product leads to axonal migration defects [34].

The results obtained with the mouse model suggest that the remaining proteins of the Ena/VASP family compensate the deficiency, leading to mild phenotypes and making the study of the mammalian Ena/VASP proteins more complicated. The double knock out Mena/VASP has been reported to be lethal at early embryonic stage and another mouse model, the Mena$^{-/-}$ /VASP-/+ present commisure formation defects more severe than those in Mena$^{-/-}$ mice [34].

2.5 Aim of the Work

As VASP deficient mice did not show any obvious dramatic phenotype (probably due to compensation by the other members of the Ena/VASP family), VASP-deficient cell lines were established in order to study in more detail the cellular function of VASP. Considering the experience in the laboratory and the interest of the group in the area of cardiovascular and heart failure research, cardiac fibroblasts were chosen as cell type to be studied.

The first part of the work includes the establishment and characterization of VASP-deficient cell lines. Detailed analysis of these cells suggested defects in the reorganization of the actin cytoskeleton. Therefore, in the second part of the work the signal transduction pathways that could be involved in actin cytoskeleton remodelling were investigated. The small GTPases of the Rho family have been shown to mediate several of the features that I found to be impaired in $VASP^{-/-}$ cells and therefore were good candidates to be studied in more detail. These studies were extended to mouse platelets. Finally, it was the aim of collaboration with Dr. Massberg (Deutsche Herzzentrum in Munich) to address possible effects of VASP on platelet adhesion *in vivo*.

3. Materials

3.1.1 Primary Antibodies

Name	Antigen	Epitope	Type	Origin	Dilution		Source	Ref.
					WB	IF		
M4	VASP	----	Polyclonal	Rabbit	1:3000	1:500		[84]
16C2	pVASP-Ser239	RKVpSKQE	Monoclonal	Mouse	1:100	---	Nanotools	[5]
Mena	Mena	NH_2-terminal	IgA	Mouse	1:1000	---	Transduction Labs	
M5	Zyxin	----	Polyclonal	Rabbit	1:2000	---	InmunoGlobe	[38]
hVin	Vinculin	----	IgG1	Mouse	1:1000	---	Sigma	
LPP	LPP	----	Polyclonal	Rabbit	1:1000	1:200	InmunoGlobe	--
Rac	Rac 1 and 2	Recombinant human Rac	Monoclonal	Mouse	1:1000	---	Upstate	[66]
Pak (N20)	Pak 1	----	Polyclonal	Rabbit	1:1000	---	Santa Cruz Biotech	[85]
pPak (Thr402)	pPak 1 and 2		Monoclonal	Goat	1:200	---	Santa Cruz Biotech	

3.1.2 Secondary Antibodies

Antibody	Label	Dilution	Company
Goat-anti-Rabbit Ig	Horseradish Peroxidase	1:5000	Amersham-Pharmacia/ Dianova
Goat-anti-Rabbit Ig	IRDye800	1:5000	Biotrend
Goat-anti-Rabbit Ig	Alexa Fluor®680	1:5000	Molecular Probes
Goat-anti-Mouse Ig	Horseradish Peroxidase	1:5000	Amersham-Pharmacia/ Dianova
Goat-anti-Mouse Ig	IRDye800	1:5000	Biotrend
Goat-anti-Mouse Ig	Alexa Fluor®680	1:5000	Molecular Probes
Goat-anti-Mouse IgA	Horseradish Peroxidase	1:5000	Sigma
anti-Rabbit Ig	Cy3	1:300	Molecular Probes
anti-Mouse Ig	Cy2	1:300	Molecular Probes
anti-Mouse Ig	Cy3	1:300	Molecular Probes

3.1.3 Fluorescent Labels

FITC Hamster anti Rat CD29 (β1 integrin)..... Pharmingen

FITC anti mouse CD61 (β3 integrin)..... Pharmingen

Oregon Green Phalloidine..... Molecular Probes

Rodamine Phalloidine..... Molecular Probes

3.1.4 Bacteria

Gold Supercompetent Cells Epicurian Coli® SoloPack™, Stratagene.

3.1.5 Plasmids

FL-VASP + Hygromycin for stable transfection, based on pCDNA3 from Invitrogen containing human full length VASP……	Dr. Martin Eigenthaler, Institute für Klinische Biochemie und Pathobiochemie
GST-PBD……	Dr. Offermanns (Pharmakologisches Institut, Heidelberg) with permission of Dr. Bokoch (The Scripps Institute, La Jolla-USA)

3.1.6 Oligonucleotide

Primers for EVL:

5’ -GAG CAG CAG CAC CGC CAG GAG-3’

5’-GGA CAG CAA CGA GGA CAC AGG-3’

Product: 590 bp

Primers for GAPDH:

5’-TTA GCA CCC CTG GCC AAG G-3’

5’-CTT ACT CCT TGG AGG CCA TG-3’

Product: 540 bp

Primers for Genotyping:

WT-PCR:

GIK 296: 5’-TTA GCT TGG TTT GGG GAC TGA ACC AGC CTC CTT TC-3’

GIK 270: 5’-CAG CCA CTC CCT GGT ACT TCC TTA CCT TGC TCA C-3’

Product: aprox. 600-700 bp

KO-PCR:

GIK 273: 5'-CGA ATA GCC TCT CCA CCC AAG CGG CCG GCG AAC-3'

GIK 274: 5'-GGC CAG CAG AAC AGT ATT GGA GAA CTA CCA GG-3'

Product: aprox. 450-500 bp

See figures 5, 6 and 7 for details of the location of the primers for genotyping

3.1.7 Antibiotics

Antibiotic-Antimycotic solution 100x..... Invitrogen Inc.
Hygromycin B 50 mg/ml..... Roche Diagnostics
Ampicillin (Stock solution: 50mg/ml)..... Sigma

3.1.8 Chemicals

PDGF-BB ..... Sigma
PGI_2..... Sigma
8p-CPT-cGMP..... BioLog
cBIMPS-cAMP..... BioLog
U46619 (thromboxane A_2 analogue)..... Sigma
Thrombin..... Sigma
Apyrase..... Sigma
Collagenase/Dispase..... Roche Diagnostics
FuGENE™..... Roche Diagnostics
Calf Serum..... BioHyb
DMEM, High Glucose..... Invitrogen Inc.
Fibronectin…… Sigma
Collagen III…… Sigma
Vitronectin …… Sigma

3.1.9 Protein Markers

Protein Molecular Weight Marker (SM0431)……. MBI Fermentas

3.1.10 DNA Markers

All DNA markers were from MBI Fermentas

1 Kb DNA Ladder……. SMO241

3 Kb DNA Ladder……. SMO321

10 Kb DNA Ladder…….. SMO311

3.1.11 Materials for Microarrays

Score Card (Standards)…….. Amersham Pharmacia

CyScribe First Strand Kit……. Amersham Pharmacia

3.2 Equipment and Software

3.2.1 Equipment

Centrifuges:

- Eppendorf 5415C
- Eppendorf 5804 R
- Hermle Z160M
- Sorvall RC5B
- Sorvall RC5B Plus

Thermocycler: Gen Amp PCR System 2400, Perkin Elmer

Eppendorf Thermomixer 5436

Rocking Platform, Biometra

Spectrophotometer: Ultrospec 2000, Amersham Pharmacia Biotech

Sonicator: Branson Sonifier 250

Aggregometer: Platelet Aggregation Profiler Model PAP-4, BioData Corporation

Fluorescence Scanner: Odyssey-Licor

UV-Transilluminator: TFX-35M, Life Technologies (Now Invitrogen)

CCD Video Camera Module XC-ST70

Power Supplies:

- Biometra Standard Power Pack P25
- Gene Power Supply GPS 200/400, Amersham Pharmacia Biotech

pH-Meter: PHM 92 LAB pH Meter, Radiometer

Speed Vac: Speed Vac® Plus SC 110A, Savant

Vortex: Vortex Genie 2, Scientific Industries

Developer: X-OMAT M35, Kodak

DNA Electrophoresis Chamber: Mini Sub DNA Cell, BioRad

Semi Dry Transfer Devise: Fast Blot B33, Biometra

Microscopes:

Axiovert 25, Zeiss

Axiovert 200, Zeiss

Microtiter Plates Counter: Wallac Victor^2 1420 MultiLabel Counter, Wallac

Cell Counter: Casy® Cell counter, Schäfer System

Confocal Laser Scanner (for microarray): ScanArray 4000, Perkin Elmer

Hybridization Station (for microarray): Amersham Pharmacia

3.2.2 Software

Imaging

Fast Capture Version 2.2.0, Fast Multimedia

Odyssey Version 1.0.58; © Li-Cor Bioscience

MetaMorph Version 4.6

NIH Scion Image

Cell Counter

Casy® 1 and Casy® Stat Version 2.1; © Schärfe System GmbH

Microtiterplate Reader

Wallac 1420 Version 2.0; © Wallac Oy

Microarrays

Acquisition: ScanAlyze; Stanford University

Analysis: GeneSpring; Silicon Genetics

4. Methods

4.1 Cell Culture

4.1.1 Isolation of mouse cardiac fibroblast.

Two 3-months-old mice of each phenotype ($VASP^{+/+}$ and $VASP^{-/-}$) were narcotized with ether. The hearts were excised, submerged in cold PBS and cut into pieces with a tissue chopper. The pieces were washed with Earl's buffer and cells were dissociated with 1mg/ml Collagenase/Dispase for 30 min at 37°C. After the incubation, the tissue pieces had settled down and the supernatant containing the isolated cells was spun at 800x *g* for 5 min. The pelleted cells were resuspended in DMEM, 10% calf serum and transferred to a 25 cm^2 culture flask. Every 3 days, the cells were trypsinized (0.1% trypsine), counted (CASY®1 cell counter) and transferred to a new flask at a density of $5x10^3$ cells/cm^2. After 3 to 4 weeks in culture, the isolated cells became spontaneously immortalized lines [86].

Phosphate-buffer saline (PBS)

140 mM NaCl

2,7 mM KCl

8,1 mM Na_2HPO_4

1,5 mM KH_2PO_4

pH 7,4

Earl's buffer

6,8 g/l NaCl

0,4 g/l KCl

0,125 g/l NaH2PO4

1 g/l Glucose

0,05 g/l Phenol Red

2,45 g/l Tris

pH 7,5

4.1.2 Cell Passage

Every 3 days cells from a 6-cm dish were washed once with PBS, trypsinized by adding 0,1% trypsine in PBS for a few minutes until the cells adopt a rounded shape. Then the trypsine solution was sucked out and cells were incubated for 1 or 2 min at 37ºC to allow to detach. Cells were resuspended in DMEM, 10% calf serum and counted with a CASY®1 cell counter. $2,5x10^3$ cells were then replated on 6-cm dishes containing 5 ml of DMEM, 10% calf serum.

4.1.3 Cell Counting

A volume of 100µl of the cell suspension was diluted in 10 ml PBS and counted with the CASY®1 cell counter as instructed by the manufacturer.

4.1.4 Cell Cloning

Cells were seed on 96-well plates at a density of 0,5 cells/well. Plates were controlled regularly until groups of growing cells were seen in some wells. Then cells were trypsinized from each well and seeded into 6-cm dishes. When they reached 80% confluence cells were passaged as usual.

4.1.5 Cell Freezing and Storage

Cells were trypsinized as described above, collected in DMEM with 10% calf serum, counted and pelleted. The pellet was resuspended in freezing medium to a final concentration of 10^6 cells/ml, and aliquoted into 1 ml cryotubes. The aliquots were stored over night at –80ºC and then in Liquid N_2.

Freezing Medium

10% DMSO in Fetal Calf Serum

4.1.6 Immunofluorescence

Cells were seeded at low density on coverslips washed with PBS containing 0.9 mM $CaCl_2$, 0.5 mM $MgCl_2$ and fixed with 3.7% formaldehyde in PBS for 20 min on ice. Cells were permeabilized for 5 min with 0.2% Triton X-100 in PBS at room temperature. After washing twice with PBS, cells were incubated with α-VASP antibody (M4 affinity purified, 1:500) 1 hour at 37°C in a moist chamber. The coverslips were washed twice with PBS and incubated with Cy2 anti-rabbit IgG and/or OregonGreen phalloidine (Molecular Probes) or Rhodamine phalloidine (Molecular probes) for 1 hour at 37°C in a moist chamber. Then the coverslips were washed, rinsed in water and mounted in Mowiol 4/88 solution. Samples were analyzed by a Leitz Aristoplan microscope and photographed with a Wild MPS46 camera (Leitz) or by an Axiovert 200 microscope connected to a digital camera.

4.1.7 Wound-Healing assay

Cells were seeded on glass coverslips or in 25 cm^2 culture flask and allow to grow until confluence with DMEM supplemented with 10% calf serum. Then, a scratch was made with a sterile pipette tip across the monolayer. Pictures of the migrating cells were taken at time 0 and 15 h after the scratch with a digital camera using MetaMorph 4.1 software

(Imaging System) connected to an Axiovert 25 microscope. Alternatively, cell migration was recorded by time-lapse video microscopy.

4.1.8 Cell adhesion assay

96-well plates were coated with Fibronectin, Collagen III or Vitronectin at different concentrations and incubated over night at 4°C. The wells were blocked with 1% BSA in PBS for 2 hours at room temperature, and washed twice with PBS. Prior the assay, cells were incubated for one hour with or without 100 µM 8-pCPT-cGMP. Cells were harvested with PBS/5 mM EDTA, counted, washed twice with serum-free DMEM containing 0.1% BSA, and resuspended at 10^5 cells/ml. 100 µl of the cell suspension was added to each well and allowed to attach for 30 min. Non-adherent cells were removed by washing twice with serum-free DMEM/1% BSA, and attached cells were fixed and permeabilized with 3 mg/ml Sigma 104 phosphatase substrat, 0,5% Triton X-100, 50 mM sodium acetate (pH 5,0) and incubated for one hour at 37°C. The reaction was completed by adding 50 µl of 1 N NaOH. Absorbance was measured at OD_{405} on a microtiter plate reader. A standard curve was set for each cell line.

4.1.9 Detachment

Detachment was followed under an Axiovert 25 microscope connected to a digital camera using MetaMorph 4.1 software (Imaging System). Cells seeded on dishes were carefully washed with PBS and treated for the time indicated with 0,1 % trypsine in PBS or PBS-EDTA solution. Pictures of the detaching cells were taken every minute after addition of the trypsine or EDTA solution.

4.1.10 Flow Cytometry analysis of β_1 and β_3 integrins

Cells were harvested with PBS/ 5 mM EDTA, counted and resuspended in PBS at 10^6 cells/ml. 10^5 cells were incubated with 0.05 µg/µl final concentration of FITC-conjugated hamster anti-rat CD29 or FITC-conjugated hamster anti-mouse CD61 monoclonal antibodies (PharMingen) for 10 min in the dark. The staining for ß3 and ß1 integrins was measured and analyzed by flow cytometry using a Becton Dickinson FACSCalibur.

4.2 DNA Manipulation

4.2.1 DNA Isolation.

Approximate 1 cm of the tail tip of an anesthetized mouse was cut and incubated with 500 µl of Proteinase K buffer containing 0,2 mg/ml Proteinase K over night at 55ºC with

gently agitation. 75 µl of 8 M potassium acetate and 500 µl Chloroform were added and samples were incubated 30 to 45 min at –20ºC. Then samples were centrifuged at full speed for 8 min, the aqueous phase was transferred to a new tube, and 2 volumes of ethanol p.a. were added and mixed 8 to 10 times by inversion. DNA was collected by centrifugation at 1700 x *g*, washed with 70% ethanol, dried at 50ºC for 5 min or at room temperature for 10 to 15 min. DNA was resuspended in 150 µl H_2O, $OD_{260/280}$ was measured and samples were diluted to 0,1 µl/µg and stored at 4ºC.

Proteinase K buffer:

0.5 % (w/v) SDS
50 mM Tris-HCl pH 8.0
3,75 mM EDTA
0,1 M NaCl

4.2.2 DNA precipitation

Two volumes of ethanol (96 %) and 3 M sodium acetate pH 5,2 were added to the DNA sample and centrifuged at full speed in a microcentrifuge for 20 to 30 min The supernatant was discarded and the pellet washed with 75% ethanol. After 10 min of centrifugation the supernatant was discarded and the tube was shortly centrifuged to collect the rest of ethanol. Samples were dried 2 to 3 min (Speed-vac) and the precipitated DNA was resuspended in an appropriate volume of water.

4.2.3 Genotyping.

Genotyping of VASP $^{-/-}$ and VASP $^{+/+}$ mice was performed by PCR.

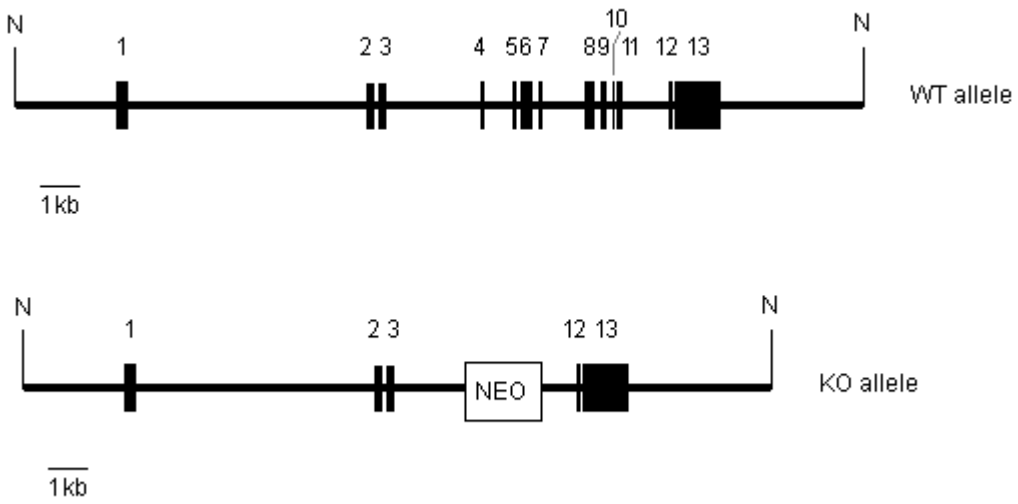

Figure 9: Scheme of VASP$^{+/+}$ and VASP$^{-/-}$ alleles. In the VASP$^{-/-}$ allele exons 4 to 11 are replaced by a Neomycin resistance cassette.

For the VASP$^{+/+}$ PCR the GIK 269 and the GIK 270 primers (GIK 296: 5'-TTA GCT TGG TTT GGG GAC TGA ACC AGC CTC CTT TC-3'; GIK 270: 5'-CAG CCA CTC CCT GGT ACT TCC TTA CCT TGC TCA C-3') were used. These primers hybridize in the intron before exon 5 and in exon 6 respectively. This region has been replaced by the Neo Cassette in the VASP$^{-/-}$ mice (see Figure 5).

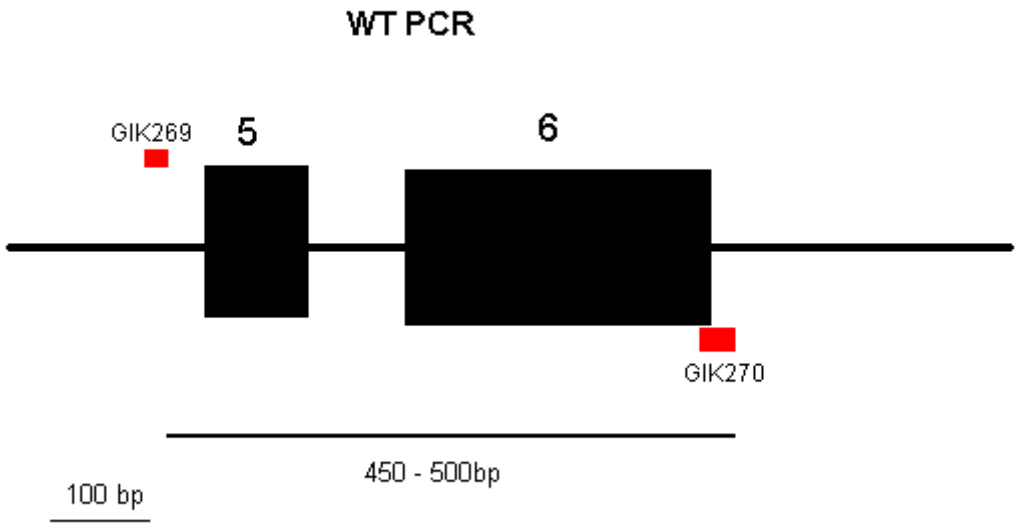

Figure 10: Detail of exons 5 and 6 where the primers for the wild type PCR hybridize.

The VASP$^{-/-}$ PCR was performed using the GIK 273 (sense) and GIK 274 (anti-sense) (GIK 273: 5'-CGA ATA GCC TCT CCA CCC AAG CGG CCG GCG AAC-3'; GIK 274: 5'-GGC CAG CAG AAC AGT ATT GGA GAA CTA CCA GG-3') primers that hybridize in the Neo Cassette and in the VASP intron between the Neo Cassette and exon 12 respectively (see Figure 7).

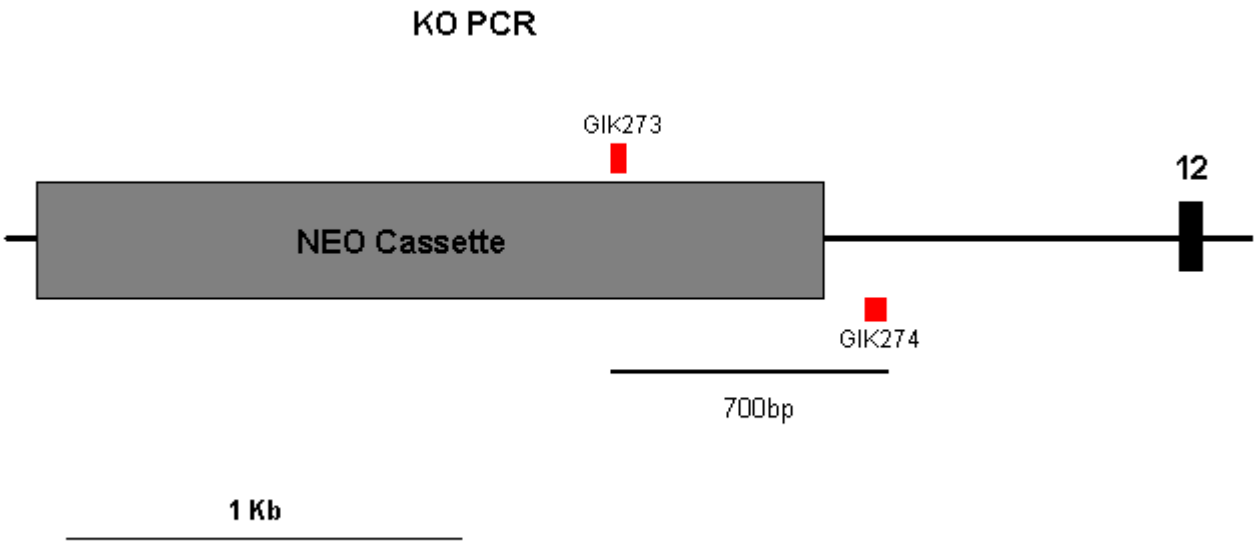

Figure 11: Detail of Neo Cassette region where the primers for the knock out PCR hybridize.

In both cases, 500 ng of genomic DNA were mixed with Taq PCR Master Mix (Qiagen) and 250 ng of each primer as follows:

	Volume	**Stock Solution**
Genomic DNA	5 µl (500 ng)	0,1 µg/µl
Taq PCR Master Mix	15 µl	2x
Primer Set (GIK273/GIK274 or GIK269/GIK270)	5 µl (250 ng of each primer)	0,1 µg/µl
H_2O	5 µl	
Final Volume	30 µl	

The PCRs were run according to the following programs:

VASP $^{+/+}$ PCR		
Temperature	**Time**	
95 ºC	5 min	
95 ºC	1 min	30 cycles
65 ºC	1 min	
72 ºC	1 min	
72 ºC	10 min	
4 ºC	∞	

VASP$^{-/-}$ PCR		
Temperature	**Time**	
95 ºC	5 min	
95 ºC	1 min	30 cycles
65 ºC	1 min	
72 ºC	2 min	
72 ºC	10 min	
4 ºC	∞	

The PCR products (20 to 30 µl of the sample) were analyzed on 1,2% agarose gels containing Etidium Bromide, and compared to size markers.

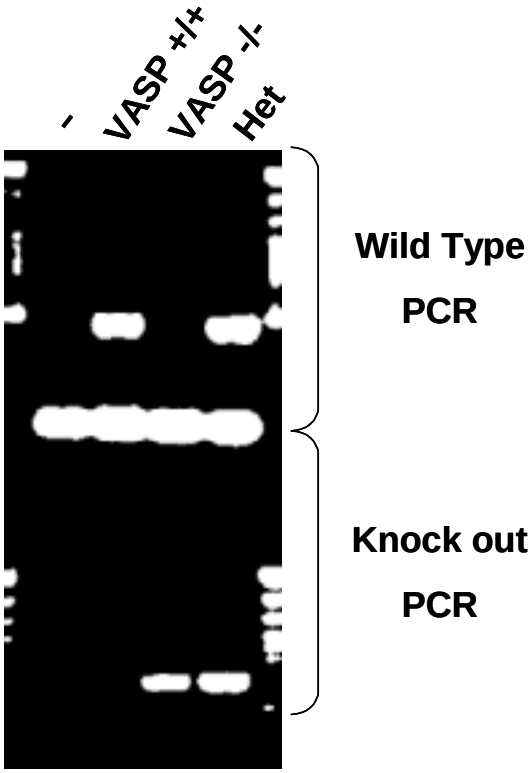

Figure 12: Example of genotyping by PCR. Upper part of the gel shows the result of a VASP$^{+/+}$ PCR (Wild type PCR) The lower part represents the VASP$^{-/-}$ PCR. Het: Heterocygotes. First line: control without template.

4.2.4 DNA Electrophoresis

For preparation of gels 1% w/v agarose was dissolved in TAE buffer by boiling for 3 min in microwave oven (450 Watts setting). When the agarose solution had cooled down to approximately 60ºC, Etidium Bromide was added and the solution was poured into gel chambers (BioRad). Samples disolved in DNA Loading Buffer (MBI Fermentas) were load into the slots of the gels and subjected to a constant voltage of about 100 V. Bands were visualized by exposing the gel to UV light and pictures were taken with a CCD Video Camera using the Fast Capture software (Version 2.2.0).

TAE Buffer

0,04 M Tris Acetate

1 mM EDTA

4.2.5 Stable transfection of mouse cardiac fibroblasts

The VASP deficient mice were generated by introducing in the VASP gene by homologous recombination the neomycin-resistance gene in the inverted position, between exons 3 and 12. Although the probability of having the neomycin resistance expressed in these cells is very low due to the inverted position in the genome, the vector used for stable transfection of a transgene in $VASP^{-/-}$ cells contains a hygromycin resistance gene, instead of the classic neomycin resistance gene, in order to avoid any interference with the neomycin resistance during the selection. $VASP^{-/-}$ cells were transfected with a vector containing the full-length human VASP cDNA and hygromycin resistance gene using FuGENE™-6 transfection reagent. One day after transfection cells were exposed to the selective medium (DMEM, 10% calf Serum, 50 µg/ml Hygromycin B). Transfected cells were maintained in selective medium routinely and transferred to DMEM 10% calf serum one day before experiments.

4.3 RNA Manipulation

4.3.1 RNA isolation from Mouse Cardiac Fibroblasts (MCFB)

Cells were seeded in 15 cm-dishes some days before the experiment in order to have a subconfluent culture when the RNA should be isolated. Cell plates were washed twice with PBS and 7,5 ml of Trizol was add to each plate. Cells were harvested with a rubber policeman in 10 ml tubes and incubated for 10 min at room temperature. Then 2 ml of Chloroform were added to each tube and immediately mixed vigorously. Samples were incubated 2,5 min at room temperature before they were centrifuged at 12000 x *g* (rotor SS34) for 15 min at 4ºC. The upper phase was transferred to a new tube, 3,75 ml

isopropanol was added and after 10 min of incubation RNA was collected at (12000 x *g*) 10 min at 4ºC. The RNA pellet was washed with 7,5 ml of 75% cold Ethanol. For this purpose sample was mixed on a vortex®, centrifuged for 5 min at 6000 x *g* (rotor SS34) at 4ºC and the pellet was resuspended in water. In order to eliminate any traces of DNA, samples were treated with 2 units DNase I in 0,1 volume DNase I buffer (Ambion) for 30 min at 37ºC. To stop the reaction 0,1 volume of DNase inactivation buffer (Ambion) was added and after 2 min samples were centrifuged at full speed in a tabletop centrifuge for 1 min The supernatant, containing the RNA, was transferred to a new tube and stored at –80ºC.

4.3.2 Northern Blotting.

Northern blots (Formaldehyde-Based System Northern Max™; Ambion) were done according to the manufacturer's instructions. After transfer, nylon membranes were crosslinked (Stratalink), prehybridized with DIG Easy Hybridization Buffer (Roche) at 50°C for 30 min, and hybridized over night at 50°C with 5 µl of probe in 10 ml of DIG Easy Hybridization Buffer. Probes for Evl and GAPDH were obtained by RT-PCR using the following primers: 5' -GAGCAGCAGCACCGCCAGGAG-3'; 5'-GGACAGCAACGAGGACACAGG-3' for Evl (Product: 590 bp) and 5'-TTAGCACCCCTGGCCAAGG-3'; 5'CTTACTCCTTGGAGGCCATG-3' for GAPDH (Product: 540 bp). The RT-PCR product was used as a template for a PCR with DIGlabeled dNTPs (Roche) and the same primers.

Membranes were washed twice with 2 x SSC (300 mM NaCl; 30 mM tris-Na-Citrate, pH 7) at room temperature for 5 min and twice with 0.1 x SSC, 0,1% SDS for 15 min at 68°C. The DIG Detection System (Roche) was used for detection.

SSC Buffer (2x)

300 mM NaCl

30 mM tris-Na-Citrate

pH 7

4.3.3 RT-PCR

RNA was isolated as described above and RT-PCR was performed using the One Step RT-PCR kit from Qiagen according to manufacturer's instructions. A touchdown program was used for the cycles:

	Temperature (ºC)	Time	Cycles
RT-PCR	50	30 min	
	95	15 min	
Amplification	94	2 min	
	94	30 sec	
	65	30 sec	5 cycles
	72	1 min	
	94	30 sec	
	60	30 sec	5 cycles
	72	1 min	
	94	30 sec	
	55	30 sec	20 cycles
	72	1 min	
	72	2 min	
	4	∞	

Results were analyzed in 1% agarose gels containing Etidium Bromide, as described for DNA electrophoresis (see section 4.2.4.).

4.3.4 Microarrays

Microarray analysis were performed by Dr. Susanne Kneitz at the Microarray Facility of the Interdisziplinäres Zentrum für Klinische Forschung (IZKF), University of Würzburg.

Mouse cDNA arrays with 4000 randomly selected known genes and 500 ESTs were used. Furthermore the array contained GAPDH (spotted 64x) and 16 commercially available standards (Score Card, Amersham Pharmacia) for spot finding and scanning.

RNA extraction was performed as described under 4.3.1 (RNA isolation from MCFB).

CyDye-labeled first strand cDNAs were generated using either Cy3 or Cy5 labeled dCTP (see 4.3.4.1). The Cy3 and Cy5 labeled probes were mixed and hybridized to the array over night. After washing to remove the unhybridized probe, the fluorescent signals for both probes were read into two different image files with a confocal laser scanner (ScanArray 4000).

Samples from $VASP^{+/+}$, $VASP^{-/-}$ and reconstituted cells (RecVASP) were analyzed by this method. RecVASP and the $VASP^{-/-}$ cells were both compared to the $VASP^{+/+}$ cells for the analysis of the data.

Data were acquired using a freely available program from M. Eisen, Stanford University (ScanAlyze). Afterwards, the data sets were normalized by setting the average of the logarithmic intensity values for each probe to 0 and standard deviation to 1. Relative intensities ($VASP^{-/-}$/$VASP^{+/+}$ or RecVASP/$VASP^{+/+}$) were calculated.

For data analysis the program GeneSpring (Silicon Genetics) was used. Differences in expression were detected by the 'drawable gene' function. This tool allows to define an intensity profile. The program then finds genes, which match this profile with a certain, user defined correlation. In this case, expression patterns of $VASP^{-/-}$ cells were supposed to be up or down regulated as compared to those from $VASP^{+/+}$ cells, whereas the reconstituted cells were not allowed to show any difference to $VASP^{+/+}$ cells. A correlation factor of 0.975 was used.

4.3.4.1 Labelling first-strand cDNA with Cy3- or Cy5-nucleotides:

This protocol for the preparation of labelled cDNA has been accomplished using the CyScribe First-Strand Kit supplied by Amersham Pharmacia Biotech.

Total RNA isolated from MCFB was mixed with random nonamers and anchored oligo(dT) as follows:

- total RNA, 10µg – 20 µg	X µl
- random nonamers	1 µl
- anchored oligo(dT)	1 µl
- water (supplied or DEPC treated)	ad 11 µl

After mixing gently by pipetting up and down, samples were incubated for 5 min at 70° C and then kept for 10 min at room temperature. Then samples were spun down for 30 s and put on ice. For first strand cDNA synthesis, dCTP CyDye-labeled nucleotides and CyScript reverse transcriptase were added to the samples as follows:

- 5 x CyScript buffer	4 µl
- 0.1 M DTT	2 µl
- dCTP nucleotide mix	1 µl
- dCTP CyDye-labeled nucleotide	1 µl
- CyScript reverse transcriptase	1 µl
Total	20 µl

Samples were mixed vigorously, spun 30 s and incubated for 1,5 h at 42° C.

4.3.4.2 Purification of labeled cDNA

RNA was degradated by addition of 2 µl of 2,5 M NaOH and by incubating the samples for 15 min at 37° C in water bath. Then, 10 µl of 2 M HEPES free acid were added, samples were mixed and spun down 30 s.

Nucleotides and short oligomers were removed by passage through AutoSeq G-50 columns.

4.3.4.2.1 Preparation of the AutoSeq G-50 columns

The resin was resuspended in the column by vortexing gently. The cap was loosened a quarter of a turn and the bottom closure was snapped off. The column was placed in a 2 ml tube as support and spun (exactly) for 1 min at 2000 x *g*. Columns were used immediately after preparation to avoid drying of the matrix.

4.3.4.2.2 Purification of the labeled cDNA

An AutoSeq G-50 column was placed in a new tube and the sample was slowly applied to the center of the angled surface of the compacted resin bed, being careful not to disturb the resin. After 1 min centrifugation at 2000 x *g* the flow through was collected and the column was discarded.

4.3.4.3 Microarray hybridization

For dual color hybridization Cy3- and Cy5-labeled cDNAs were combined into one tube and mixed with:

labeled cDNA	121 µl
PolyA (0.5 mg/ml)	1.5 µl
Formamide	62,5 µl
5x SSC	62,5 µl
10% SDS	2,5 µl
H_2O	ad 250 µl

After 5 min incubation at 95° C samples were spun for 2 min to cool down and to collect the condensate. Samples should not be put on ice. If necessary, the probe can be kept at 70° C until the slide is ready.

Slides should be prehybridized with Prehybridization Solution

Prehybridization Solution

25% formamide

5X SSC

0,1% (w/v) SDS

1% (w/v) BSA (optional, to reduce background)

The prehybridization solution was warmed on a hot plate to 45-50° C with constant stirring. The slide was put into the prehybridization buffer for 45 min at 42° C, then rinsed with distilled water and centrifuged in a 50 ml tube until it dried not more than 800 rpm for 5 min.

4.3.4.4 Hybridization

For hybridization a hybridization station (Amersham Pharmacia Biotech) was used.

4.3.4.5. Scanning

For scanning a ScanArray4000 (Packard Biochip) was used.

4.4 Protein Manipulation

4.4.1 Determination Protein Concentration

Protein concentrations were determinated using the DC BioRad Protein Assay. This assay is based in the Bradford method for determination of protein concentration. BSA standard solutions and samples (0; 0,25 ; 0,5 ; 0,75 ; 1 µg/µl - 25 µl each) were mixed with the reagent as follows:

Standard or Sample:	25 µl
Reagent A‘:	125 µl
Reagent B:	1 ml

(Reagent A‘ = 20 µl Reagent S in 1 ml reagent A)

Samples were mixed vigorously and after 15 min incubation at room temperature the OD_{750} was measure. Absorbance obtained was correlated to the protein concentration according to the standard values.

4.4.2 SDS-Polyacrylamide Gel Electrophoresis (PAGE) and Immunoblotting (Western Blot)

Sodium dodecyl sulfate polyacrylamide gel electrophoresis (SDS-PAGE) was performed using 12% or 8% (w/v) polyacrylamide separating gels [87]. Proteins were loaded into the slots of the gel and separated with a current of 100 V. Then, proteins in the gel were transfer onto nitrocellulose membranes with a semi-dry blotter at 300 mA for 30 min according to manufacturer’s instructions.

After the transfer, membranes containing the proteins were stained with Ponceau dye and subsequently blocked with 2% milk in PBS for 30 min. Membranes were incubated 2 hours to overnight with the first antibody freshly diluted in TBS-T-2% milk. Then, membranes were washed 3 times with TBS-T-2% milk, and incubated with the secondary antibody

(diluted in TBS-T-2% milk). According to secondary antibody used, Western blots were either analyzed using the enhanced chemo luminicence (ECL, Amersham) detection kit, or by scanning with the Odyssey scanner (Licor).

Separating Gels

	Stock	**12%**	**8%**
acrylamide/bisacrylamide	30% (w/v) (29:1)	3,2 ml	2,145 ml
Tris-HCl (pH 8.6)	1 M	3 ml	3 ml
SDS	10% (w/v)	0,08 ml	0,08 ml
APS	10% (w/v)	0,075 ml	0,075 ml
H_2O		1,64 ml	2,7 ml
TEMED	99%	0,005 ml	0,005 ml
Total Volume		8 ml	8 ml

Stacking gel

	Stock	**4%**
Acrylamide/Bisacrylamide	30% (w/v) (29:1)	0,65 ml
Tris-HCl (pH 6,8)	1 M	0,65 ml
SDS	10% (w/v)	0,05 ml
APS	10% (w/v)	0,025 ml
H_2O		3,6 ml
TEMED	99%	0,005 ml
Total Volume		5 ml

Sample Loading buffer (3x)

150 mM Tris HCl, pH 6,8

300 mM DTT

6% (w/v) SDS

0,03% (w/v) Bromophenol Blue

30% glycerol

Electrophoresis buffer

25 mM Tris, pH 8,6
192 mM glycin
0,1% (w/v) SDS

Transfer buffer

25 mM Tris, pH 8,3
192 mM glycin
20% (v/v) methanol

TBS-T

25 mM Tris , pH 7.5
140 mM NaCl
2,7 mM KCl
0,01% Tween 20

4.4.3 Two-Dimensional Gel Electrophoresis

Cells were harvested in Laemmli SDS sample buffer and proteins were precipitated and SDS was removed with chloroform/methanol extraction. Isoelectric focussing for two-dimensional gel electrophoresis was performed using the Protean-IEF cell (BioRad) according to the manufacturer's instructions. 100 µg of protein were solubilized in 350 µl of solubilization buffer. Cell extracts were loaded on a 17 cm ReadyStrip IPG strip (linear pH range 3-10) (BioRad) during 16 - 24 h active rehydration at 50 V. Focusing was for 30 min at 250 V, 30 min at 500 V, followed by a linear increase to 4000 V within 5 h, and a final step at 4000 V for 16 h. After equilibration in equilibration buffer, the strips were immediately applied to vertical SDS gels (10% acrylamide/bis-acrylamide). Gels were then transferred onto nitrocellulose membranes and Pak 1 was detected by immunoblotting with N20 antibody.

Solubilization buffer

7 M urea
2 M thiourea
4% (w/v) CHAPS
15 mM dithiothreitol
0,5% (w/v) Bio-Lyte
3/10 Ampholyte (pH range 3-10)
10 nM Okadaic acid

Equilibration Buffer

50 mM Tris HCl pH 8.8

6 M urea

30% (w/v) glycerol

2 % (w/v) SDS

4.4.4 Preparation of GST-PBD Sepharose Beads for Rac Pull Down assay

Bacteria containing the expression plasmid for GST fused to the Rac/Cdc42 binding domain of Pak (GST-PBD) were cultured over night in LB-Ampicillin medium at 37ºC with an agitation of 200 rpm until they reached an OD_{600}= 1 (log phase). The expression of the fusion protein was induced by addition of 0,5 mM IPTG, 3 h incubation at 37ºC. Bacteria were pelleted by centrifugation at 5000 x *g* for 15 min at 4ºC and resuspened in PBS. Lysozyme was added to a final concentration of 1 mg/ml and lysis was carried out for 30 min on ice. Then 10 ml of 0,2% (w/v) Triton X-100 in PBS and 5 µg/ml each of DNase and RNase were added per 100 ml of original culture medium. After 10 min incubation at 4ºC the suspension was centrifuged at 3000 x *g* for 30 min at 4ºC in order to pellet intact cells membranes rest and chromosomal DNA. The supernatant containing the expressed GST-PBD was collected and 1 mM DTT was added. A 50% (v/v) slurry of glutathion sepharose was added. The GST-PBD was allowed to bind to the glutathion sepharose beads for 30 min at room temperature with gentle agitation. The sample was then centrifuged at 500 x *g*, the supernatant was removed and the GST-PBD sepharose beads were washed three times with PBS. Finally the beads were resuspended in one volume of PBS and stored in 50 µl aliquots at –80ºC.

LB-medium

1% (w/v) Bacto-tryptone

0,5% (w/v) Bacto-yeast extract

1% (w/v) NaCl

50µg/ml Ampicillin

4.4.5 Determination of Rac activation (Rac Pull Down Assay)

Activated Rac was determined as described [88]. Cells were starved for 24 h with serum free DMEM and stimulated with 5 ng/ml of PDGF-BB [89] for the times indicated. After stimulation, cells were washed twice with ice cold PBS and harvested in 2-fold lysis buffer. After lysis for 15 min at 4°C, the samples were centrifuged at full speed in a microcentrifuge at 4°C, and 50 µl of the supernatant was used to estimate the total amount of Rac. The rest of the supernatant was mixed with approximately 20 µg of the Rac-GTP binding domain of PAK as a GST fusion protein (GST-PBD for 45 min at 4°C. Then the samples were

centrifuged at 320 x *g* at 4°C and the beads were washed 3 times with washing buffer. Finally, the pelleted beads were resuspended in 15 µl of Laemmli sample buffer and analyzed by 12% SDS-PAGE using an anti-Rac antibody. As controls, unstimulated cells were lysed and clarified as described above. 0.1 volume of 150 mM EDTA was added to the samples, immediately followed by an addition of 200 µM GTPγS to the positive control or 1 mM GDP to the negative control. The samples were incubated for 15 min at 30°C. Then reactions were stopped by addition of $MgCl_2$ to a final concentration of 60 mM and transfer to 4°C. The samples were then incubated with the GST-PBD construct coupled to GSH-sepharose beads, washed and analyzed as described above. The pulled down material and aliquots of the supernatants were also analyzed by SDS-PAGE to check for the efficiency of the method.

MCFB Lysis buffer (2x)

50 mM Tris-HCl, pH 7,5
10 mM $MgCl_2$
200 mM NaCl
2% (v/v) Nonidet P-40
10% (w/v) glycerol
0,5% (w/v) sodium deoxicholate
Proteases inhibitors (Complete Mini®, Roche)

Platelet Lysis buffer (2x)

50 mM Tris-HCl, pH 7,2
1% (v/v) Triton X-100
0,5% (w/v) sodium deoxicholate
0,1% (w/v) SDS
500 mM NaCl
10 mM $MgCl_2$
Proteases Inhibitors (Complete Mini®, Roche)

Washing buffer

50 mM TrisCl, pH 7,5
10 mM $MgCl_2$
150 mM NaCl
1% (v/v) Triton X-100
5 mM EGTA
Proteases inhibitors (Complete Mini®, Roche)

4.4.6 Pak In-Gel Kinase Assay

MCFB samples, either unstimulated or stimulated 2 min with FCS, were loaded on an 8% SDS-polyacrylamide gel containing 1 μg/ml Myelin basic protein (MBP) dissolved in the gel mixture. After electrophoresis the gel was soaked twice in Buffer 1 at room temperature for 40 min and 20 min, respectively. The gel was then transferred to Buffer 2 for 2 h, with a buffer change after one hour. Then, the gel was incubated in Buffer 3 for 2 h, changing it again after one hour. Thereafter, the gel was soaked overnight at 4ºC in Buffer 4. The next morning, the gel was soaked in new Buffer 4 for a total of 90 min, with buffer changes every 30 min. After this, the gel was incubated, first 30 min at room temperature, and then 30 min at 30ºC in Buffer 5 (Kinase Buffer). In order to perform the in-gel kinase assay, 25 μM ATP and 10 μl [P^{32}]ATP (Amersham, Stock: 4500 Ci/mmol) were added to the Kinase Buffer, and the gel was incubated for other 30 min at 30ºC, with gentle agitation. After the reaction, the gel was incubated 6 hours in Wash Buffer, changing the solution frequently, and finally washed overnight at room temperature. The next morning the gel was stained with Coomasie Blue, dried, and exposed to Kodak X-OMAT film overnight.

Buffer 1

20% (v/v) propanol
50 mM Tris-HCl pH 7,5

Buffer 2

50 mM Tris-HCl pH 7,5
5 mM 2-Mercaptoethanol

Buffer 3

50 mM Tris-HCl pH 7,5
6 M Guanidinium

Buffer 4

50 mM Tris-HCl pH 7,5
0,04% Tween 40
5 mM 2-Mercaptoethanol

Buffer 5 or Kinase Buffer

10 mM HEPES pH 8.0
1 mM DTT
0,1 M EGTA
1 mM EDTA
5 mM $MgCl_2$

Wash Buffer

5% TCA

1% Na-Pyrophosphate

Coomasie Blue Staining Solution

0,25 g Coomasie Brilliant Blue R250

90 ml MeOH:H_20 (1:1)

10 ml glacial acetic acid

Coomasie Destaining Solution

20% MeOH

30% glacial acetic acid

4.5. Blood Manipulation

4.5.1 Blood sampling (mice)

Adult mice were narcotized with ether, a midline abdominal incision was made and the organs were moved to one side to facilitate the location of the inferior *Vena cava*, which is then punctured using a 0.60 mm needle [90]. The Blood sample is withdrawn into a 2 ml plastic syringe containing 1/10 volume of CCD buffer as anticoagulant. 1 to 2 ml of blood can be obtained from one adult mouse.

Alternatively, blood from the retroorbital veins was taken with a capillary from narcotized mice into a tube containing 1/10 volume of CCD buffer. With this method, only a maximum of 700 µl of blood can be taken per mouse. However, the animal survives and blood can be taken again one week later (4 to 5 times from the same mouse).

CCD Buffer

100 mM tri-Na-citrate, pH 6.5

7 mM citric acid

140 mM glucose

0,5 mM acetylsalicylic acid

1 mM EGTA

4.5.2 Preparation of Washed Mouse Platelets.

Blood from 3 to 4 mice was pooled for each experiment and diluted with ½ volume of Hepes Tyrode Buffer pH 6.3 [66]. Apyrase was added to a final concentration of 1 Unit/ml and centrifuged at 200 x *g* for 8 min at 37ºC. The upper layer (platelets rich plasma, PRP) was transferred to a second tube and centrifuged at 1000 x *g* for 5 min at 37ºC. The pelleted platelets were then washed by resuspension with Hepes-Tyrode buffer pH 6.3 and centrifuged again at 1000 x *g* for 5 min. Finally, the pelleted platelets were resuspended at a density of approximately $1x10^9$ platelets/ml in Hepes-Tyrode Buffer containing 2 mM Ca^{2+}, pH 7,3. Platelets were counted using a Neubauer chamber.

Hepes-Tyrode Buffer (without Ca^{2+}) pH 6,3

137 mM NaCl
2 mM KCl
0,3 mM NaH_2PO_4
12 mM $NaHCO_3$
1 mM $MgCl_2$
5,5 mM Glucose
5 mM Hepes sodium salt
0,35% (w/v) BSA

Hepes-Tyrode Buffer (with Ca^{2+}) pH 7,3

137 mM NaCl
2 mM KCl
0,3 mM NaH_2PO_4
12 mM $NaHCO_3$
1 mM $MgCl_2$
2 mM Ca^{2+}
5,5 mM Glucose
5 mM Hepes sodium salt
0,35% BSA

4.5.3 Preparation of Washed Human Platelets.

Venous blood from healthy volunteers was collected into a tube containing CCD Buffer (see 4.5.1) with 15 mM EGTA. Platelet rich plasma (PRP) was obtained after centrifugation of whole blood at 300 x *g* in a swinging bucket rotor for 20 min. PRP was incubated for 10 min at room temperature. Platelets were pelleted by centrifugation at 400 x *g* for 10 min, resuspended in resuspension buffer at a final concentration of $2x10^8$ platelets/ml and left for 20 min at room temperature prior to use.

Resuspension Buffer pH 7,4

145 mM NaCl

5 mM KCl

1 mM $MgCl_2$

10 mM Hepes

10 mM Glucose

4.5.4 Stimulation of Washed platelets

Platelets were preincubated for 20 min (unless otherwise indicated) with or without cGMP or cAMP analogs at 37ºC. Then 300 µl of the platelet suspension was transferred to a glass tube with constant stirring in an aggregometer to monitor aggregation of the sample. 3 µl of U46619 (Thromboxan A_2 (TxA_2) analog) (final concentration 1 µM) was added for the indicated time and the stimulation was stopped by adding 300 µl of 2x cold platelet lyses buffer (see 4.4.5, Determination of Rac activation). Samples were immediately transferred to ice.

4.5.5 *In vivo* fluorescence microscopy

(By Dr. Massberg, Deutsches Herzzentrum und 1. Medizinische Klinik, Klinikum rechts der Isar, Technische Universität München)

Platelets isolated from $VASP^{-/-}$ or $VASP^{+/+}$ mice as described [91], were labeled ex vivo with 5-carboxyfluorescein diacetat succinimidyl ester (DCF). Fluorescent platelets (2 x 10^8/250µl) were infused intravenously via polyethylene catheters (Portex, Hythe, England) implanted into the right jugular vein of $VASP^{-/-}$ or $VASP^{+/+}$ recipient mice and were visualized in situ by *in vivo* video microscopy of the right common carotid artery. Platelet endothelial cell interactions were monitored using a Zeiss Axiotech microscope (20 x water immersion objective, W 20x/0.5, Zeiss) with a 100 W HBO mercury lamp for epi-illumination. All videotaped images were evaluated using a computer-assisted image analysis program (Cap Image 7.1, Dr. Zeintl, Heidelberg). The number of adherent platelets was assessed by counting the cells that did not move or detach from the endothelial surface within 10 seconds.

4.5.6 Assessment of platelet adhesion following vascular injury – inhibition of platelet adhesion by nitric oxide

(By Dr. Massberg, Deutsches Herzzentrum und 1. Medizinische Klinik, Klinikum rechts der Isar, Technische Universität München)

Wild type mice were anesthetized by intraperitoneal injection of a solution of midazolame (5 mg/kg body weight, Ratiopharm, Ulm), medetomidine (0.5 mg/kg body weight, Pfizer, Karlsruhe) and fentanyl (0.05 mg/kg body weight, CuraMed Pharma GmbH, Munich). Polyethylene catheters (Portex, Hythe, England) were implanted into the right jugular vein. The right common carotid artery was dissected free and ligated vigorously near the carotid bifurcation for 5 min to induce vascular injury. Fluorescent wild type or $VASP^{-/-}$ platelets (2 $x10^8$/250 µl) were preincubated at room temperature for 5 min with either PBS (control) or the NO-donor spermine-NO (Alexis, Grünberg; 100 nM final concentration). After preincubation, the samples were prestimulated with 0.2 U/ml murine thrombin (Sigma) for 5 min (at this concentration of thrombin, platelets were preactivated but do not aggregate). Subsequently, the fluorescent platelets were infused intravenously and platelet adhesion to the injured carotid artery was monitored *in situ* by *in vivo* video microscopy. Tethered platelets were defined as all platelets establishing initial contact with the injured vessel wall, followed by slow surface translocation (at a velocity significantly lower than the centerline velocity) or by firm adhesion; their numbers are given as cells per mm^2 endothelial surface. The number of adherent platelets was assessed by counting the cells that did not move or detach from the endothelial surface within 10 seconds.

5. Results

5.1 Mouse Cardiac Fibroblast (MCFB)

5.1.1 Establishment of a mouse cardiac fibroblast cell line

In order to study in more detail the role of VASP, mouse cardiac fibroblast cell linee were established from both VASP-wild type and VASP-deficient adult mouse hearts.
When cells from normal mammalian tissues (that means not from tumors) are cultured in standard conditions *in vitro* they usually can be kept in culture for only a limited number of cell division cycles (about 50 for human fibroblasts and 5 - 10 for mouse fibroblast). Thereafter, they stop dividing and die. This process is called *cellular or replicative senescence*. However, during the propagation of some cell cultures, especially those derived from rodents, a few cells often arise that are able to escape senescence and divide indefinitely [92,93]. The immortal cells that overcome senescence are defined as a *cell line*. Although these immortal cells resemble normal cells in most aspects, the fact that they can divide indefinitely is reflecting one or more mutations that have altered their proliferative properties [93]. Nevertheless, cell lines are used widely for cell biology studies because they provide a source of standardized and genetically homogenous cells.

This was the strategy used to establish a mouse cardiac fibroblast (MCFB) cell line from $VASP^{+/+}$ and $VASP^{-/-}$ mice [86]. As described in the Materials and Methods section, cells isolated form the mouse heart were counted after splitting and were seeded in a new dish at a density of 5×10^3 cells/cm^2. With this data the Cumulative Passage Doublings (CPD) was calculated as follows:

$$\Delta n_t = \frac{ln\,(Nt) - ln\,(No)}{ln\,(2)}$$

No= number of cells seeded on a dish
Nt= number of cells counted at passage number t

$$CPD = \sum \Delta n$$

A graphical representation of cell number at every passage vs. CPD allows visualizing how the primary cells go into a senescent period after 4 passages and then some of them can divide indefinitely as a cell line (compare the theoretical curve [93] with the one obtained for the $VASP^{+/+}$ MCFB in figure 13) The cell line was considered established when Δn became constant.

A.

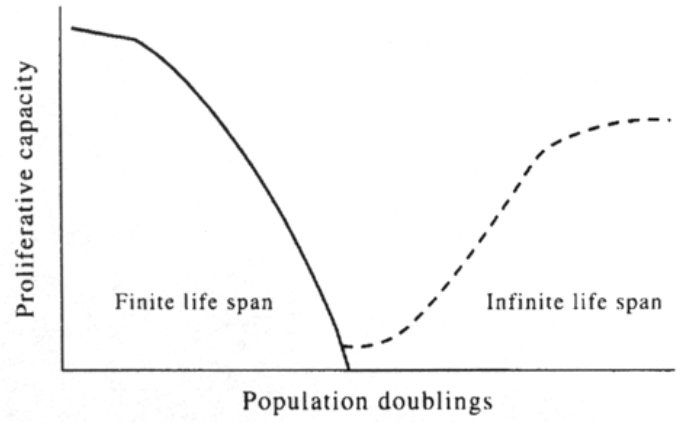

B.

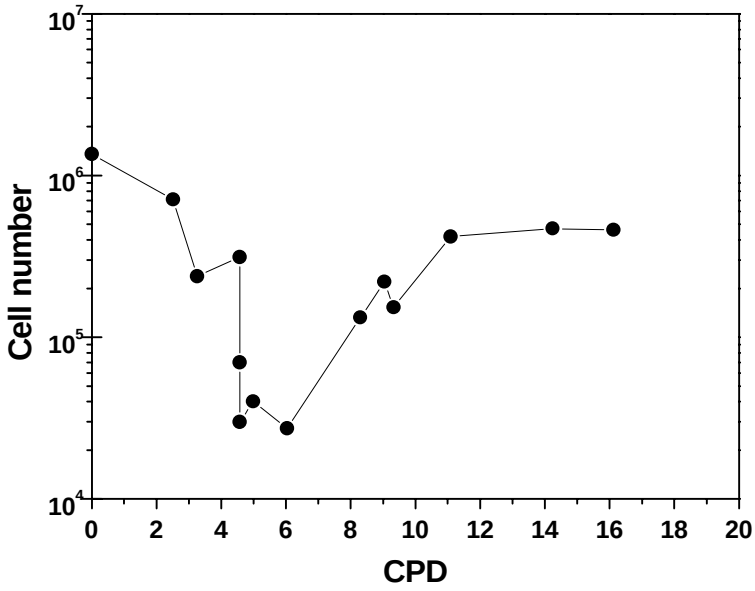

Figure 13: A. Replicative Senescence, theoretical curve. The proliferative capacity of most somatic mammalian cells declines more or less exponentially with each doubling (finite life span). Cells from many rodent species may spontaneously escape senescence (infinite life span) [93] **B. Curve showing the cell number vs. CPD for $VASP^{+/+}$ cells.** A similar curve was obtained for $VASP^{-/-}$ cells.

DMEM and McCoy 5A medium as well as fetal calf serum versus supplemented calf serum were tested in order to find the best condition for the culture of this cell lines. As

shown in figure 14, DMEM (high glucose) combined with supplemented calf serum was the best combination tried and was used within the whole study unless stated otherwise.

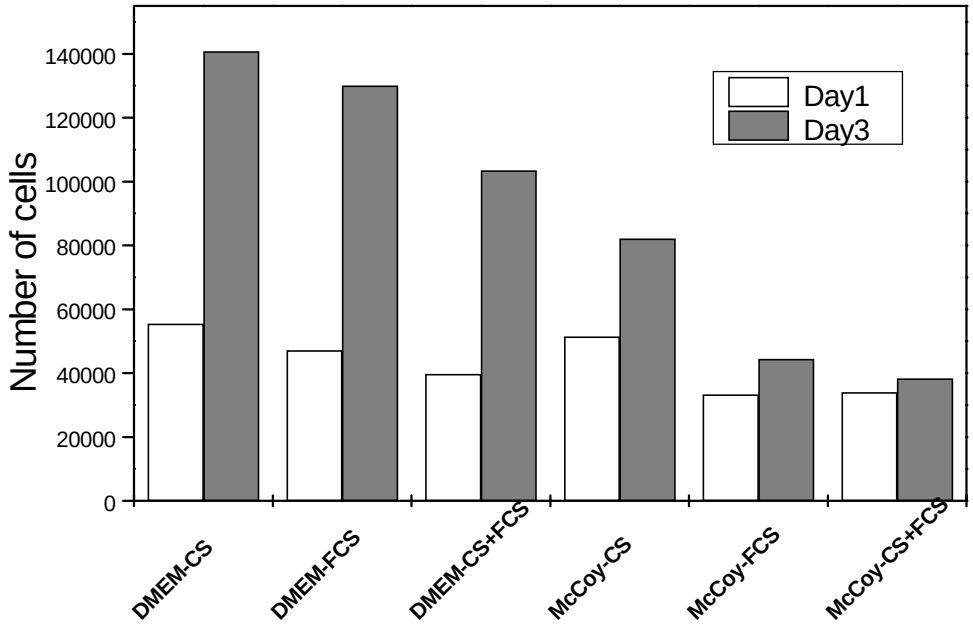

Figure 14: Selection of the most convenient media for MCFB cells. Proliferation of cells during 3 days was investigated using different media. Assays were done on wild type cells. CS: calf serum; FCS: fetal calf serum.

5.1.2 Mena and Evl expression are not up- or down- regulated in VASP$^{-/-}$ cells

The mammalian Ena (Mena), the Ena/VASP like protein (Evl) and VASP share the same domain structure [6,9]. It has been shown that VASP can interact with the other members of the family by forming heterotetramers [9] [19]. It is possible that in the absence of VASP the expression levels of Mena and Evl change to compensate for the lack of VASP. Both Mena and Evl are expressed in MCFB (Figure 15). Mena was checked by Western blotting of total cell lysates with a specific antibody. The absence of VASP did not induce any changes in Mena expression (Figure 15 A). It was not possible to check the levels of Evl expression by Western blotting because the antibody available was not sensitive enough. Northern blotting using total RNA isolated from MCFB was used to answer this question. Evl expression was also not changed by the absence of VASP (Figure 15 B). These observations coincide with the published data on VASP$^{-/-}$ mouse organs [52]. It is worth to note that the expression level of Evl was very low in heart [52] and MCFB. (This result on Evl expression was later also confirmed by the microarray technique. Unfortunately *Mena* cDNA

is not present on the mouse chip used here and its expression levels could therefore not be checked by this method.)

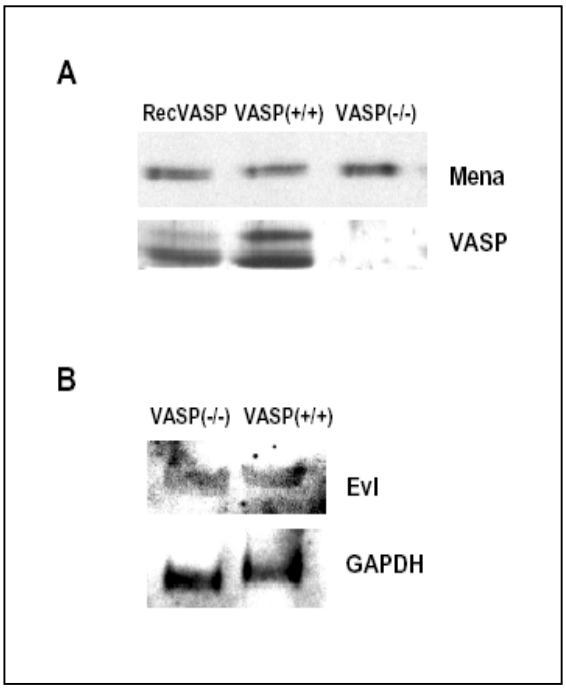

Figure 15: Expression levels of Mena and Evl do not change in VASP$^{-/-}$ cardiac fibroblasts. A: 30 µg of total cell lysates were separated by SDS-PAGE and Mena and VASP expression were analyzed by immunoblotting with specific antibodies. In SDS gel electrophoresis VASP migrates as a doublet due to phosphorylation of Ser-153 (mouse VASP), which causes a mobility shift from 46 to 50 kDa. B: Northern blot analysis of Evl and GAPDH (loading control) mRNA expression in wild type and knockout MCFB cells.

5.1.3 VASP$^{+/+}$ and VASP$^{-/-}$ cell lines have similar growth rates

Once the cell lines were established, proliferation was studied. Cells from both lines were seeded at the same density on 12-well plates, resuspended using trypsin at different time points and counted. The results are shown in figure 16 as the log [cell number] vs. time in days. VASP$^{-/-}$ showed a tendency to grow more slowly than the wild type cells, however this difference was not significant (VASP$^{+/+}$: 0,9728 doubling/day vs. VASP$^{-/-}$: 0,8632 doubling/day). The growth speed was calculated as the slope of the proliferation curve before confluence. At day 6 cells reached confluence and stopped dividing by cell-contact inhibition.

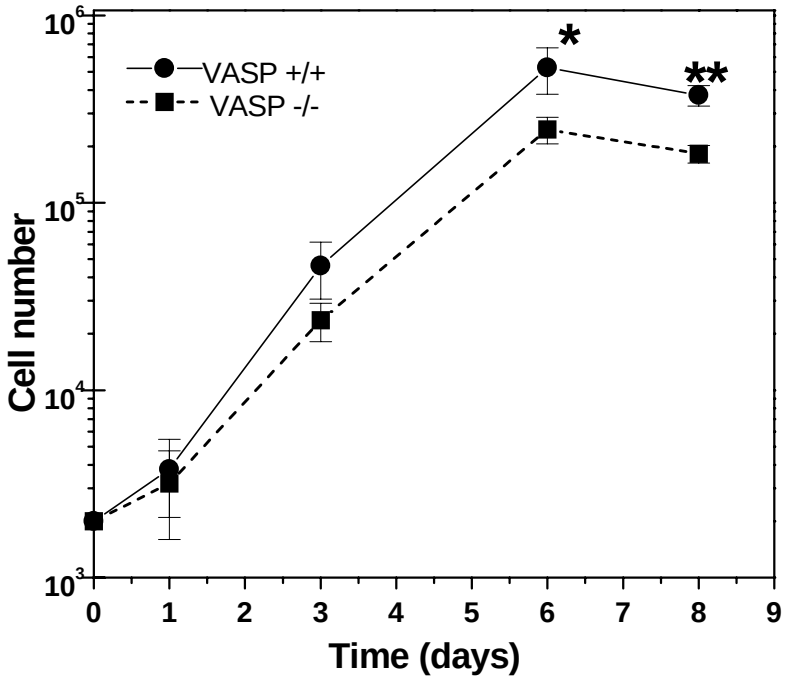

Figure 16: Proliferation of VASP$^{+/+}$ and VASP$^{-/-}$ MCFB cells. 2x10^3 cells were seeded in each well of a 12-well plate. Cells were counted at day 1; 3; 6 and 8 after seeding with the Casy® Cell counter. ---●--- VASP$^{+/+}$; - - ■- - VASP$^{-/-}$. (*: p<0,05; **p<0,01; unpaired t-test) n = 4.

5.1.4 VASP$^{-/-}$ cells are more spread

Even if the growth rates were not significantly different, the maximum of VASP$^{+/+}$ cells was about the double that of VASP deficient cells (see figures 16 and 17). This difference could be due to a different response to the medium and the concentration of serum. The amount of cells counted on a confluent dish was independent of the serum concentration (between 5 and 20%), as it can be observed in figure 18.

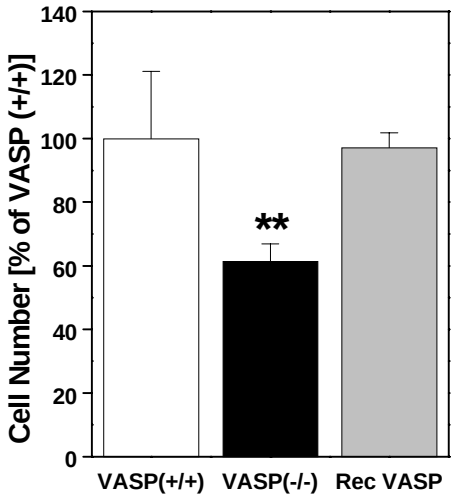

Figure 17: Relative number of cells in a 6-well plate at confluence (3 days after splitting). Data are relative numbers with the number of VASP$^{+/+}$ cells set as 100%. (**: $p<0.05$, unpaired t-test). RecVASP: VASP$^{-/-}$ cells stably transfected with full length human VASP DNA.

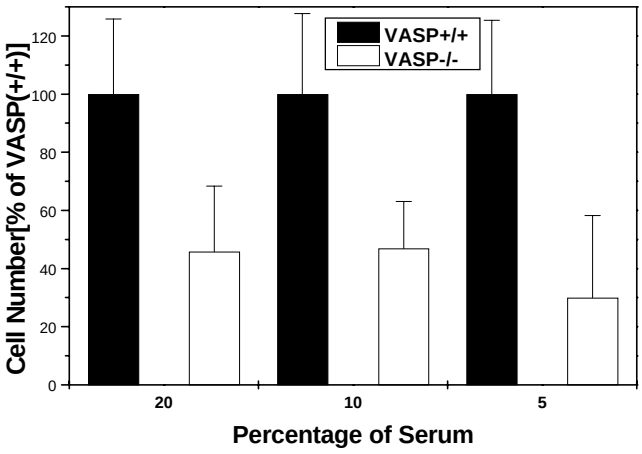

Figure 18: The lower relative number of VASP$^{-/-}$ cells at confluence is not dependent on the serum concentration. Cells were seeded at the same density on a 6-well plate and were kept in culture with DMEM containing 20% (A); 10% (B) or 5% (C) calf serum. When they reached confluence, cells were counted with the Casy® cell counter. Cells were not dividing at serum concentration lower than 5%.

The lower number of VASP$^{-/-}$ cells at confluence suggested differences of the size of these cells; that would mean that VASP$^{-/-}$ cells, being bigger than VASP$^{+/+}$ cells, reaches confluence with a lower number of cells. In order to check this hypothesis the estimated volume and diameter of the cells in suspension after trypsinization was measured with the Casy® cell counter. Surprisingly, the volume of both cells lines was similar: 4,96 ± 0,11 pl for VASP$^{+/+}$ cells and 5,07 ± 0,12 pl for VASP$^{-/-}$ cells (figure 19).

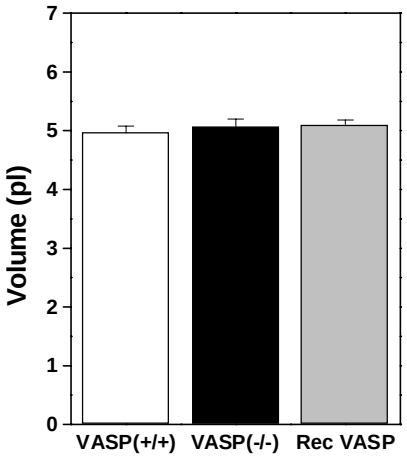

Figure 19: Average volumes of cells in suspension. Volumes of the cells were measured with a Casy® cell counter (n= 40 cells for $VASP^{+/+}$; 32 cells $VASP^{-/-}$ and 40 cells RecVASP).

As the lower $VASP^{-/-}$ cell number at confluence was not a consequence of a difference in growth, neither a difference in volume, the only explanation for this observation would be a difference in the surface area occupied by the cells. Cells were seeded at low density in order to have a sparse culture. Pictures of several fields were taken with a digital camera connected to the microscope and the cell area of at least 50 cells was measured with Scion Image software. Indeed, the area of $VASP^{-/-}$ cells was about twice the area (2,61 ± 0,90 arbitrary units) of the wild type cells (1,00 ± 0,45) (Figure 20). As it can be seen in figure 21 VASP deficient cells exhibit larger lamellipodia and are more spread than the $VASP^{+/+}$ cells.

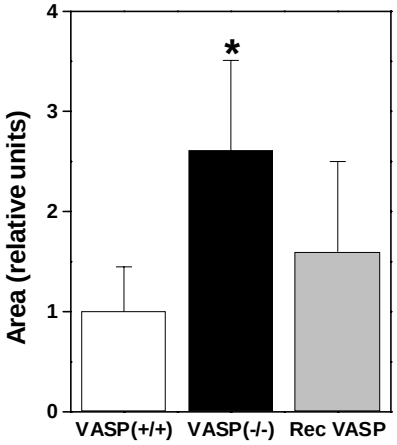

Figure 20: Average area covered by a single cell (relative units). The mean area of $VASP^{+/+}$ cells (n=40) was set as 1; $VASP^{-/-}$ n=32; RecVASP n=40; *: p<0,001, unpaired t-test.

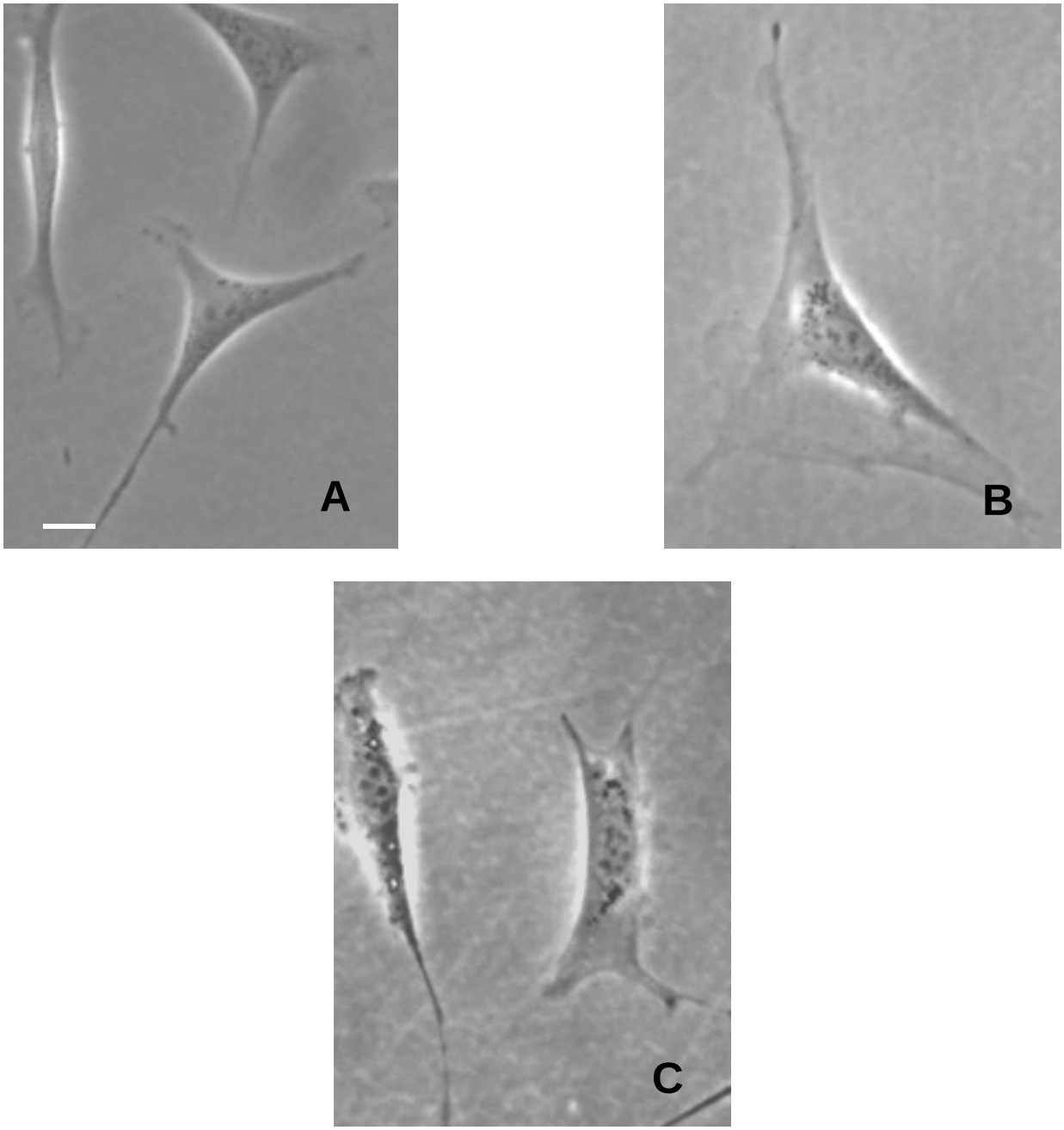

Figure 21: VASP$^{+/+}$ and VASP$^{-/-}$ mouse cardiac fibroblasts show different cell shape.
VASP$^{+/+}$ (A), VASP$^{-/-}$ (B), and RecVASP (C) mouse cardiac fibroblasts Bar = 10 μm.

The differences seen between VASP$^{+/+}$ and VASP$^{-/-}$ cells could be due to an artifact, namely a consequence of the spontaneous cell transformation that is required for the establishment of the cell line. To confirm that the enhanced spreading of the VASP deficient cells was indeed VASP-dependent, the knock out cells were stably transfected with full length human VASP. After transfection with lipofectamine, cells were incubated in selective media containing 50 μg/ml Hygromycin. The level of VASP expression was checked by

Western blotting of cells surviving in the presence of the antibiotic (Figure 15). Surviving cells were called Reconstituted VASP cells (RecVASP).

The reintroduction of VASP into the VASP$^{-/-}$ cells reverted the enlarged spreading phenotype observed in the absence of VASP (figure 21) suggesting a VASP effect rather than a cloning artefact.

Isolated clones of RecVASP cells, expressing different levels of VASP show a gradually decrease in lamellipodium formation as the levels of VASP increase (figure 22), confirming once more that VASP expression down-regulates excessive cell spreading.

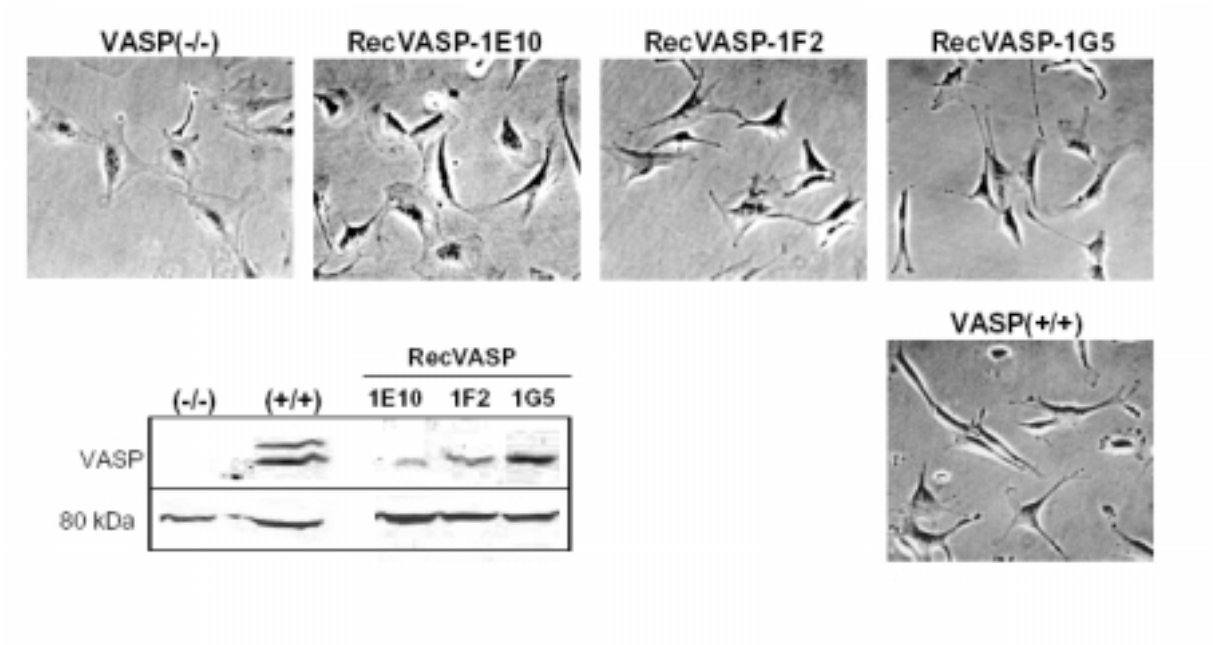

Figure 22: Lamellipodia formation is dependent on VASP expression levels in RecVASP cells. Phase contrast images: Cell shapes of different RecVASP clones. Lower left: Immunoblot analysis of VASP expression (upper panel) in RecVASP cell clones. The lower panel shows an 80 kDa protein recognized by the M4 antiserum in rodent cells, which serves as a loading control. VASP expression levels increase gradually from VASP$^{-/-}$, RecVASP-1E10, -1F2, -1G5 to VASP$^{+/+}$ cells, while the tendency to form extended lamellipodia decreases in the same order.

In order to rule out that enhanced spreading was a cell type dependent effect, another cell type was analyzed. The same phenotype difference was observed in Mesangial cells derived form the kidney of both wild type and VASP knock out mice (Figure 23).

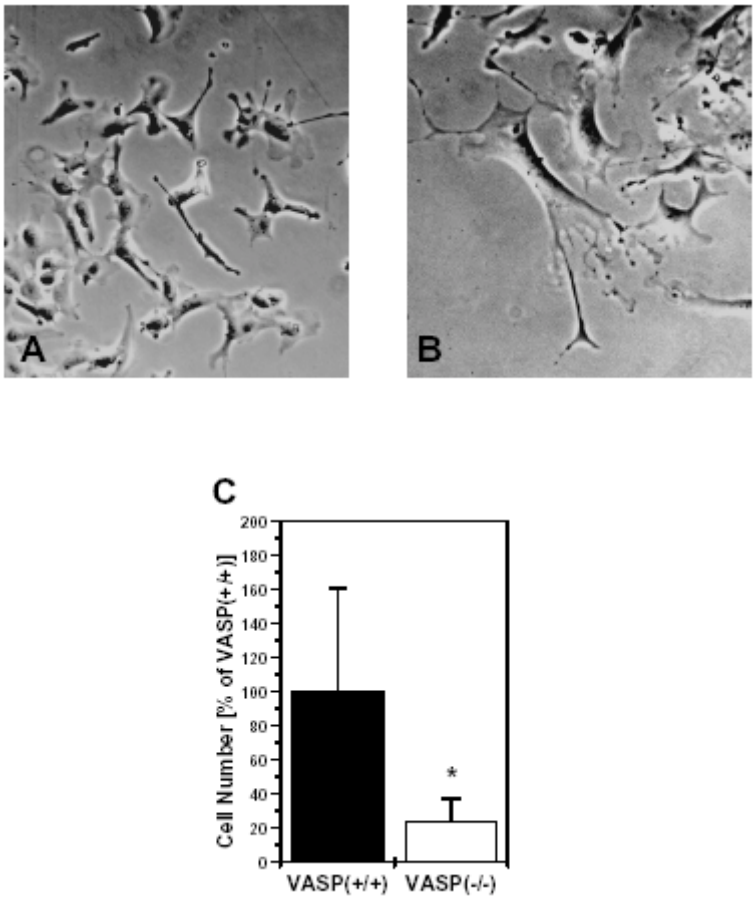

Figure 23: Cell shape difference in mouse mesangial cells. Upper panel: Phase contrast micrographs of VASP$^{+/+}$ **(a)** and VASP$^{-/-}$ **(b)** mesangial cells. Lower panel: Relative number of cells at confluence. Data are shown as percentage with the number of VASP$^{+/+}$ cells set as 100%. (n= 28 confluent dishes for VASP$^{+/+}$; n= 32 confluent dishes for VASP$^{-/-}$).

5.1.5 VASP$^{-/-}$ cells have thicker stress fibers

VASP is a cytoskeletal protein that colocalizes with focal adhesions [8] and stress fibers and has binding domains for vinculin [10], zyxin [10], LPP [11] and F-acting [24] and other proteins linked to the cytoskeleton (reviewed in [6,9]). Therefore it was interesting to investigate if the absence of VASP alters the organization of the actin cytoskeleton. Staining of MCFB with fluorescent phalloidine revealed that VASP$^{-/-}$ cells have thicker stress fibers in comparison to the wild type cells (figure 24). This phenotype was reverted by the reintroduction of VASP into VASP$^{-/-}$ cells (RecVASP cells; figure 24, C). At larger magnification it is apparent that filaments crossover between adjacent filament bundles (see inserts in figure 24). These results were unexpected, since similar actin filaments bundles result from overexpression of VASP in PtK_2 and NIH3T3 cells [36,94]. Moreover, Ena/VASP proteins have been shown to bundle actin filaments *in vitro* [20,24]. As both overexpression

and ablation of VASP leads to a similar morphology of the stress fibers, it is likely that this phenotype involves other mechanisms than the actin filament bundling activity of VASP. Possible mechanisms explaining these results will be discussed later.

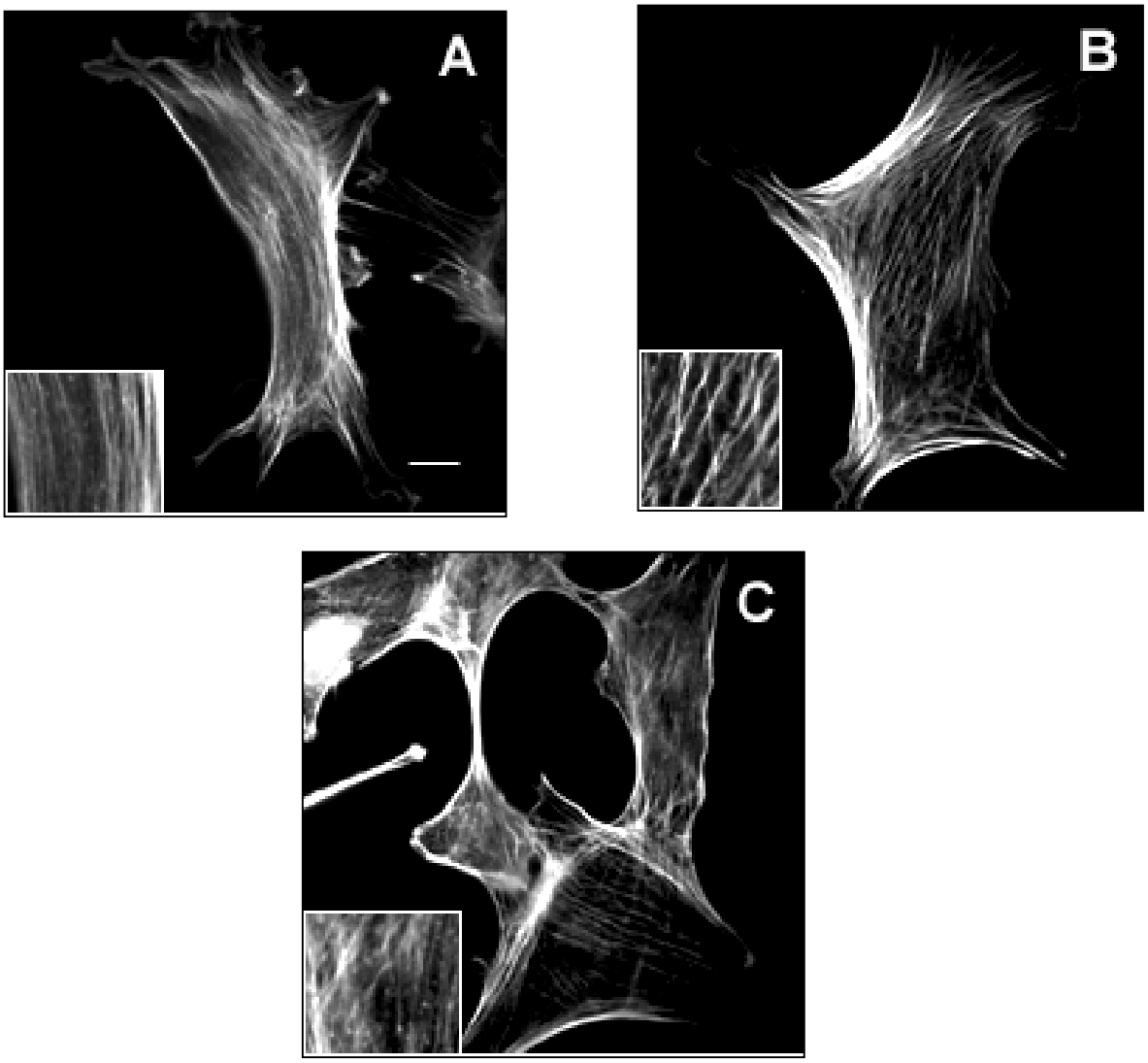

Figure 24: VASP$^{-/-}$ cells have thicker stress fibers. VASP$^{+/+}$ (A), VASP$^{-/-}$ (B) and RecVASP cells (C) were stained for F-actin with Oregon Green Phalloidine. Insets in panels A, B and C show a detailed view of the stress fibers. Bar = 15 µm.

5.1.6 VASP$^{-/-}$ stress fibers are also more stable

Serum deprivation is known to lead to stress fiber break down and disassembly [95]. Indeed after 24 h of serum starvation VASP$^{+/+}$ cells lost most of their prominent stress fibers and showed only thin actin filament structures (Figure 24, A and A'). After addition of serum stress fibers reappeared in these cells (Figure 25, C and C'). In contrast, VASP$^{-/-}$ cells mostly maintained their stress fiber structures during starvation (Figure 25, B and B') with a similar morphology as in the presence of serum (Figure 25, D and D').

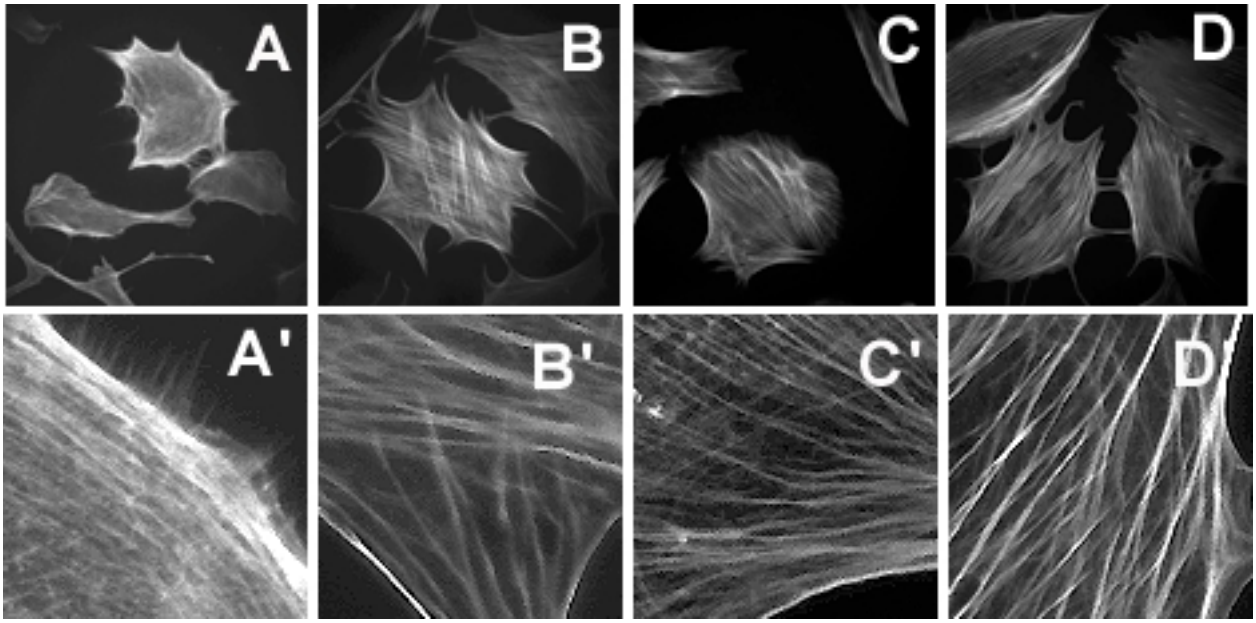

Figure 25: Stress fiber persistence in VASP$^{-/-}$ cells during starvation. Cells were seeded on coverslips and kept in DMEM with 0,2% fetal calf serum for 24 hours. Stress fibers were stained with Rhodamine phalloidine. VASP$^{+/+}$ cells (A and C) and VASP$^{-/-}$ cells (B and D) starved for 24 hours (A and B) and 5 minutes after stimulation with 10% fetal calf serum (C and D). The lower panels (A', B', C' and D') show a 63-fold magnification of A, B, C and D respectively.

In collaboration with Annette B. Galler, phosphorylation of myosin light chain (MLC) was checked in two-dimensional gel electrophoresis as a biochemical marker of stress fiber stabilization [96]. During starvation, MLC phosphorylation was reduced in the VASP$^{+/+}$ cells while it remained at high levels in the VASP$^{-/-}$ cells [97].

The thicker stress fibers and their stabilization in the knockout cells, together with the results obtained with the overexpression of VASP, suggest that a balanced level of VASP is needed for regulation of stress fibers remodeling.

5.1.7 VASP$^{-/-}$ cells have prominent focal adhesion sites

Focal contacts or focal adhesion sites are located at the ends of the stress fibers, where cells attache to the substratum via integrins. Focal adhesion sites have a precise protein composition that includes VASP and some of its binding partners, such as Vinculin, [10] Zyxin [10] and LPP [11]. It has been shown that stimulation of cGK with concomitant phosphorylation of VASP depletes VASP from focal adhesion sites apparently without affecting their structure [98]. Therefore, it was of interest to investigate if the complete absence of VASP was influencing either the morphology or the function of the focal contacts. Immunofluorescent staining of wild type and VASP-deficient MCFB cells with the focal adhesion marker protein LPP revealed that VASP$^{-/-}$ cells have more prominent focal adhesion sites, both in the periphery of the cells and at central position within the cells (Figure 26).

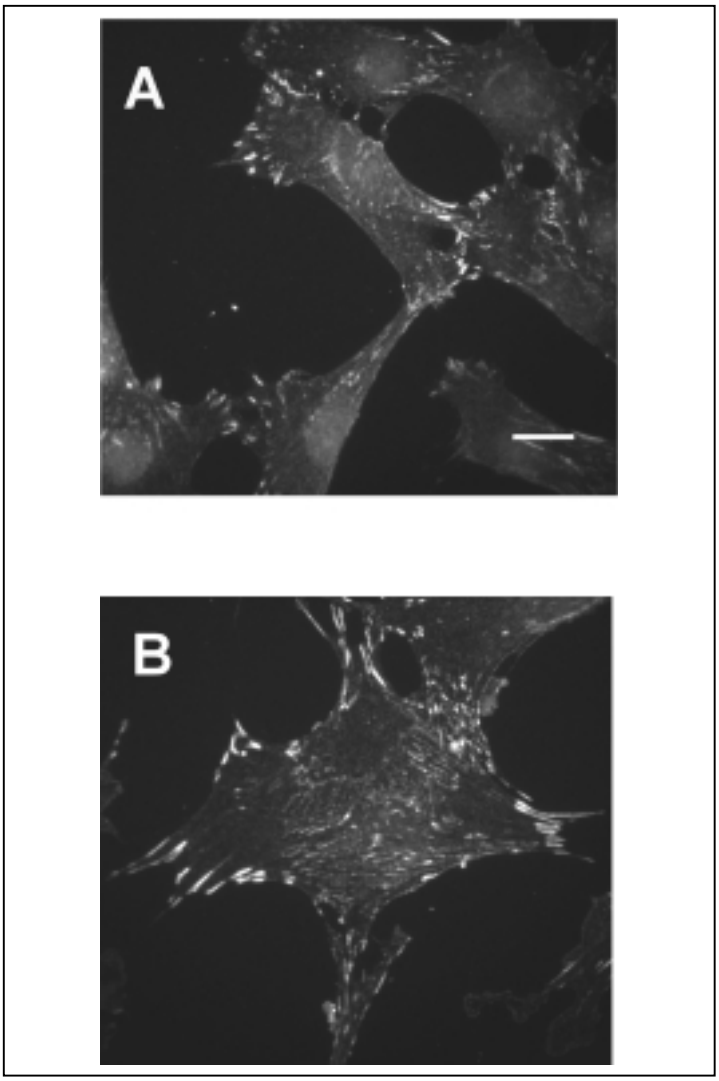

Figure 26: Increased focal adhesion sites of VASP$^{-/-}$ cells. Focal adhesions of wild type (A) and VASP deficient (B) MCFB were labelled with an anti-LPP antibody. Note the more elaborated focal adhesion sites of VASP$^{-/-}$ cells. Bar = 20 μm**.**

In order to confirm that the difference observed was a cytoskeletal disorder and not due to differential expression levels of LPP, expression levels of Zyxin, LPP and Vinculin were checked by Western blotting (Figure 27). None of the three proteins were up- or down regulated in the absence of VASP, in accordance with the results of Hauser and collaborators [52] obtained for different tissues of the VASP deficient mouse.

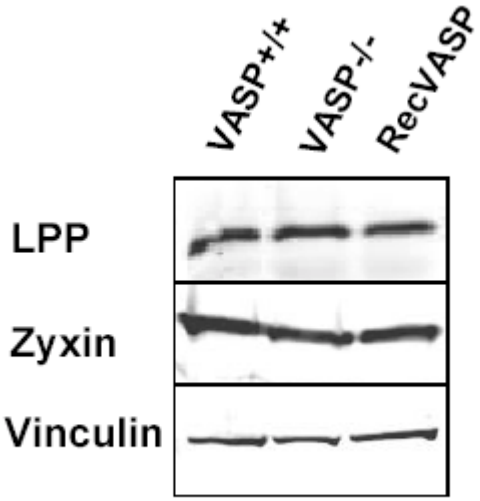

Figure 27: Expression level of focal adhesion binding partners of VASP. Total MCFB lysates (20 µg for the LPP and Zyxin blots and 10 µg for the Vinculin blot) were separated by SDS-PAGE and LPP, Zyxin and Vinculin expression were analyzed by immunoblotting with specific antibodies.

5.1.8 Adhesion and detachment rates decrease in VASP$^{-/-}$ cells.

Enhanced spreading, thicker and more stable stress fibers and the more prominent focal adhesion sites in VASP deficient cells suggested that the dynamic cellular processes leading to reorganization of the actin cytoskeleton are altered in these cells. Working routinely with the cells, I observed that the time needed for detachment of the VASP$^{-/-}$ cells by trypsinization or with PBS-EDTA was significantly longer than the time needed for VASP$^{+/+}$ cells (figure 28). Considering the difference in the focal adhesion sites between the cells lines it is not surprising that in the absence of VASP cells adhere stronger to the substrate.

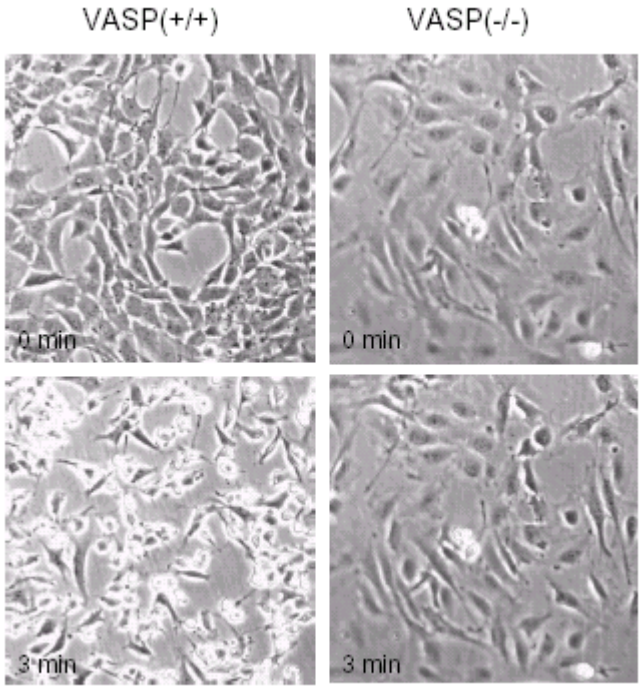

Figure 28: Decreased detachment rates in VASP$^{-/-}$ cells. Phase contrast micrographs showing that wild type, but not VASP$^{-/-}$ cells, round off and begin to detach within 3 min of incubation in the presence of 0.1% trypsin.

On the other hand, adhesion requires a very precise rearrangement of the cytoskeleton to be properly achieved. That includes spreading, lamellipodia and filopodia formation, assembling of focal contacts and actin stress fibers. As most of these parameters were altered in VASP deficient cells, an *in vitro* adhesion assay was performed. A known number of cells were allowed to adhere to fibronectin coated 96-well plates for 30 min. A difference was only observed at low concentrations of fibronectin (1 μg/ml). Surprisingly, significantly less VASP$^{-/-}$ cells adhered to the fibronectin-coated surface within 30 min as compared with the wild type cells (Figure 29). No difference could be observed at the other fibronectin concentrations investigated (3 to 10 μg/ml). After 2-3 hours, both cells lines attached almost quantitatively also at 1μg/μl. This indicates that there is considerable delay in the cell attachment of the VASP$^{-/-}$ cells at low fibronectin concentration rather than a difference in the cell number due to the enhanced spreading of the VASP deficient cells.

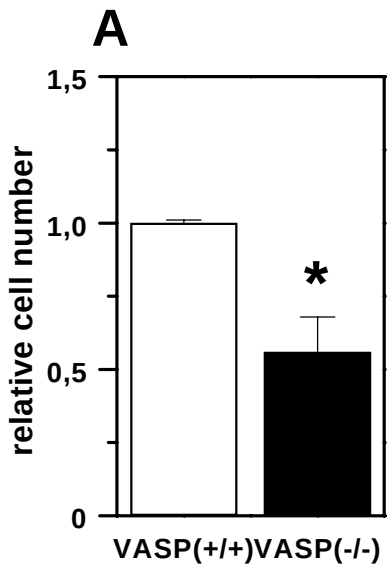

Figure 29: Decreased cell adhesion in VASP$^{-/-}$ cells. Relative number of VASP$^{+/+}$ cells and VASP$^{-/-}$ cells attaching within the first 30 min to 96-well plates coated with 1 µg/ml fibronectin (Average of 4 different experiments ± SEM; *: p<0,05)

Taken together, these results suggest that the reorganization of the cellular structure required for the transition from a suspended to an adhesive cellular state and vice versa are compromised in the absence of VASP.

5.1.9 The cGMP analog 8p-CPT-cGMP accelerates attachment of MCFB cells

During cell detachment cAMP-dependent protein kinase is activated and is thought to mediate detachment induced inactivation or disassembly of adhesion related protein complexes [69]. Lawrence et al have shown that VASP is phosphorylated upon neutrophil spreading, and have suggested that both events, VASP phosphorylation and spreading, are dependent on cGMP-stimulated protein kinase [99]. As VASP is a substrate of both cAMP- and cGMP- dependent protein kinases, it was of interest to investigate whether VASP phosphorylation is involved in the cellular transition from a suspended to an adherent phenotype. Therefore, both VASP$^{+/+}$ and VASP$^{-/-}$ cells were pre-incubated in the absence or presence of the cGMP analog 8-pCPT-cGMP under conditions for which cGK-mediated VASP phosphorylation had been established in NIH3T3 cells [98]. The adhesion on Fibronectin was tested as described before. When stimulated with the cGMP analogue, significantly more VASP$^{+/+}$ cells attached to the substratum within 30 min as compared to non-treated cells (Figure 30, A). If the effect of the 8-pCPT-cGMP was mediated by VASP it

should be abolished in VASP$^{-/-}$ cells. Indeed, adhesion of VASP$^{-/-}$ cells was essentially unaffected by the pre-treatment (Figure 30, B).

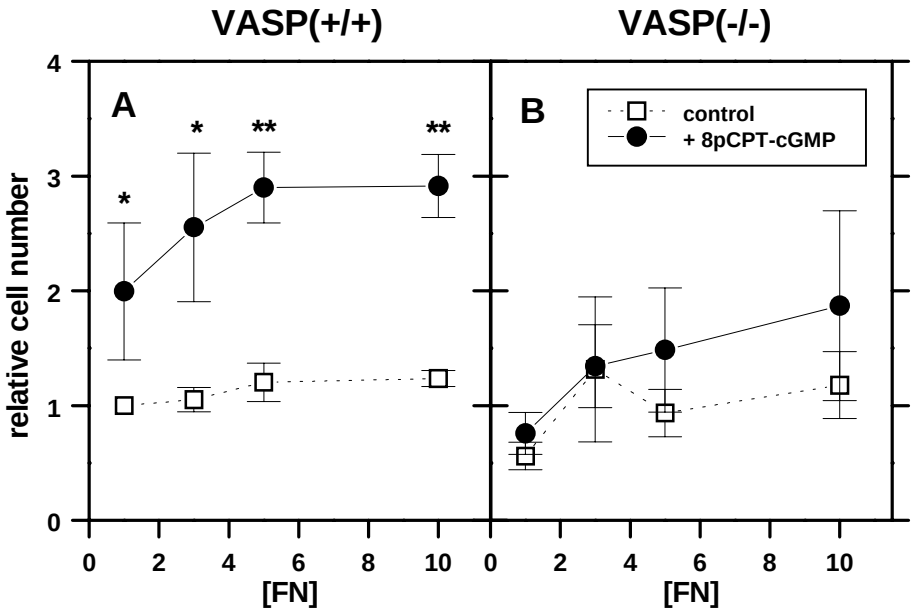

Figure 30: Cell Adhesion as function of fibronectin concentration and the effect of stimulation with 8p-CPT-cGMP. Panels **A** and **B** represent the relative cell number of adherent cells of VASP$^{+/+}$ and VASP$^{-/-}$ respectively preincubated with (—●—) or without (– –□– –) 100µM of 8pCPT-cGMP for one hour. Adhesion was tested using 1, 3, 5 and 10 µg/ml fibronectin as a substrate. The data are averages of 4 different experiments ± SEM. Due to the variability between different experiments in the cell numbers, adhesion of VASP$^{+/+}$ cells at 1 µg/ml was considered 1 and all the other values were related to it. (*: $p<0.05$; **: $p<0.005$, unpaired t-test)

5.1.10 Reorientation and motility of VASP$^{-/-}$ cells are impaired in a wound healing assay

Remodeling of the cytoskeletal structure plays an important role in cell migration. In order to accomplish a proper movement, the reorganization of the cytoskeleton must be tightly regulated and coordinated at precise subcellular locations. A motile cell will first polarize. That requires a clear distinction of a „front“ and a „rear“ part of the cell not only in terms of morphology but also in terms of protein localization. At the front, actin polymerization and new focal adhesion formation take place, leading to the protrusion of the lamella in the direction of movement. At the rear side, however, focal adhesions will have to be released and the cell will retract the rear [100].

As VASP deficient cells showed anomalies in adhesion, detachment, stress fibermorphology and spreading, migration was investigated in these cell lines. To this end, cells were scratched off of a confluent cell layer to allow cells next to the scratched area to migrate into the empty space. Pictures of the cells were taken immediately after scratching

(Figure 31, A-C) and 15 hours later (Figure 31, D-F). Twelve to 15 h after scratching, $VASP^{+/+}$ cells in the outermost cell row were mostly orientated parallel to the wound (Figure 31, D/D‘), whereas $VASP^{-/-}$ cells after 15 h were perpendicular to the wound (Figure 31 E/E’). This obvious difference in the orientation of the cells could be reverted by reintroducing VASP into $VASP^{-/-}$ cells (Figure 31 F/F’). The orientation of stress fibers coincided with that of the cells (Figure 32). Using time-lapse microscopy, the wound-healing assay was analysed in more detail over a period of 24 h. Whereas all three cell lines were able to close the scratch within about 20 to 22 hours, the motility of the cells was different. Twelve to 15 h after scratching, $VASP^{+/+}$ cells started to detach from their neighbours in the monolayer and were migrating with highly active frontal lamellipodia and retraction of their rear ends, resulting in an orientation parallel to the scratch. In contrast, $VASP^{-/-}$ cells were protruding highly mobile lamellipodia into the direction of the wound without retracting at their rear ends from the adjacent cell monolayer. Overall this resulted in a more perpendicular orientation relative to the scratch. Ultimately, dividing cells considerably contributed to wound closure. RecVASP cells behaved as wild type cells, indicating that the reduced translocational speed of $VASP^{-/-}$ cells was indeed due to the lack of VASP. In conclusion, the capability of $VASP^{-/-}$ cells to reorient their stress fibers and cell axis and to detach their rear ends appears to be markedly compromised when compared to VASP expressing cells. Together, this results in decreased cell motility.

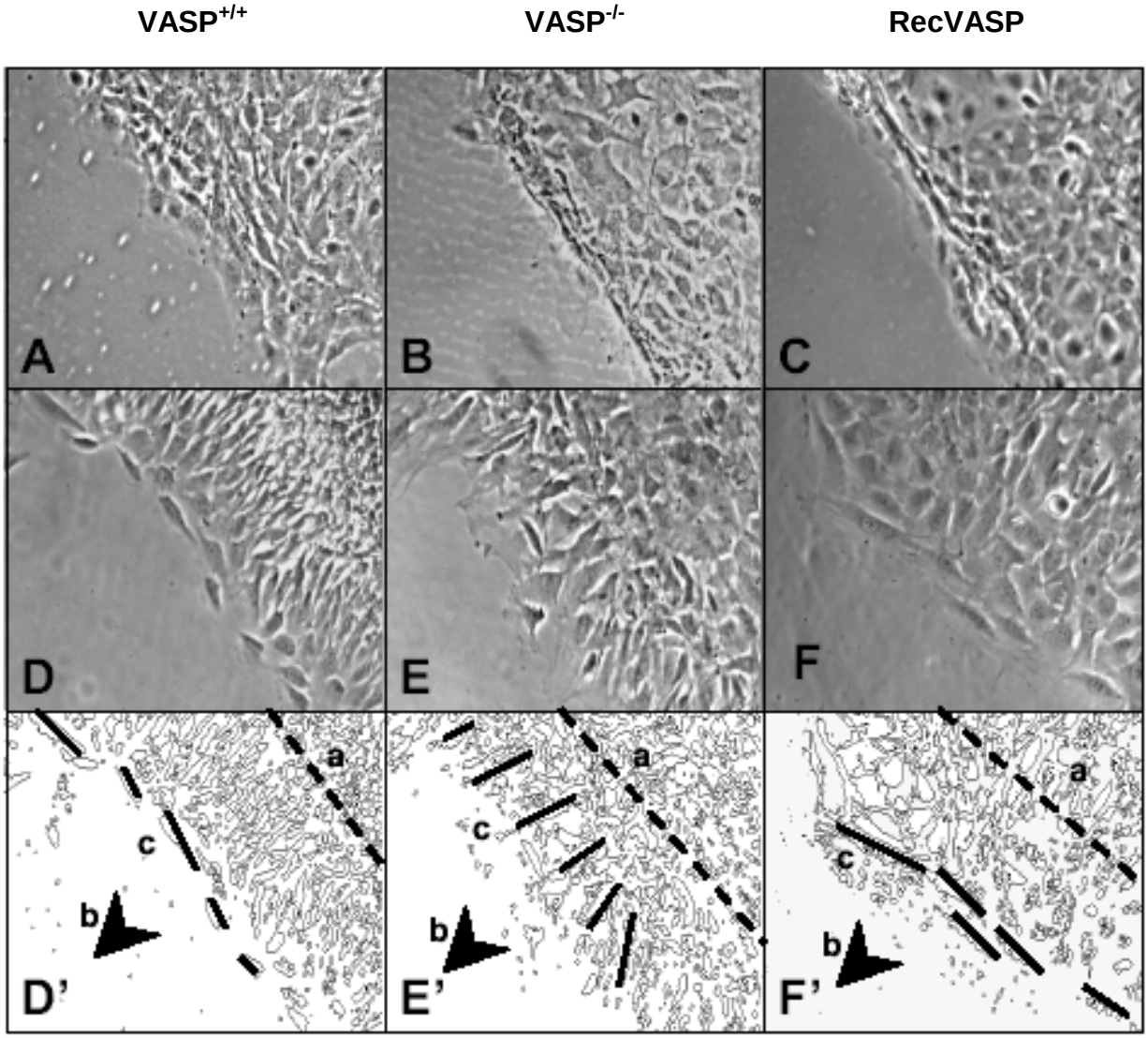

Figure 31: VASP$^{-/-}$ cells fail to reorient in a wound-healing assay. VASP$^{+/+}$ cells (left column: A, D, D'); VASP$^{-/-}$ cells (middle column: B, E, E') and VASP$^{-/-}$ cells reconstituted with human VASP cDNA (right column: C, F, F') immediately after (A, B, C) and 15 h after (D, E, F) the confluent monolyer has been scratched. D', E', F' show a graphic visualization of cell orientation (c) and direction of movement (arrowhead; b), where the dashed line (a) indicates the position of the cell border at t=0. Note that only wild type cells and VASP$^{-/-}$ cells stably transfected with VASP are able to reorient their cell axis perpendicular to the direction of movement. VASP$^{-/-}$ cells are unable to reorient and detach their rear ends.

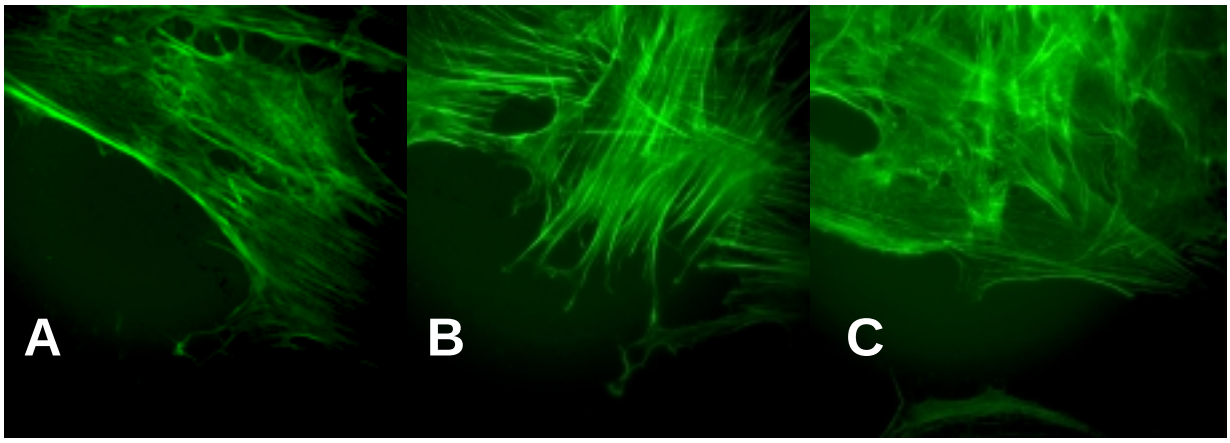

Figure 32: VASP$^{-/-}$ cells fails to reorient in a Wound-healing assay. Actin staining of motile cells during the wound healing assay. The assay was performed for 15 hours and then the cells were fixed, permeabilized and F-actin was stained with Oregon Green Phalloidine. **(A)** VASP$^{+/+}$; **(B)** VASP$^{-/-}$ and **(C)** RecVASP.

5.1.11 Prolonged Rac activation in the absence of VASP

Since Rac, Cdc42, and Pak are key regulators of lamellipodia formation and cell spreading and the Rac/Pak pathway is known to play an essential role in cell motility, [101,102], this pathway was analyzed in VASP$^{-/-}$ cells. In order to investigate Rac activation a Rac pull-down assay has been used. A GST fusion of the Rac/Cdc42 binding (CRIB) motif of Pak was used to affinity precipitate the activated form of Rac (Rac-GTP) [66,88].

As shown in Figure 33, PDGF-BB (5 ng/ml) induced a rapid and transient activation of Rac in VASP$^{+/+}$ cells with a maximal activity at around two minutes. After five minutes of stimulation Rac activity decreased again and reached background levels at about 10-15 min. Interestingly, Rac activation in VASP$^{-/-}$ cells was significantly faster as compared to VASP$^{+/+}$ cells. The maximal degree of Rac activation was seen after one minute of stimulation, and was maintained at a high level for at least 15 minutes (Figure 33, upper panels). If prolonged Rac activation were specifically due to VASP deficiency, it should be possible to reverse this effect by reintroducing VASP into VASP$^{-/-}$ cells. Indeed, reconstituted cells were characterized by a transient PDGF-induced Rac activation, comparable to VASP$^{+/+}$ cells (Figure 33). RecVASP cells showed a maximal Rac activation at around one minute after stimulation, which within one additional minute returned to levels of unstimulated controls or even below. All these cell lines expressed similar amounts of Rac, confirming that an enhanced activation of the small GTPase is observed here rather than increased expression levels of the protein. These data, together with the morphological differences described above, strongly suggest that VASP is involved in the regulation of Rac activity.

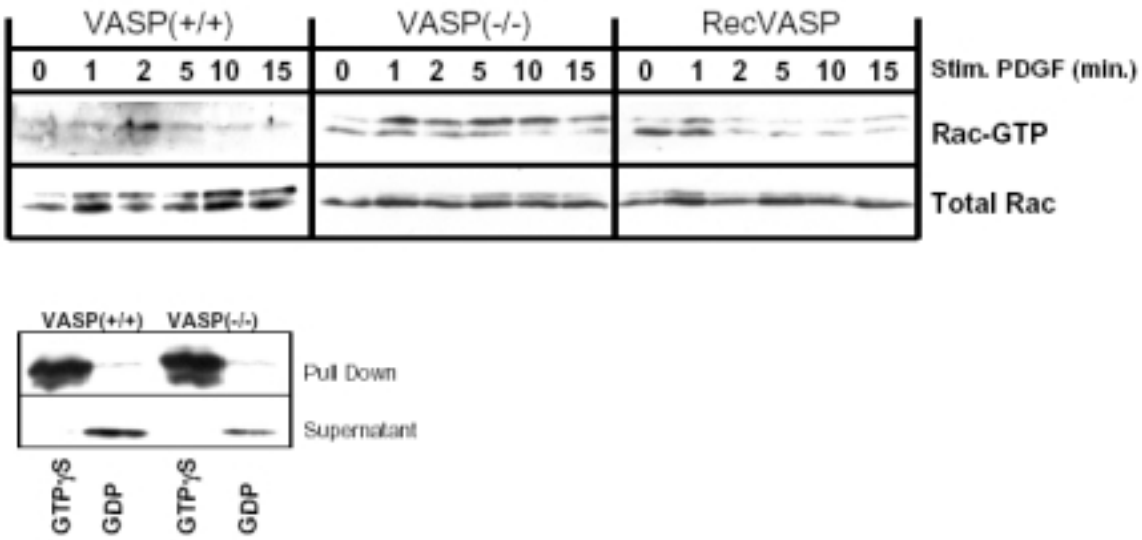

Figure 33: Prolonged Rac activation in VASP$^{-/-}$ mouse cardiac fibroblasts. Upper panel: Cells were starved for 24 h in serum free medium and subsequently stimulated with 5 ng/ml of PDGF-BB for the time indicated. Activated Rac (GTP-Rac) was precipitated using a fusion protein of GST and the Pak CRIB motif. Precipitates (Rac-GTP) and aliquots of total cell lysates (Total Rac) were analysed with a Rac specific antibody. Results are representative for a total of 5 independent experiments. Lower panel: As controls, unstimulated cells were loaded with GTPγS (positive control) or with GDP (negative control). Only the Rac-GTP form was pulled down, while Rac-GDP remains in the supernatant. In contrast to other tissues, Rac of cardiac fibroblasts or total heart lysates appears as a doublet band when analysed by SDS gel electrophoresis and immunoblotting.

5.1.12 Pak is activated in VASP$^{-/-}$ cells

The Pak family of proteins appears to be a central element in pathways that lead to cell spreading, since it functions both as a direct target of activated Rac and Cdc 42 and as an upstream activator of Rac [103]. Therefore, in order to assess activation of this signaling pathway in more detail in MCFB cells, I also analysed Pak activation. Upon interaction with their activators, Paks undergo autophosphorylation at multiple sites [70,104]. One of these sites, which is involved in substrate recognition [104], is conserved in Pak-1 to Pak-3 and is centred around Thr-423 (human Pak-1;α-Pak), Thr-402 (Pak-2;γ-Pak), and Thr-421 (Pak-3; β-Pak), respectively [70,104].

Analysis using an antibody directed against this phosphorylated autophosphorylation site showed that wild type cells displayed a transient Pak phosphorylation ceasing within about 5 min of FCS stimulation, whereas a profound and more sustained elevation of

phospho-Pak was observed with VASP$^{-/-}$ MCFB (Figure 34). In another approach, MCFB$^{-/-}$ and wild type cells were serum starved for 24 hours. Cell lysates were separated by two-dimensional gel electrophoresis and were immunoblotted using an anti-Pak antibody that recognizes Pak-1 independent of its phosphorylation state. After serum stimulation for 2 h, Pak-1 from VASP deficient cells, as compared to VASP$^{+/+}$ cells, showed a much more pronounced shift to a lower isoelectric point, indicating Pak-1 phosphorylation (Figure 35).

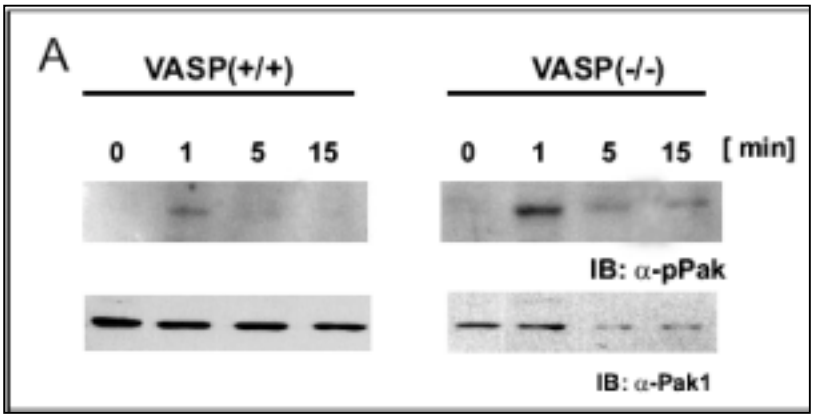

Figure 34: Pak phosphorylation in VASP$^{-/-}$ cells. After stimulation with 10 % FCS for the times indicated, cells were harvested and lysates were separated by SDS-PAGE. Pak expression and Pak phosphorylation were analysed by immunoblotting with anti-Pak1 antibody (N20) and anti-phospho Thr-423 Pak antibody, respectively.

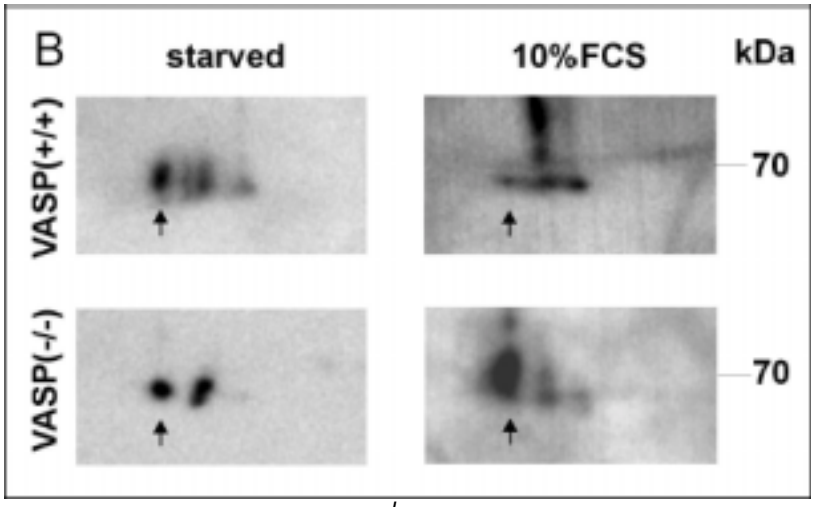

Figure 35: Pak phosphorylation in VASP$^{-/-}$ cells. Cells lysates were separated by 2-D gel electrophoresis and Pak-1 was detected by immunoblotting. The acidic region of the isoelectric focussing strip is oriented to left. Corresponding spots are marked with an arrow. This is a representative out of three independent experiments.

An in-gel kinase assay was used as a third method to confirm this data (Figure 36). Total cell lysates were run on a 10% SDS gel containing myelin basic protein (MBP) as an *in vitro* Pak substrate. After electrophoretical separation, the proteins were renatured and the

kinase assay was performed in the gel. MBP contained in the gel is phosphorylated by its kinase(s) revealing their position after separation in the gel. The bands obtained by autoradiogrphy coincided with the size of the Pak kinase studied. However, this assay is here only orientating as one cannot exclude that other kinases migrate at a similar position as Pak. For example, LIM kinase (LIMK), a substrate for Pak, can also phosphorylate MBP and has a similar molecular weight.

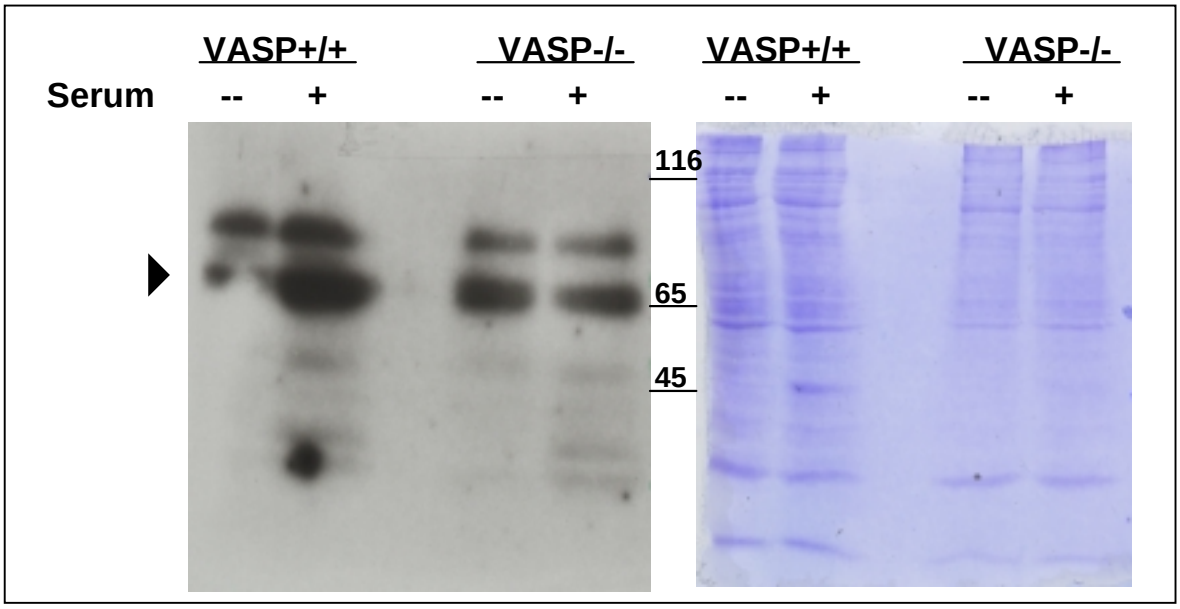

Figure 36: Pak activity in VASP$^{-/-}$ cells. Cells were starved over night and subsequently stimulated with serum and harvested in loading sample buffer. Left panel: Autoradiography of the in-gel kinase assay. Right panel: Comassie staining of the same gel. Arrowhead indicates the molecular size of Pak.

In conclusion, not only morphological data, but also two lines of biochemical evidence indicate that the Rac/Pak pathway is activated in MCFB cells in the absence of VASP.

5.1.13 Differences in the expression pattern of VASP$^{+/+}$ and VASP-deficient MCFB analyzed by Microarrays.

In order to investigate if the absence of VASP has any influence on the RNA expression profile of MCFB cells we used mouse cDNA arrays with 4000 randomly selected known genes and 500 ESTs. RNA from VASP$^{+/+}$, VASP$^{-/-}$ and RecVASP were isolated and CyDye-labeled first strand cDNAs were generated using either Cy3 or Cy5 labeled dCTP. The cDNA derived from VASP$^{-/-}$, VASP$^{+/+}$ and RecVASP was labeled using different color to allow ratio imaging. The Cy3 and Cy5 labeled probes were mixed and hybridized over night

to the array. After washing away the unhybridized probe the fluorescent signals for both probes are read into two different image files with a confocal laser scanner (ScanArray 4000, Perkin Elmer). Figure 37 shows and example of the image obtained after hybridization.

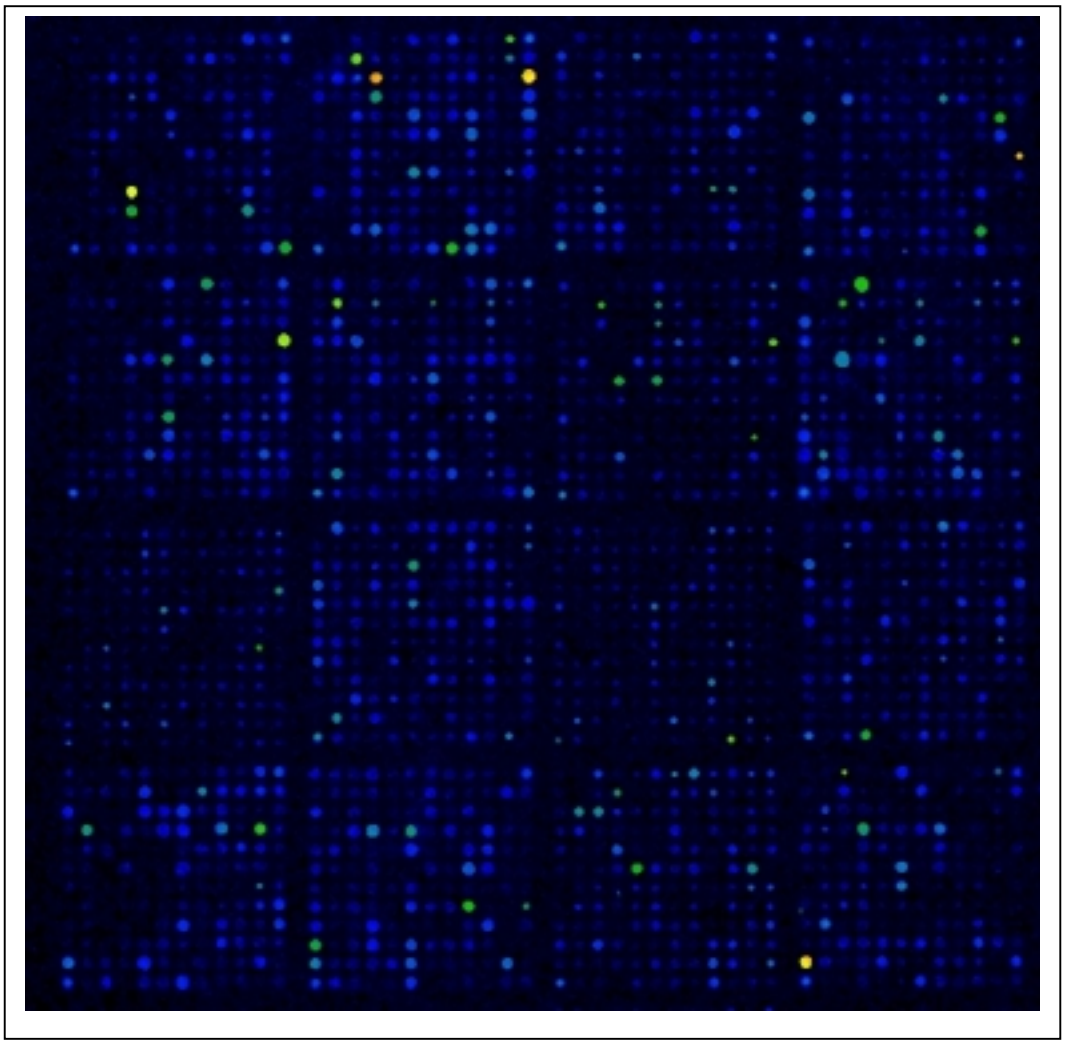

Figure 37: Example of an image of a mouse array obtained after hybridization with labeled cDNA. The picture corresponds to the array hybridized with $VASP^{+/+}$ Cy3-labelled cDNA. The gradation of colors correlates with expression level of the spotted genes (black or dark blue= not expressed; yellow= highly expressed). The same array was also hybridised with Cy5-cDNA from $VASP^{-/-}$ or RecVASP cells, and both fluorescent labels were read with a confocal laser scanner (ScanArray 4000, Perkin Elmer) and analysed with the ScanAlyze software.

To be able to compare all three probes, the RecVASP cells and the $VASP^{-/-}$ cells were both compared to the $VASP^{+/+}$ cells. In order to avoid false positives and/or negatives due to differences in the incorporation of the CyDye-CTP, samples were alternatively labelled with Cy3 and Cy5. Differences in gene expression should be independent of the dye used for the labelling of the probe.

Array Name	Cy3 dCTP	Cy5 dCTP
6 M ng 28_R	RecVASP	$VASP^{+/+}$
6 M ng 29_KO	$VASP^{-/-}$	$VASP^{+/+}$
6 M ng 30_R	$VASP^{+/+}$	RecVASP
6 M ng 31_KO	$VASP^{+/+}$	$VASP^{-/-}$
6 M ng 32_R	RecVASP	$VASP^{+/+}$

Table 2: Identification of the samples for the analysis of the mouse arrays. Each "array name" corresponds to a set of two competitively hybridized RNA probes, where one has always been hybridized with $VASP^{+/+}$ CyDye labelled cDNA and the other was either RecVASP cDNA or $VASP^{-/-}$ cDNA.

The ScanAlyze program was used for data acquisition. Afterwards, the data sets were normalized by setting the average of the logarithmic intensity values for each probe to 0 and standard deviation to 1. Relative intensities ($VASP^{-/-}/VASP^{+/+}$ or $RecVASP/VASP^{+/+}$) were calculated. The data were analysed with the program GeneSpring.

Differences in expression were detected by the 'drawable gene' function. This tool allows defining an intensity profile. The program then finds genes, which match this profile with a certain, user defined, correlation. In this case the $VASP^{-/-}$ set of genes were supposed to be up or down regulated as compared to the wild type cells, whereas the RecVASP cells were not allowed to show any difference to the $VASP^{+/+}$ cells. A correlation of 0.975 was used (Figure 38). Using this method, a total of 21 genes differentially expressed were identified: 15 were up-regulated and 6 were down-regulated in VASP deficient cells. A list of the genes obtained is presented in table 3. As stated before, only genes that have shown differences between $VASP^{-/-}$ and $VASP^{+/+}$ but not between RecVASP and $VASP^{-/-}$ were considered. RecVASP have been generated by stably transfecting full-length human VASP in VASP deficient cells and the random insertion of the transfected gene into the genome can cause variations in the expression pattern. For that reason only those genes in the RecVASP sample that were not changed when compared to the wild type cells were accepted during the screening, this fraction represented 62% of the 4500 genes spotted in the microarray chip. That means the differences observed in $VASP^{-/-}$ cells could be reverted by the addition of VASP.

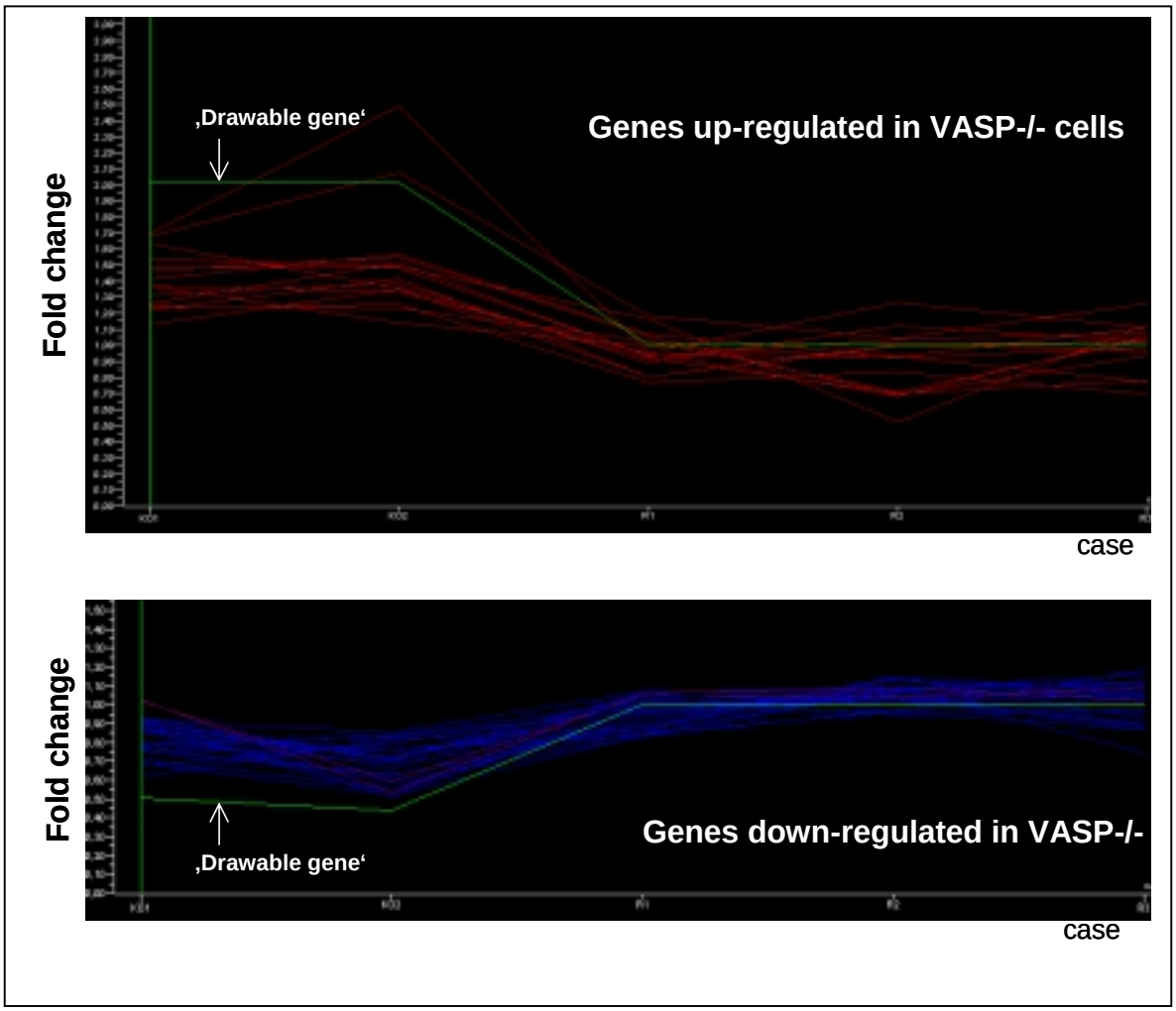

Figure 38: Graphic representing the analysis of the MicroArrays. Green lines correspond to a theoretical "user defined gene" that represent the expected intensity for each case or assay for an up regulated gene in the $VASP^{-/-}$ cells (upper panel) and a down-regulated gene in $VASP^{-/-}$ cells (lower panel). The theoretical "drawable" genes were set as follow: ratio of the normalized intensities was calculated (KO= $VASP^{-/-}$ /$VASP^{+/+}$ and R= RecVASP/$VASP^{+/+}$); KO was defined as 2 for up-regulated genes and 0,5 for down-regulated genes, R was defined as 1 for both cases. Genes that fit to the "drawable gene" with a correlation factor of 0,975 were taken as candidate genes (represented as blue or red lines). KO1 and KO2 and R1 to R3 are independent hybridization assays.

Relative Intensity		Arrays					Genes	Description
		28_R	30_R	32_R	29_KO	31_KO		
	Genes up-regulated in VASP$^{-/-}$ cells	1,06	0,69	0,93	1,46	1,55		ESTs
		0,93	1,04	1,07	1,26	1,51	**Mpg**	N-methylpurine-DNA glycosylase
		0,77	0,83	0,70	1,24	1,26	**Numb**	numb gene homolog (Drosophila)
		1,07	0,93	1,11	1,41	1,56	**Tgfb**	latent TGF beta binding protein
		1,00	0,93	0,98	1,37	1,14	**Mafb**	v-maf musculoaponeurotic fibrosarcoma oncogene family, protein B (avian)
		0,92	0,70	0,78	1,63	1,36	**Deb2**	differentially expressed in B16F10 2
		1,17	0,52	1,13	1,54	1,49		ESTs, Moderately similar to DNA NUCLEOTIDYLEXOTRANSFERASE [Bos taurus]
		0,95	0,68	1,06	1,37	1,33	**Man2a1**	mannosidase 2, alpha 1
		0,95	1,27	1,11	1,70	2,49	**Bcl7b**	B-cell CLL/lymphoma 7B
		1,02	0,71	1,04	1,25	1,23	**Crygf**	crystallin, gamma F
		0,93	0,93	0,77	1,48	1,48	**Capn5**	calpain 5
		1,18	1,04	1,26	1,68	2,08	**Mrg2**	myeloid ecotropic viral integration site-related gene 2
		0,90	1,12	1,03	1,31	1,39	**Robo1**	roundabout homolog 1 (Drosophila)
		0,81	1,00	0,97	1,13	1,35		ESTs
		0,80	0,99	1,03	1,22	1,41	**Zfp61**	Zinc finger protein 61
	Genes down-regulated in VASP$^{-/-}$ cells	0,98	1,02	1,08	0,78	0,84	**Smpd1**	sphingomyelin phosphodiesterase 1, acid lysosomal
		0,91	1,13	1,05	0,76	0,62	**Apaf1**	Apoptotic protease activating factor 1
		1,02	1,04	1,08	0,78	0,84	**Npr1**	natriuretic peptide receptor 1
		0,95	1,10	1,11	0,90	0,72	**Tcfl4**	Transcription factor like 4
		0,99	1,04	0,90	0,68	0,80	**Nucb2**	nucleobindin 2
		0,97	1,02	1,10	0,79	0,83	**Ltbp3**	latent transforming growth factor beta binding protein 3

Table 3: Differential gene expression in VASP deficient cells. The same names used in Table 2 are used to identify the arrays. Relative intensities were calculated as the ratio of intensities for each set of arrays as for figure 38: VASP$^{-/-}$/VASP$^{+/+}$ (29_KO and 31_KO) and RecVASP/VASP$^{+/+}$ (28_R, 30_R and 32_R)

The genes obtained with this method give new possibilities to study VASP function. New experiments need to be done in order to confirm the changes in the expression profile of VASP deficient cells. Special attention will be given to the roundabout homolog 1 (Robo), as the protein product of this gene is able to interact with the EVH1 domain of Ena in

Drosophila, and is the only known binding partner of the Ena/VASP family which expression seems to be altered in the absence of VASP.

5.2 Platelets

5.2.1 Rac activity regulation by VASP

In platelets VASP is the most predominant member of the Ena/VASP family of proteins present. Moreover, they contain high levels of Rac. Therefore, it was of great interest to investigate the effect of VASP in this system. In collaboration with the group of Dr. Offermanns in the Institute of Pharmacology, University of Heidelberg, I studied the effect of the absence of VASP in murine platelets stimulated with thromboxane A_2 (TxA_2). Dr. Gratacap and colleagues showed that Rac is activated by the platelet agonist TxA_2 [66]. Also, thrombin activation of platelets induced a more than 2-fold higher surface expression of P-selectin and fibrinogen binding in $VASP^{-/-}$ platelets in comparison to wild type platelets, indicating enhanced agonist induced activation [52]. Considering the prolonged Rac activation obtained on MCFB cells stimulated with PDGF-BB, a similar result was expected in platelets treated with TxA_2. Unfortunately, I could not observe a prolonged activation of Rac in the $VASP^{-/-}$ platelets after the agonist stimulation (figure 39). In contrast to MCFB stimulated cells, Rac activation by TxA_2 in platelets is very fast (maximum activation is reached after 10 sec of stimulation) and lasts for several minutes. As the activation of Rac coincides with the general activation of platelets by TxA_2 and, moreover, upon stimulation platelets also secrete TxA_2, it is probably not possible to observe a transient Rac regulation in this system.

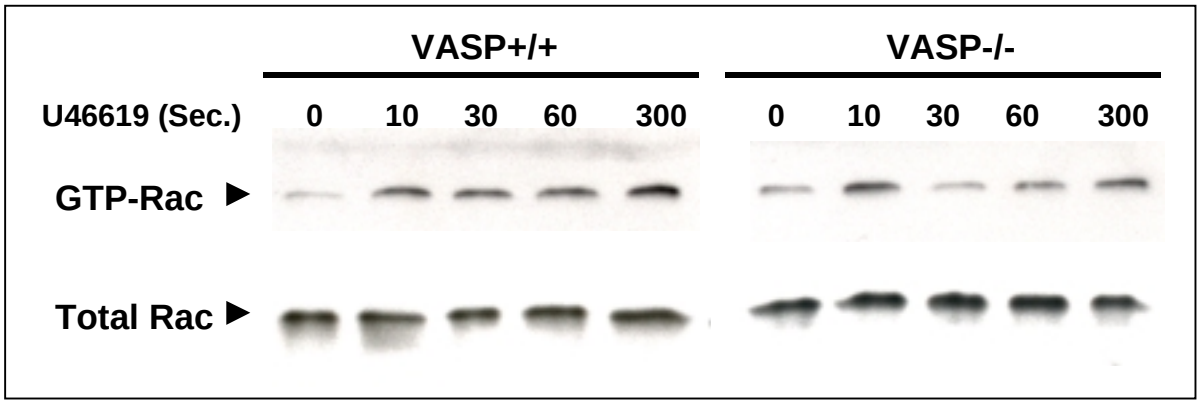

Figure 39: Rac activation is not enhanced in VASP deficient platelets. Washed platelets were prepared from blood of both, $VASP^{+/+}$ and $VASP^{-/-}$ mice. Platelets were stimulated with the TxA_2 analogue U46619 (1 μM) for the indicated times. Reactions were stopped with lyses buffer and Rac activity was determined performing a pull down assay as described for MCFB cells.

The activation of Rac by TxA_2 can be inhibited by preincubation of platelets with cGMP and cAMP analogues (8p-CPT-cGMP and cBIMPS-cAMP, respectively) [66]. This inhibition likely involves the cGMP and cAMP dependent kinases. Cyclic nucleotides are potent inhibitors of platelet activation and aggregation. VASP, as substrate of both kinases, is located at the intersection of two inhibitory pathways induced by cGMP and camp, respectively. Hence, it was worth to investigate if VASP was playing a role in the inhibition of Rac by cyclic nucleotides. The platelets from $VASP^{-/-}$ and $VASP^{+/+}$ mice were preincubated with cBIMPS-cAMP (100 μM) or 8p-CPT-cGMP (1 mM) for 20 minutes and stimulated with TxA_2 (1 μM). The Rac pull down was performed in the same way as it was done for the MCFB. The inhibition of Rac by the cGMP analog was abolished in VASP deficient platelets while there was no difference between $VASP^{+/+}$ and $VASP^{-/-}$ when the platelets were preincubated with the cAMP analog (figure 40). However, note that the Rac pull down assay on mouse platelets is very variable. Mouse platelets are extremely sensitive to manipulation and basal levels of Rac are usually high, making it difficult to detect the activation by TxA_2. The basic problem of this method is to obtain murine platelets on a good resting state. The results presented here show a trend, which needs to be confirmed by more experiments.

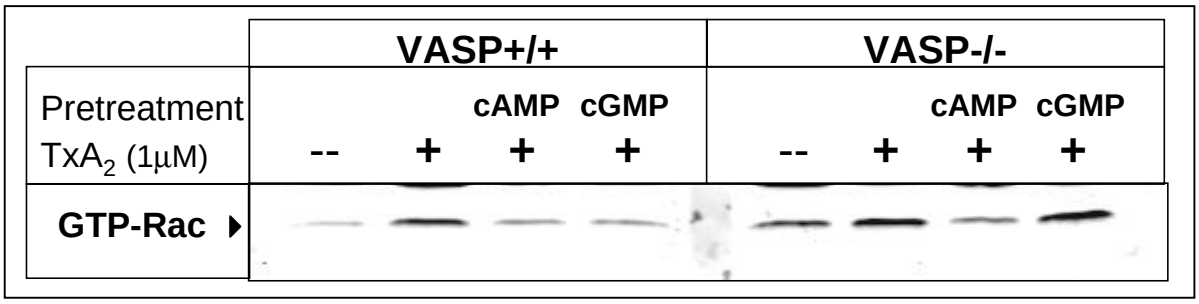

Figure 40: Rac inhibition by the cGMP analog is impaired in $VASP^{-/-}$ cells. Washed platelets were prepared from blood of both, $VASP^{+/+}$ and $VASP^{-/-}$ mice. Platelets were pre-incubated 20 min with 100 μM cBIMPS-cAMP (cAMP) or with 1 mM 8pCPT-cGMP (cGMP) and stimulated with the TxA_2 analogue U46619 (1 μM) for 1 min. Samples were stopped with lysis buffer and Rac activity was determined performing a pull down assay as described for MCFB cells.

5.2.2 Enhanced Platelet adhesion in VASP deficient mice: An *in vivo* approach.[2]

5.2.2.1 VASP regulation of platelet adhesion in vivo

To address the significance of VASP for the homeostasis of platelet-endothelium interactions *in vivo*, we assessed platelet adhesion in the carotid artery of $VASP^{-/-}$ mice in

[2] The experiments shown in this section were performed by the group of Dr.Steffen Massberg (Deutsches Herzzentrum 1.Medizinische Klinik, Technische Universität München) with $VASP^{-/-}$ and VASP +/+ mice provided from our group.

collaboration with Dr. Massberg. Fluorescent wild type or VASP$^{-/-}$ platelets were transfused into wild type or VASP$^{-/-}$ mice, respectively, and were visualized by intravital videofluorescence microscopy. Wild type platelets did not interact with wild type endothelium under physiological conditions. Interestingly, the loss of VASP significantly enhanced platelet-endothelial cell interactions *in vivo* (Figures 41a and 41b). Platelet tethering to the endothelial surface was increased approximately 11-fold, while the number of platelets firmly attached to the vascular wall was found to increase more than 4-fold in VASP$^{-/-}$ as compared with wild type mice.

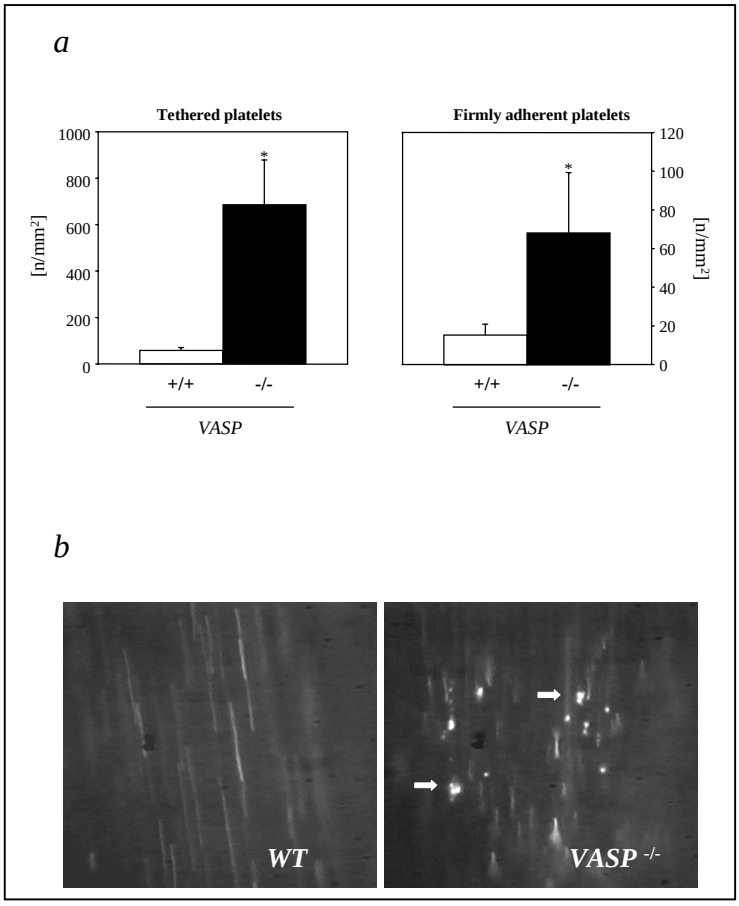

Figure 41 Role of *VASP* in the regulation of platelet adhesion in the common carotid artery *in vivo*. (a) Platelet-endothelial cell interactions were investigated in *VASP*$^{-/-}$ mice by *in vivo* fluorescence microscopy of the common carotid artery *in situ.* Wild type animals served as controls. The upper panels summarize platelet tethering (left) and firm platelet adhesion (right). Numbers of tethered and adherent platelets are given per mm^2 of vessel surface. Mean ± SEM, n=10 each group, asterisk indicates significant difference compared to wild type mice, $P < 0.05$. **(b)** The microphotographs show representative *in vivo* fluorescence microscopy images. White arrows indicate adherent platelets. Monitor magnification 500-fold. (Dr. Steffen Massberg)

5.2.2.2 VASP deficient platelets show enhanced adhesion following endothelial denudation.

In advanced atherosclerosis, rupture of the atherosclerotic lesion leads to endothelial denudation and exposure of the thrombogenic subendothelial matrix to circulating platelets, initiating platelet recruitment to the injured vessel wall. In order to address whether VASP might be involved in regulation of platelet adhesion to the subendothelial matrix, platelet-vessel wall interactions after vascular injury were investigated. Carotid Vascular injury was induced in wild type animals by vigorous ligation for 5 min, causing complete loss of endothelial cell layer. Then, adhesion of thrombin-preactivated (0.2 U/ml of murine thrombin) $VASP^{+/+}$ or $VASP^{-/-}$ platelets to the injured carotid was determined by *in vivo* fluorescence microscopy. Within the first minutes after endothelial denudation a high number of $VASP^{+/+}$ platelets were tethered to the vascular wall (2530 $\pm$ 82 platelets/mm^2, Figure 42a). Basically all the platelets contacting the subendothelium showed irreversible stable adhesion (2089 $\pm$ 58 platelets/mm^2, Figure 42b and c). In contrast $VASP^{-/-}$ platelets significantly increased tethering and stable adhesion to the subendothelium after vascular injury (3191 $\pm$ 144 and 2753 $\pm$ 128 platelets/mm^2 for tethering and stable adhesion respectively; Figure 42).

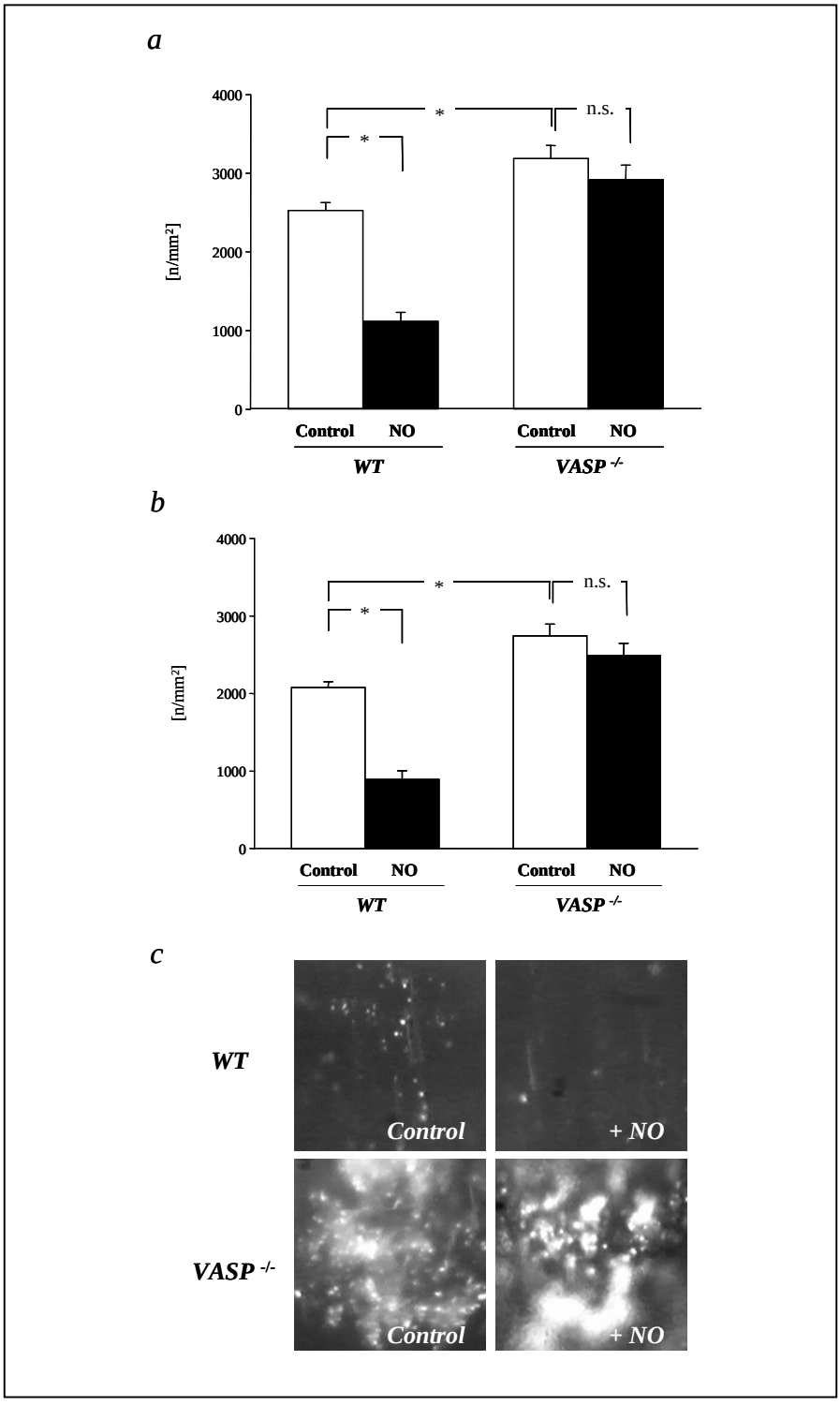

Figure 42 Platelet adhesion following endothelial denudation. Endothelial denudation induces platelet adhesion. Fluorescent wild type or *VASP*$^{-/-}$ platelets were preincubated with either PBS (control) or the NO-donor spermine-NO. After preincubation, the samples were stimulated with 0.2 U/ml mouse thrombin. **(a)** Platelet tethering and **(b)** Firm platelet adhesion to the carotid artery was assessed by intravital videofluorescence microscopy. Mean ± SEM, n=5 each group, asterisk indicates significant difference compared to control, $P < 0.05$. **(c)** The microphotographs show representative *in vivo* fluorescence microscopy images in illustrating adhesion of wild type or *VASP*$^{-/-}$ platelets following endothelial denudation in the absence or presence of spermine-NO. Monitor magnification 500-fold.

5.2.2.3 VASP deficient platelets are unresponsive to nitric oxide

NO is known to be a very important endogenous platelet antagonist [105,106] that mediates platelet inhibition through cGMP/cGK I. To determine the role of VASP in NO/cGMP-dependent regulation of platelets adhesion, the effects of NO on adhesion of $VASP^{+/+}$ and $VASP^{-/-}$ platelets to the injured vascular wall were investigated. Fluorescent platelets ($VASP^{+/+}$ and $VASP^{-/-}$) were preincubated with the NO donor spermine-No followed by stimulation with thrombin. Platelet adhesion to the carotid artery of wild type mice was monitored by intravital videofluorescence microscopy. In $VASP^{+/+}$ platelets, pre-treatment with NO donors decreased platelet tethering and adhesion to the injured vessel wall by approximately 56 and 57% respectively. In contrast, $VASP^{-/-}$ platelets showed nearly no response to NO, tethering was only reduced by 8% and firm platelet adhesion by 9% (Figure 42).

The data presented here show for the first time *in vivo* that VASP down regulates platelet adhesion to the vascular wall under physiological and pathophysiological (endothelial denudation) conditions.

6. Discussion

The Vasodilator stimulated phosphoprotein, VASP, was originally discovered as substrate for both cAMP- and cGMP- dependent protein kinases in human platelets. Further investigations demonstrated that VASP binds to F-actin and colocalizes with stress fibers, focal contacts and highly dynamic membrane structures. Moreover, studies with the model system of Listeria motility established that VASP,located at the head of the actin tail of Listeria, is an important stimulatory component for the actin-based motility of this intracellular pathogen. Although many of these data depict VASP and the Ena/VASP protein family as enhancers of actin filament formation, other data strongly suggest that these proteins also have inhibitory functions in integrin regulation, cell motility and axon guidance [9]. However, at the molecular level the precise biological function of VASP remains to be established. A major goal of this work was to acquire a better understanding of the biological VASP function using a VASP deficient cell model.

It has been suggested that the proteins of the Ena/VASP family can functionally replace each other and may therefore compensate the loss of one of them. This idea of redundancy within the Ena/VASP family is supported by several facts. Proteins of the Ena/VASP family have a similar structure, and the three domains (EVH1, EVH2 and PRR) are highly conserved in all members. Moreover Ena/VASP proteins are able to form multimeric complexes via their EVH2 domain in vitro and in cells [19]. In agreement with this and studied at a systemic level, human VASP is able to rescue the lethal phenotype of $Ena^{-/-}$ Drosophila melanogaster, indicating that VASP may compensate for the loss of Ena in vivo. In mammals, three members of the family are expressed: VASP, Mena and Evl. In most tissues and cell types all three proteins are expressed with some exceptions. In brain, Mena is predominant, and platelets appear to exclusively express VASP. Mice deficient in one of the family proteins show a mild phenotype with a clear effect only in those tissues or cells where the lacking protein is more abundantly or exclusively expressed. (See chapter 2.4 for a description of the Ena/VASP deficient animal models). But if two family members are “knocked out” at the same time, the result is lethality at an early embryonic stage. These observations support the idea of redundancy of the Ena/VASP proteins [9].

However, Ena/VASP proteins are biochemically and functionally not identical. A major result of my work presented here is that the absence of VASP alone is sufficient to cause a clear phenotype at the cellular level. Mouse cardiac fibroblast (MCFB) cells isolated from $VASP^{-/-}$ mouse heart are more spread and present stronger and stable stress fibers as well as bigger focal adhesions. These morphological differences have important consequences on other cellular parameters such as adhesion and migration.

6.1 Function of VASP in the stabilization of stress fibers and its consequence in cell morphology and behavior

6.1.1 Function of VASP in stabilization of stress fibers

VASP is not only highly concentrated in focal adhesions and stress fibers [107], but binds F-actin [36,107] via its EVH2 domain [24,29,36] through a conserved region of this domain (Block B) and has also the property of cross-linking actin filaments via the coiled-coil domain [24]. In addition, tetramerization of VASP has been shown to enhance F-actin binding and bundling [24]. Moreover, VASP and Mena as well are involved in promoting actin polymerization [7,15]. Over-expression of VASP and certain mutants containing the EVH2 domain [24,94] leads to thicker stress fibers. This is in agreement with the bundling capacities of VASP reported by Bachmann et al. [24].

According to these observations VASP has been considered as a cytoskeletal protein with a structural and stimulatory role in F-actin polymerization and stress fiber formation. Cells deficient in VASP would be predicted to have either reduced bundling of actin filaments or to have no cytoskeletal effect if the possibility is considered that the other members of the Ena/VASP family present in the cells will compensate for its absence. However, as it has been shown here, $VASP^{-/-}$ cells present thicker and more prominent stress fibers when compared with wild type cells. This result shows that VASP is not merely a structural protein facilitating actin polymerization but may be involved in more complex processes leading to the regulation of the actin cytoskeleton turnover and/or remodeling. More precisely, this result suggests a dual function of VASP: on the one hand the actin binding, bundling and polymerization activity performed directly by VASP; on the other hand a negative VASP effect on cell signaling pathways involved in actin cytoskeleton remodeling. In the case of VASP over-expression, the first function may be predominant; in the case of the VASP deficient cells, the second functional role is observed.

It has been postulated that proteins with this characteristics (over-expression and reduced expression cause similar effects) are considered to be or act as scaffold proteins [108,109]. Scaffold proteins are proteins that bring together the components of an active complex. If the ratio of scaffold protein and binding partners is different than the stoichiometric one the active signaling complex fails to triggers the right signal. VASP may have a scaffold function during actin cytoskeleton remodeling.

6.1.2 VASP and the regulation of membrane tension

Raucher and Sheetz showed that lamellipodial extension rates are inversely correlated with the apparent membrane tension [110]. They also showed that membrane tension could be reduced by the addition of detergents at sublytic concentrations, which leads to an enhanced spreading rate and acceleration of lamellipodia formation. In addition, stimulation of lamellipodia formation by PDGF induces a reduction in membrane tension [110]. These authors also showed that PIP_2 regulates plasma membrane tension [110]. $VASP^{-/-}$ MCFB cells require more time to adhere (Figure 28) and start spreading when compared to control cells [97], however the final result is stronger adhesion and enhanced spreading of $VASP^{-/-}$ cells. When cells adhere to the substratum, they start to spread, assemble stress fibers and induce new actin polymerization. Membrane tension also has to be reduced in order to allow new actin polymerization at that place. For example, it is not possible to incorporate actin monomers to the growing fiber at the location were the membrane is extended if the membrane tension is high. [110]. In collaboration with Annette Galler from our group and the group of D. Drenckhahn (Dept. of Anatomy and Cell Biology), the membrane tension of $VASP^{-/-}$ and $VASP^{+/+}$ was therefore measured using a laser tweezers. Interestingly and in support of the hypothesis discussed above, we observed an enhanced tension in VASP deficient cells [97]. The enhanced MLC phosphorylation and the cell surface stiffening observed in $VASP^{-/-}$ cells appear to lead to an enhanced strength of the actin cytoskeleton. Moreover, this enhanced contractility may cause the promotion of focal adhesion assembly, integrin clustering and strengthening of cell adhesion, as has been experimentally observed with VASP deficient cells.

6.2. VASP deficient cells show no differences in Mena and Evl expression levels

In this work, I demonstrated that the absence of VASP alone is sufficient to induce distinct differences at the cellular level including cell shape, stress fibers and focal adhesion. However, since Bear et al. [40] described a reduction in lamellipodia protrusion and a reduced random motility in cells deficient in all three mammalian Ena/VASP family members, the results obtained here could have been a consequence of an altered regulation and expression of other Ena/VASP proteins. For example, in the absence of VASP, Mena or Evl expression could be up-regulated and the cellular effects observed could have been due to the over-expression of Mena (or Evl) rather than due to the absence of VASP. However, neither Mena nor Evl expression levels were significantly changed in VASP deficient MCFB indicating that VASP (and probably every Ena/VASP family member) has a function per se,

independently of the other Ena/VASP proteins present in the cell. This suggests that Ena/VASP proteins, in addition to partially overlapping and therefore redundant functions, have clearly distinct functions which cannot be replaced by other family members.

6.3. VASP may modulate the expression pattern of some binding partners

Differences between $VASP^{+/+}$ and $VASP^{-/-}$ cells could not be explained by an altered expression of other Ena/VASP family members (as discussed above) but could perhaps be due to an altered expression and/or function of proteins which interact with Ena/VASP proteins. Interestingly, results from microarray analysis show that VASP deficiency affects the expression pattern of these cells. One of the genes up-regulated in VASP deficient MCFB was of particular interest: Robo. The Roundabout (robo) gene was originally identified in a large scale Drosophila mutant screen for genes related to the control of midline crossing of axons. The gene encodes for a transmembrane protein of the immunoglobuline superfamily [111]. Robo contains two FP4 motifs that bind to the EVH1 domain of Ena [112]. In Drosophila, it was shown that Ena strengthens the repulsive function of Robo during axon guidance [12].

Robo has been found in mammalian brain [113] and spinal cord [114]. An alternative splicing of the Robo messenger codes for Dutt 1. Dutt1 and Robo are expressed in a number of tissues (Brain, muscle, lung, kidney, eye and liver) during embryogenesis. In general, the expression of these proteins diminishes in adult mice. In mouse heart, Dutt 1 is preferentially expressed during development and its expression is dramatically reduced in adult mice heart [115]. If VASP, in mammals, has a function similar to that of Ena in Drosophila (i.e. strengthening the function of Robo), then cells may compensate for the absence of VASP by up-regulating the expression level of Robo as has been observed experimentally. Clearly, the functional significance of this microarray finding has to be investigated in future experiments, i.e. analysis of the equivalent of repulsive forces.

6.4. Rac and other small GTPases are good candidates to be involved in VASP dependent regulation of actin cytoskeleton

Since the phenotype of $VASP^{-/-}$ cells could not be explained by a differential expression of other Ena/VASP family members, additional mechanisms of regulation of the actin cytoskeleton should be investigated. Small GTPases of the Rho family were good candidates, as they are known to mediate several of the cytoskeletal processes impaired in $VASP^{-/-}$ MCFB. Among the Rho-GTPases, Rac has been shown to regulate lamellipodia

formation and spreading, two features that were particularly altered in the absence of VASP. Indeed, Rac/Pak pathway activation was enhanced and prolonged in VASP$^{-/-}$ cells suggesting a VASP dependent regulation responsible for the phenotype observed.

I showed here using a wound healing assay that VASP deficient MCFB cells failed to align in parallel to the edges of the wound when compared to wild type MCFB. Using a similar approach, Nobes and colleagues had demonstrated that Rac activity was essential for primary rat embryo fibroblasts (REF1) to extend lamellipodia [116]. REF1 cells normally extend the lamellipodium toward the empty space, showing after two hours a position perpendicular to the wound. Cells injected with a dominant negative form of Rac (N17Rac) did not form lamellipodia and had their stress fibers oriented in parallel to the wound [116]. When compared to the results presented here, the Rac dominant negative injected cells resemble VASP$^{+/+}$ cells (cells with low Rac activity) whereas VASP-deficient MCFB cells (cells with elevated Rac activity) are similar to control REF cells. Although these are different cell systems, direct (N17Rac injection) or indirect (VASP knock-out) manipulation of Rac activity in both experiments obviously led to changes in cell motility. Cell orientation and lamellipodia formation therefore may be explained as secondary effects due to Rac/Pak activation in VASP$^{-/-}$ cells. When cells were monitored by time lapse video microscopy we observed that the failure of VASP-deficient cells to reorient their cell axis coincides with compromised detachment of their rear ends. This is in agreement with the observation that stress fibers and cell adhesion are markedly increased in VASP$^{-/-}$ cardiac fibroblasts and may contribute to the overall decrease in cell motility, as revealed by the wound healing assay. Interestingly, Kiosses and colleagues [117] suggested a model according to which regulated Pak activity is required for induction of tail retraction. This would also be in line with the deregulation of Pak activity and the motility phenotype of VASP$^{-/-}$ cells. In contrast to our observations, a Mena/VASP double knockout cell line was reported to show increased random motility [40]. These data may be reconciled with our present data if the adhesive phenotype found in VASP$^{-/-}$ cells is less pronounced in these double null cells. Then, Rac/Pak pathway activation (de-suppression) is likely to result in an increased plasma membrane protrusive activity and an increase in random migration, indeed, this has been experimentally observed by Bear and colleagues [40].

The small GTPases are know to be involved in regulation of adhesion, another feature that is impaired in VASP$^{-/-}$ cells. Upon adhesion, small GTPases are activated, initially a transient Rac activation followed by a more prolonged Rho activation [68,118]. Rac can induce new actin polymerization [119], a process possibly accelerated by VASP as has been clearly observed with the *Listeria* model [77,120]. In the absence of VASP, actin polymerization is slower, and the negative regulation of Rac is missing (Figure 32) leading to

enhanced spreading due to prolonged Rac-induced lamellipodia formation. Rho causes reorganization of existing [118] stress fibers and focal adhesion assembly [121,122].
Raucher and Sheetz have shown that stimulation of lamellipodia formation with PDGF reduce membrane tension. This stimulus also activates Rac in different cell types including the MCFB studied here. However this is not in contradiction with the enhanced membrane tension measured with VASP$^{-/-}$ cells, in which Rac activation is also enhanced. Membrane tension was determined in cells that were firmly attached to the substrate, i.e. the spreading process was already completed and PDGF stimulation was absent. The membrane tension data obtained indicate stabilization of the cytoskeleton in VASP deficient cells (thicker stress fibers, prominent focal adhesion, enhanced MLC phosphorylation) and suggest that Rho activation is also enhanced in the absence of VASP. It would be interesting to investigate changes in membrane tension during dynamic processes such as spreading in the absence of VASP.

6.4.1 How does VASP regulate the Rac/Pak pathway?

It is not clear, whether there is some mechanism regulating the Rac level or activity in response to the mobile capacity or actin organization in cells, as discussed for Gelsolin$^{-/-}$ cells [123]. Thus, it is conceivable that (as part of a compensatory reaction) VASP absence/deficiency indirectly leads to an enhanced Rac/Pak pathway activation. However, also several not mutually exclusive modes can be envisaged, how VASP might regulate Rac/Pak signaling in a more direct manner. One pathway resulting in Rac and Pak activation involves integrins which are candidates for VASP dependent regulation. Integrin dependent adhesion can be modified by VASP (Refs. [52,53] and additional unpublished observations from our group) and is a prerequisite for PAK activation by GTP-bound Rac [68,124]. Through an interaction with PIX1, a guanine nucleotide exchange factor for Rac, Pak can feed back to Rac activation [103,125]. Actually, there is increasing evidence suggesting that the ordered interaction between these mediators is important for the regulation of Rac-dependent signaling: First, a PIX-Pak-Nck complex via PKL1 is linked to Paxillin [126] and Pak localization to integrin-based focal contacts is dependent on the Paxillin-PKL interaction [127]). A Paxillin mutant that is deficient in PKL binding leads to drastically prolonged Rac activity and highly protrusive lamellipodia [127]. Second, the scaffold protein SLP-76 potentiates adhesion-dependent Pak activation [30]. Tyrosine phosphorylation of SLP-76 stimulates its association with the Pak binding adapter protein Nck and the Rac exchange factor Vav1 [30]. In platelets, adhesion to fibrinogen stimulated the association of SLP-76 with SLAP-130 and its binding partner VASP [30], thus placing VASP probably into the same molecular complex as Rac, its exchange factor Vav1, and its effector Pak.

Similarly, Zyxin harbors binding sites for the EVH1 domain of VASP [10,16] and the SH3 domain of Vav [128] in proximity within its proline-rich domain. Functionally, VASP and Zyxin cooperate in the formation of actin-rich cell surface protrusions and during cell spreading in different experimental systems [25]. There is also evidence for a possible link between Ena/VASP proteins and yet another exchange factor, Trio (a protein with two separate GEF1 domains acting on Rac/RhoG and Cdc42, respectively). Thus, genetic data indicate that Trio and the *Drosophila* Ena/VASP family protein Ena have opposing functions in the same pathway [80]. Also, Trio has been shown to interact genetically both with Rac and Pak in *Drosophila*. There, these proteins define a pathway that, similar to the role of Ena [12,80], links guidance receptors to the actin cytoskeleton [129]. Together these data suggest a possible mode of VASP-dependent inhibition of Rac/Pak signaling through modulation of Trio-mediated guanine nucleotide exchange of Rac and/or Cdc 42. Moreover, knock-out of the gene encoding the Trio interacting protein Tara causes cell spreading and stress fiber thickening [130]. This phenotype resembles VASP$^{-/-}$ cells, and Trio is therefore a putative player in VASP deficient cells . (See Figure 43 for a summary).

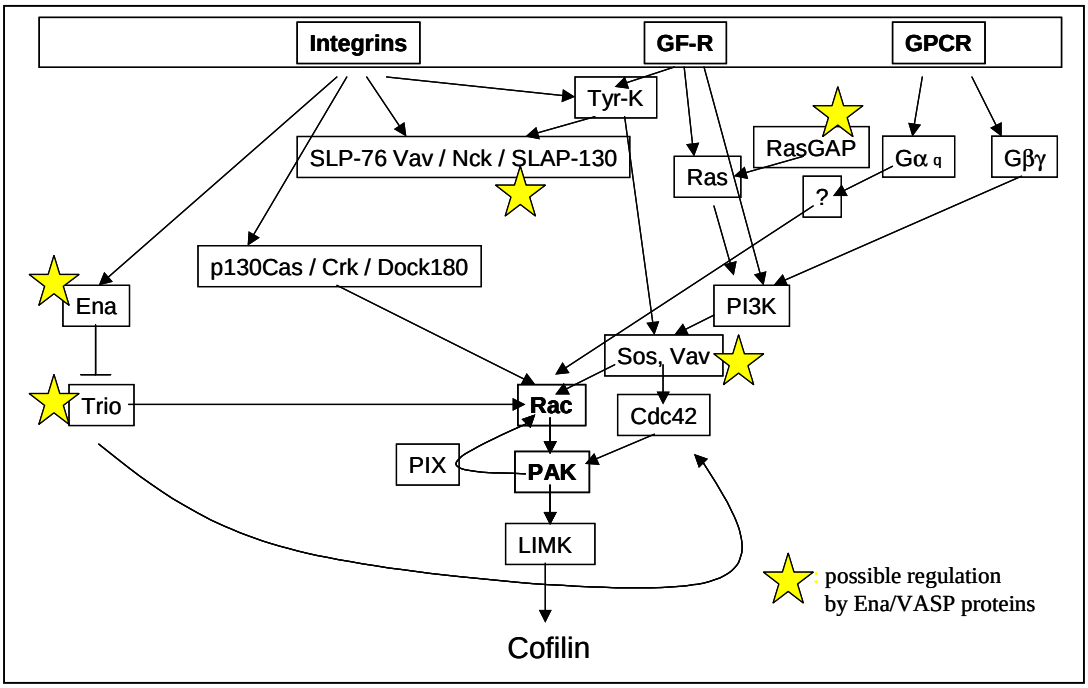

Figure 43: Summary of Rac regulation and possible steps where Ena/VASP proteins could interact. Summary includes pathways and information from several cell types.

However, we cannot exclude that VASP may actually intersect with signaling pathways at an upstream level: VASP specifically interacts *in vitro* with a proline-rich peptide derived from the N-terminal segment of p120RasGAP3, a protein that is also involved in stress fiber turnover and reorientation during cell migration (see Ref. [131] for a review).

6.5. Adhesion: observations in vitro and in vivo point to the importance of VASP in this cellular process

In this work, I showed that VASP deficient cells attach more slowly to fibronectin but , once attached, stronger. This indicates delayed primary adhesion but stronger stable adhesion. The membrane tension assays using laser tweezers discussed earlier also confirmed the strong adhesion of MCFB cells. In the in vitro assays used in this work only the interaction to fibronectin is investigated without any other factor influencing the process. However, the situation in vivo is quite different. Usually there is more than one cell type involved and secretion of neighboring cells may regulate adhesion, by modification of the ECM composition or by acting directly on the attaching cell. This is particularly true for adhesion of platelets in vivo.

Platelets normally circulate without binding to the vessel wall. Adhesion is prevented by endothelial cells, which secrete prostacyclin and nitric oxide, inhibitors of platelet activation and adhesion. Upon vascular injury, the subendothelium is exposed to the circulating platelets in the flowing blood. As the adhesion of platelets occurs under flow conditions, adhesion must be fast and resist the shear forces. This has led to the development of a particular set of ligands and receptors. Platelets come into contact with ECM constituents such as collagen and other molecules secreted/produced locally in response to the injury such as von Willebrand factor (vWf). After a superficial disruption of the endothelium, the main basement membrane components that are exposed to the blood are vWf, proteoglycans, collagen type IV laminin and fibulin. The first platelet contact takes place via its glycoprotein GPIb, able to interact with vWf. Collagen IV can elicit platelet response but is less effective than other types of collagen such as type I, III and VI that are exposed by deeper injury. Mainly the integrin $\alpha_2\beta_3$ and the glycoprotein GPVI interact with collagen. Fibrinogen is normally not present in the subendothelial ECM but can be immobilized at the injury region and is involved in thrombus formation by mediating platelet-platelet interactions via the αIIbβ3. The binding of platelet membrane receptor to the ECM and associated molecules elicits the activation of platelets and signaling cascades within them (outside-in signaling). The activation of signaling pathways in the platelets will modulate their adhesion and interaction with subendothelium and other cells. Upon activation, platelets

secrete P-selectin that can be recognized by leukocyte membrane receptors. During atherosclerosis, abnormal endothelial cells increasingly expose adhesive molecules such as P-selectin and vWf that contribute to the adhesion of platelets to the atherosclerotic plaque. (for a review see [132]). It is clear that adhesion under in vivo situations involves a higher number of parameters/molecules to be coordinated and controlled than adhesion studied by an in vitro model.

Therefore, it was of particular interest to study platelet adhesion using in-vivo conditions which was done in a collaborative project with Dr. Massberg (Herzzentrum, Munich). Platelet-endothelial cell interactions were significantly enhanced with $VASP^{-/-}$ platelets under normal (basal) conditions (probably due to enhanced activation of the integrin $\alpha IIb\beta 3$ in $VASP^{-/-}$ platelets), during ischemia/reperfusion periods and after endothelial denudation. At first sight, these in-vivo results apparently disagree with the in vitro assays performed with MCFB reported here. Clearly, the difference between the in-vivo and in vitro model (cell types and different adhesive proteins involved; flow conditions; parameters to be controlled) may be responsible for differences in the kinetics of adhesion. However, it should be stressed here that the final result, a stronger and more stable adhesion of VASP deficient cells, was observed in both situations.

6.5.1 Influence of cGMP analogs in cell adhesion

Treatment of platelets with cGMP analogs (such as 8pCPT-cGMP) inhibits their activation, but the shape change prior aggregation still takes place. In vivo platelet adhesion experiments were also performed in the presence of NO donors that will activate the guanylate cyclase (GC), increase cGMP levels, activate the cGMP-dependent protein kinase (cGK) and cause VASP phosphorylation in platelets. Treatment with NO donors inhibited adhesion to the endothelium of wild type but not cGK-I-deficient platelets in vivo [133]. Similar data were obtained in vitro with rat mesangial cells, endothelial cells and leukocytes [134,135]. The inhibition of adhesion by NO/cGMP is apparently VASP dependent: adhesion of VASP deficient platelets was not effectively inhibited by NO-donor pretreatment (Massberg et al., submitted for publication). These in vivo results agree with in-vitro data obtained earlier [52,53] which demonstrated that platelet inhibition by cyclic nucleotides is impaired in the absence of VASP

In apparent contrast to the inhibitory effect of cGMP in platelet adhesion, I showed here that treatment of wild type MCFB with the cGMP analog 8pCPT-cGMP induces an enhanced VASP dependent adhesion in vitro. Considering that 8pCPT-cGMP selectively activates cGK it would be reasonable to suggest a phospho-VASP effect in cell adhesion. It cannot be excluded that the effect of cGMP observed in MCFB is cell-type specific and that 8p-CPT-cGMP or cGMP induce or inhibit adhesion depending on the cell type. The adhesion

assay performed with MCFB is certainly complex. Although primary MCFB cells express both isoforms of cGK I (Iα and Iβ) it has been observed that cells in culture express reduced or even undetectable cGK levels after 15 to 20 passages, depending on the preparation. This reduction of cGK expression in cell culture has also been observed in Jurkat cells [136], but not in rat mesangial cells (Dr. Stepan Gambaryan, personal comunication). The results presented here were obtained with cells in passage 25 (where cGK was not detectable) indicating that the VASP dependent effect of 8pCPT-cGMP in cell adhesion may be not due to cGK activation and consequent VASP phosphorylation. The 8pCPT-cGMP compound is also poor activator of cAK. Therefore, (particularly at high concentrations or long-term incubation times) a cross activation of PKA leading to phosphorylation of VASP is difficult to rule out. A very weak phosphorylation of the Ser239 has been seen in cells pretreated with the cGMP analog at passage 25. This phosphorylation is probably due to a residual cGK level (that is below the detection range of the anti-cGK antibody) or, alternatively, cross-activation of the PKA. However, this low amount of phospho-VASP obtained in 8p-CPT-cGMP treated MCFB is most likely not enough to induce a 2-fold increase in adhesion. Very recently, it has been shown that the cGMP analog 8pCPT-cGMP (but not cGMP) activates a GEF (Guanosine Exchange Factor) for the small GTPase Rap: Epac (Exchange protein directly activated by cAMP) [137]. Epac is activated in vivo and in vitro by cAMP, which releases an autoinhibitory domain [138]. Rap1, on the other hand, has been involved in the control of integrin-mediated cell adhesion [139,140]. Over-expression of activated Rap1 stimulates integrin-dependent adhesion in human T-cell and mouse pre-B cell leukemia lines, and a dominant negative form of Rap1 (RapN17) inhibits T-cell receptor (TCR) induced adhesion. The role of Rap 1 in platelets is still controversial. Activation of the integrin αIIbβ3, the inhibition of which is correlated with VASP phosphorylation, results in Rap 1 activation; however, integrin-mediated adhesion is also required for subsequent Rap 1 inactivation (See Bos et al (2001) [141] for a review).

In conclusion, the data presented in this dissertation strongly suggest that VASP appears not only to regulate various aspects of actin filament formation and architecture [9], but also modifies Rac/Pak pathway signaling and, as consequence, cell motility and polarization. On the basis of the results shown, VASP appears to be involved in processes related to the turnover / remodeling of the actin cytoskeleton by regulating actin polymerization both directly and indirectly, ie. via signaling pathways such as Rac/Rho-GTPases. Finally, the absence of VASP strengthens cell adhesion, both in vitro and in vivo. In particular the platelet in vivo results demonstrate the participation of VASP in processes such as adhesion, which may become an important novel target for future anti-platelet/ anti-thrombotic therapies.

6.6 Future perspectives

The results presented here open new ways for the study of VASP as a regulator of the actin cytoskeleton. The mechanism of the regulation of the Rac/Pak pathway by VASP remains to be elucidated. As Rac is activated by different stimuli (Integrin activation, growth factor receptors, G protein coupled receptors) it is interesting to evaluate the involvement of VASP in the different mechanisms of Rac activation using different agonists. Further experiments are planned to investigate if the inhibitory, VASP-dependent effects of 8p-CPT-cGMP on TxA_2 (via G_q) stimulated Rac activation in platelets is valid also for other cell types. VASP would appear closer to the Rac activation cascade if the inhibitory effect of VASP is independent of the stimulus used to activate Rac.

As also discussed earlier, the cellular phenotypes analyzed here suggest an enhanced Rho activity in VASP deficient cells. Efforts and experimental approaches to demonstrate this are on the way. Such experiments, combined with the use of novel and validated inhibitors of Rho and Rho pathways (e.g. Y-27632, C3), may help to understand the role of VASP in the regulation of small GTPases.

Another topic to be clarified is the question if the enhanced adhesion observed in wild type MCFB pretreated with the cGMP analog 8p-CPT-cGMP is mediated by Epac, involving VASP in the regulation of Rap. More specific activators of cGK and Epac have been recently developed that could be useful to answer this question.

Several genes have been found to be differentially expressed in the absence of VASP, as suggested by the results obtained using the microarray approach. Many of these data need to be confirmed and advanced by other techniques and approaches. Of particular interest is the functional significance of enhanced Robo1 expression in VASP deficient cells.

Finally, the role of VASP phosphorylation in the cellular processes studied here remains to be investigated in detail. Phosphorylation sites are one aspect of the main difference between members of the Ena/VASP family members. They may be, at least partially, responsible for the exclusive functions of VASP.

The ultimate goal is to understand the structural and functional in vivo role of VASP and its binding partners in regulating actin filament formation, signal transduction pathways and cellular processes such as adhesion, motility and gene expression profiles.

7. References

1. Gawaz M: *Das Blutplättchen: Physiologie, Pathophysiologie, Membranrezeptoren, antithrombozytäre Wirkstoffe und Therapie bei koronarer Herzerkrankung*. Stuttgart; New York: Georg Thieme Verlag; 1999.
2. Halbrugge M, Walter U: **Purification of a vasodilator-regulated phosphoprotein from human platelets**. *Eur J Biochem* 1989, **185**:41-50.
3. Halbrügge M, Friedrich C, Eigenthaler M, Schanzenbacher P, Walter U: **Stoichiometric and reversible phosphorylation of a 46-kDa protein in human platelets in response to cGMP- and cAMP-elevating vasodilators**. *J Biol Chem* 1990, **265**:3088-3093.
4. Butt E, Abel K, Krieger M, Palm D, Hoppe V, Hoppe J, Walter U: **cAMP- and cGMP-dependent protein kinase phosphorylation sites of the focal adhesion vasodilator-stimulated phosphoprotein (VASP) in vitro and in intact human platelets**. *J Biol Chem* 1994, **269**:14509-14517.
5. Smolenski A, Bachmann C, Reinhard K, Honig-Liedl P, Jarchau T, Hoschuetzky H, Walter U: **Analysis and regulation of vasodilator-stimulated phosphoprotein serine 239 phosphorylation in vitro and in intact cells using a phosphospecific monoclonal antibody**. *J Biol Chem* 1998, **273**:20029-20035.
6. Reinhard M, Jarchau T, Reinhard K, Walter U: **VASP**. In *Guidebook to the Cytoskeletal and Motor Proteins*. Edited by Kreis T, Vale R: Oxford University Press; 1999:168-171.,
7. Gertler FB, Niebuhr K, Reinhard M, Wehland J, Soriano P: **Mena, a relative of VASP and Drosophila Enabled, is implicated in the control of microfilament dynamics**. *Cell* 1996, **87**:227-239.
8. Haffner C, Jarchau T, Reinhard M, Hoppe J, Lohmann SM, Walter U: **Molecular cloning, structural analysis and functional expression of the proline-rich focal adhesion and microfilament-associated protein VASP**. *Embo J* 1995, **14**:19-27.
9. Reinhard M, Jarchau T, Walter U: **Actin-based motility: stop and go with Ena/VASP proteins**. *Trends Biochem Sci* 2001, **26**:243-249.
10. Niebuhr K, Ebel F, Frank R, Reinhard M, Domann E, Carl UD, Walter U, Gertler FB, Wehland J, Chakraborty T: **A novel proline-rich motif present in ActA of Listeria monocytogenes and cytoskeletal proteins is the ligand for the EVH1 domain, a protein module present in the Ena/VASP family**. *Embo J* 1997, **16**:5433-5444.
11. Petit MM, Fradelizi J, Golsteyn RM, Ayoubi TA, Menichi B, Louvard D, Van de Ven WJ, Friederich E: **LPP, an actin cytoskeleton protein related to zyxin, harbors a nuclear export signal and transcriptional activation capacity**. *Mol Biol Cell* 2000, **11**:117-129.
12. Bashaw GJ, Kidd T, Murray D, Pawson T, Goodman CS: **Repulsive axon guidance: Abelson and Enabled play opposing roles downstream of the roundabout receptor**. *Cell* 2000, **101**:703-715.
13. Klostermann A, Lutz B, Gertler F, Behl C: **The orthologous human and murine semaphorin 6A-1 proteins (SEMA6A- 1/Sema6A-1) bind to the enabled/vasodilator-stimulated phosphoprotein- like protein (EVL) via a novel carboxyl-terminal zyxin-like domain**. *J Biol Chem* 2000, **275**:39647-39653.
14. Krause M, Sechi AS, Konradt M, Monner D, Gertler FB, Wehland J: **Fyn-binding protein (Fyb)/SLP-76-associated protein (SLAP), Ena/vasodilator-stimulated phosphoprotein (VASP) proteins and the Arp2/3 complex link T cell receptor (TCR) signaling to the actin cytoskeleton**. *J Cell Biol* 2000, **149**:181-194.

15. Chakraborty T, Ebel F, Domann E, Niebuhr K, Gerstel B, Pistor S, Temm-Grove CJ, Jockusch BM, Reinhard M, Walter U, et al.: **A focal adhesion factor directly linking intracellularly motile Listeria monocytogenes and Listeria ivanovii to the actin-based cytoskeleton of mammalian cells**. *Embo J* 1995, **14**:1314-1321.
16. Ball LJ, Kuhne R, Hoffmann B, Hafner A, Schmieder P, Volkmer-Engert R, Hof M, Wahl M, Schneider-Mergener J, Walter U, et al.: **Dual epitope recognition by the VASP EVH1 domain modulates polyproline ligand specificity and binding affinity**. *Embo J* 2000, **19**:4903-4914.
17. Fedorov AA, Fedorov E, Gertler F, Almo SC: **Structure of EVH1, a novel proline-rich ligand-binding module involved in cytoskeletal dynamics and neural function**. *Nat Struct Biol* 1999, **6**:661-665.
18. Prehoda KE, Lee DJ, Lim WA: **Structure of the enabled/VASP homology 1 domain-peptide complex: a key component in the spatial control of actin assembly**. *Cell* 1999, **97**:471-480.
19. Ahern-Djamali SM, Comer AR, Bachmann C, Kastenmeier AS, Reddy SK, Beckerle MC, Walter U, Hoffmann FM: **Mutations in Drosophila enabled and rescue by human vasodilator-stimulated phosphoprotein (VASP) indicate important functional roles for Ena/VASP homology domain 1 (EVH1) and EVH2 domains**. *Mol Biol Cell* 1998, **9**:2157-2171.
20. Lambrechts AI, Kwiatkowski A, Lanier LM, Bear JE, Vandekerckhove J, Ampe C, Gertler FB: **PKA phosphorylation of EVL, a Mena/VASP relative, regulates its interaction with actin and SH3-domains**. *J Biol Chem* 2000, **275**:36143-36151.
21. Ahern-Djamali SM, Bachmann C, Hua P, Reddy SK, Kastenmeier AS, Walter U, Hoffmann FM: **Identification of profilin and src homology 3 domains as binding partners for Drosophila enabled**. *Proc Natl Acad Sci U S A* 1999, **96**:4977-4982.
22. Reinhard M, Giehl K, Abel K, Haffner C, Jarchau T, Hoppe V, Jockusch BM, Walter U: **The proline-rich focal adhesion and microfilament protein VASP is a ligand for profilins**. *Embo J* 1995, **14**:1583-1589.
23. Ermekova KS, Zambrano N, Linn H, Minopoli G, Gertler F, Russo T, Sudol M: **The WW domain of neural protein FE65 interacts with proline-rich motifs in Mena, the mammalian homolog of Drosophila enabled**. *J Biol Chem* 1997, **272**:32869-32877.
24. Bachmann C, Fischer L, Walter U, Reinhard M: **The EVH2 domain of the vasodilator-stimulated phosphoprotein mediates tetramerization, F-actin binding, and actin bundle formation**. *J Biol Chem* 1999, **274**:23549-23557.
25. Drees B, Friederich E, Fradelizi J, Louvard D, Beckerle MC, Golsteyn RM: **Characterization of the interaction between zyxin and members of the Ena/Vasodilator-stimulated phosphoprotein family of proteins**. *J Biol Chem* 2000, **275**:22503-22511.
26. Harbeck B, Huttelmaier S, Schluter K, Jockusch BM, Illenberger S: **Phosphorylation of the vasodilator-stimulated phosphoprotein (VASP) regulates its interaction with actin**. *J Biol Chem* 2000, **275**:30817-30825.
27. Hüttelmaier S, Mayboroda O, Harbeck B, Jarchau T, Jockusch BM, Rüdiger M: **The interaction of the cell-contact proteins VASP and vinculin is regulated by phosphatidylinositol-4,5-bisphosphate**. *Curr Biol* 1998, **8**:479-488.
28. Loisel TP, Boujemaa R, Pantaloni D, Carlier MF: **Reconstitution of actin-based motility of Listeria and Shigella using pure proteins**. *Nature* 1999, **401**:613-616.
29. Laurent V, Loisel TP, Harbeck B, Wehman A, Grobe L, Jockusch BM, Wehland J, Gertler FB, Carlier MF: **Role of proteins of the Ena/VASP family in actin-based motility of Listeria monocytogenes**. *J Cell Biol* 1999, **144**:1245-1258.

30. Obergfell A, Judd BA, del Pozo MA, Schwartz MA, Koretzky GA, Shattil SJ: **The molecular adapter SLP-76 relays signals from platelet integrin alphaIIbbeta3 to the actin cytoskeleton**. *J Biol Chem* 2001, **276**:5916-5923.
31. Lanier LM, Gates MA, Witke W, Menzies AS, Wehman AM, Macklis JD, Kwiatkowski D, Soriano P, Gertler FB: **Mena is required for neurulation and commissure formation**. *Neuron* 1999, **22**:313-325.
32. Jonckheere V, Lambrechts A, Vandekerckhove J, Ampe C: **Dimerization of profilin II upon binding the (GP5)3 peptide from VASP overcomes the inhibition of actin nucleation by profilin II and thymosin beta4**. *FEBS Lett* 1999, **447**:257-263.
33. Lambrechts A, Verschelde JL, Jonckheere V, Goethals M, Vandekerckhove J, Ampe C: **The mammalian profilin isoforms display complementary affinities for PIP2 and proline-rich sequences**. *Embo J* 1997, **16**:484-494.
34. Lanier LM, Gertler FB: **From Abl to actin: Abl tyrosine kinase and associated proteins in growth cone motility**. *Curr Opin Neurobiol* 2000, **10**:80-87.
35. Comer AR, Ahern-Djamali SM, Juang JL, Jackson PD, Hoffmann FM: **Phosphorylation of Enabled by the Drosophila Abelson tyrosine kinase regulates the in vivo function and protein-protein interactions of Enabled**. *Mol Cell Biol* 1998, **18**:152-160.
36. Hüttelmaier S, Harbeck B, Steffens O, Messerschmidt T, Illenberger S, Jockusch BM: **Characterization of the actin binding properties of the vasodilator-stimulated phosphoprotein VASP**. *FEBS Lett* 1999, **451**:68-74.
37. Carl UD, Pollmann M, Orr E, Gertlere FB, Chakraborty T, Wehland J: **Aromatic and basic residues within the EVH1 domain of VASP specify its interaction with proline-rich ligands**. *Curr Biol* 1999, **9**:715-718.
38. Reinhard M, Jouvenal K, Tripier D, Walter U: **Identification, purification, and characterization of a zyxin-related protein that binds the focal adhesion and microfilament protein VASP (vasodilator-stimulated phosphoprotein)**. *Proc Natl Acad Sci U S A* 1995, **92**:7956-7960.
39. Vasioukhin V, Bauer C, Yin M, Fuchs E: **Directed actin polymerization is the driving force for epithelial cell-cell adhesion**. *Cell* 2000, **100**:209-219.
40. Bear JE, Loureiro JJ, Libova I, Fassler R, Wehland J, Gertler FB: **Negative regulation of fibroblast motility by Ena/VASP proteins**. *Cell* 2000, **101**:717-728.
41. Offermanns S: **The role of heterotrimeric G proteins in platelet activation**. *Biol Chem* 2000, **381**:389-396.
42. Gohla A, Offermanns S, Wilkie TM, Schultz G: **Differential involvement of Galpha12 and Galpha13 in receptor-mediated stress fiber formation**. *J Biol Chem* 1999, **274**:17901-17907.
43. Klages B, Brandt U, Simon MI, Schultz G, Offermanns S: **Activation of G12/G13 results in shape change and Rho/Rho-kinase- mediated myosin light chain phosphorylation in mouse platelets**. *J Cell Biol* 1999, **144**:745-754.
44. Schwarz UR, Walter U, Eigenthaler M: **Taming platelets with cyclic nucleotides**. *Biochem Pharmacol* 2001, **62**:1153-1161.
45. Eigenthaler M, Ullrich H, Geiger J, Horstrup K, Honig-Liedl P, Wiebecke D, Walter U: **Defective nitrovasodilator-stimulated protein phosphorylation and calcium regulation in cGMP-dependent protein kinase-deficient human platelets of chronic myelocytic leukemia**. *J Biol Chem* 1993, **268**:13526-13531.
46. Geiger J, Nolte C, Butt E, Sage SO, Walter U: **Role of cGMP and cGMP-dependent protein kinase in nitrovasodilator inhibition of agonist-evoked calcium elevation in human platelets**. *Proc Natl Acad Sci U S A* 1992, **89**:1031-1035.

47. Hettasch JM, Sellers JR: **Caldesmon phosphorylation in intact human platelets by cAMP-dependent protein kinase and protein kinase C**. *J Biol Chem* 1991, **266**:11876-11881.
48. Fox JE, Berndt MC: **Cyclic AMP-dependent phosphorylation of glycoprotein Ib inhibits collagen-induced polymerization of actin in platelets**. *J Biol Chem* 1989, **264**:9520-9526.
49. Butt E, Walter U: **Cyclic nucleotides: measurement and function**. In *Platelets: A practical approach*. Edited by Watson S: Oxford, University Press; 1996:259-278.,
50. Fischer TH, Gatling MN, Lacal JC, White GC, 2nd: **rap1B, a cAMP-dependent protein kinase substrate, associates with the platelet cytoskeleton**. *J Biol Chem* 1990, **265**:19405-19408.
51. Soderling SH, Beavo JA: **Regulation of cAMP and cGMP signaling: new phosphodiesterases and new functions**. *Curr Opin Cell Biol* 2000, **12**:174-179.
52. Hauser W, Knobeloch KP, Eigenthaler M, Gambaryan S, Krenn V, Geiger J, Glazova M, Rohde E, Horak I, Walter U, et al.: **Megakaryocyte hyperplasia and enhanced agonist-induced platelet activation in vasodilator-stimulated phosphoprotein knockout mice**. *Proc Natl Acad Sci U S A* 1999, **96**:8120-8125.
53. Aszodi A, Pfeifer A, Ahmad M, Glauner M, Zhou XH, Ny L, Andersson KE, Kehrel B, Offermanns S, Fassler R: **The vasodilator-stimulated phosphoprotein (VASP) is involved in cGMP- and cAMP-mediated inhibition of agonist-induced platelet aggregation, but is dispensable for smooth muscle function**. *Embo J* 1999, **18**:37-48.
54. Goldberg MB: **Actin-based motility of intracellular microbial pathogens**. *Microbiol Mol Biol Rev* 2001, **65**:595-626, table of contents.
55. Mullins RD, Heuser JA, Pollard TD: **The interaction of Arp2/3 complex with actin: nucleation, high affinity pointed end capping, and formation of branching networks of filaments**. *Proc Natl Acad Sci U S A* 1998, **95**:6181-6186.
56. Welch MD, Rosenblatt J, Skoble J, Portnoy DA, Mitchison TJ: **Interaction of human Arp2/3 complex and the Listeria monocytogenes ActA protein in actin filament nucleation**. *Science* 1998, **281**:105-108.
57. van der Flier A, Sonnenberg A: **Function and interactions of integrins**. *Cell Tissue Res* 2001, **305**:285-298.
58. Hall A: **Rho GTPase family**. In *Extracellular Matrix, Anchor, and Adhesion Proteins*, edn Second. Edited by Kreis T, Vale R: Oxford University Press; 1999:71-78.,
59. Chardin P, Madaule P, Tavitian A: **Coding sequence of human rho cDNAs clone 6 and clone 9**. *Nucleic Acids Res* 1988, **16**:2717.
60. Yeramian P, Chardin P, Madaule P, Tavitian A: **Nucleotide sequence of human rho cDNA clone 12**. *Nucleic Acids Res* 1987, **15**:1869.
61. Ridley AJ, Hall A: **The small GTP-binding protein rho regulates the assembly of focal adhesions and actin stress fibers in response to growth factors**. *Cell* 1992, **70**:389-399.
62. Nobes CD, Hawkins P, Stephens L, Hall A: **Activation of the small GTP-binding proteins rho and rac by growth factor receptors**. *J Cell Sci* 1995, **108**:225-233.
63. Leung T, Chen XQ, Manser E, Lim L: **The p160 RhoA-binding kinase ROK alpha is a member of a kinase family and is involved in the reorganization of the cytoskeleton**. *Mol Cell Biol* 1996, **16**:5313-5327.
64. Nobes CD, Hall A: **Rho, rac, and cdc42 GTPases regulate the assembly of multimolecular focal complexes associated with actin stress fibers, lamellipodia, and filopodia**. *Cell* 1995, **81**:53-62.

65. Soulet C, Gendreau S, Missy K, Benard V, Plantavid M, Payrastre B: **Characterisation of Rac activation in thrombin- and collagen-stimulated human blood platelets**. *FEBS Lett* 2001, **507**:253-258.
66. Gratacap MP, Payrastre B, Nieswandt B, Offermanns S: **Differential regulation of Rho and Rac through heterotrimeric G- proteins and cyclic nucleotides**. *J Biol Chem* 2001, **276**:47906-47913.
67. Missy K, Van Poucke V, Raynal P, Viala C, Mauco G, Plantavid M, Chap H, Payrastre B: **Lipid products of phosphoinositide 3-kinase interact with Rac1 GTPase and stimulate GDP dissociation**. *J Biol Chem* 1998, **273**:30279-30286.
68. del Pozo MA, Price LS, Alderson NB, Ren XD, Schwartz MA: **Adhesion to the extracellular matrix regulates the coupling of the small GTPase Rac to its effector PAK**. *Embo J* 2000, **19**:2008-2014.
69. Howe AK, Juliano RL: **Regulation of anchorage-dependent signal transduction by protein kinase A and p21-activated kinase**. *Nat Cell Biol* 2000, **2**:593-600.
70. Lim L, Manser E, Leung T, Hall C: **Regulation of phosphorylation pathways by p21 GTPases. The p21 Ras- related Rho subfamily and its role in phosphorylation signalling pathways**. *Eur J Biochem* 1996, **242**:171-185.
71. Sanders LC, Matsumura F, Bokoch GM, de Lanerolle P: **Inhibition of myosin light chain kinase by p21-activated kinase**. *Science* 1999, **283**:2083-2085.
72. Zeng Q, Lagunoff D, Masaracchia R, Goeckeler Z, Cote G, Wysolmerski R: **Endothelial cell retraction is induced by PAK2 monophosphorylation of myosin II**. *J Cell Sci* 2000, **113**:471-482.
73. Edwards DC, Sanders LC, Bokoch GM, Gill GN: **Activation of LIM-kinase by Pak1 couples Rac/Cdc42 GTPase signalling to actin cytoskeletal dynamics**. *Nat Cell Biol* 1999, **1**:253-259.
74. Daniels RH, Bokoch GM: **p21-activated protein kinase: a crucial component of morphological signaling?** *Trends Biochem Sci* 1999, **24**:350-355.
75. Lawler S: **Regulation of actin dynamics: The LIM kinase connection**. *Curr Biol* 1999, **9**:R800-802.
76. Chernoff J: **Close encounters of the LIM-kinase**. *Nat Cell Biol* 1999, **1**:E115-117.
77. Cameron LA, Giardini PA, Soo FS, Theriot JA: **Secrets of actin-based motility revealed by a bacterial pathogen**. *Nature Rev. Mol. Cell. Biol.* 2000, **1**:110-119.
78. Borisy GG, Svitkina TM: **Actin machinery: pushing the envelope**. *Curr Opin Cell Biol* 2000, **12**:104-112.
79. Fradelizi J, Noireaux V, Plastino J, Menichi B, Louvard D, Sykes C, Golsteyn RM, Friederich E: **ActA and human zyxin harbour Arp2/3-independent actin-polymerization activity**. *Nat Cell Biol* 2001, **3**:699-707.
80. Liebl EC, Forsthoefel DJ, Franco LS, Sample SH, Hess JE, Cowger JA, Chandler MP, Shupert AM, Seeger MA: **Dosage-sensitive, reciprocal genetic interactions between the Abl tyrosine kinase and the putative GEF trio reveal trio's role in axon pathfinding**. *Neuron* 2000, **26**:107-118.
81. Krugmann S, Jordens I, Gevaert K, Driessens M, Vandekerckhove J, Hall A: **Cdc42 induces filopodia by promoting the formation of an IRSp53:Mena complex**. *Curr Biol* 2001, **11**:1645-1655.
82. Higgs HN, Pollard TD: **Regulation of actin filament network formation through Arp 2/3 complex: activation by a diverse array of proteins**. *Annu Rev Biochem* 2001, **70**:649-676.
83. Wear MA, Schafer DA, Cooper JA: **Actin dynamics: assembly and disassembly of actin networks**. *Curr Biol* 2000, **10**:R891-895.
84. Halbrugge M, Walter U: **Analysis, purification and properties of a 50,000-dalton membrane- associated phosphoprotein from human platelets**. *J Chromatogr* 1990, **521**:335-343.

85. Howe AK: **Cell adhesion regulates the interaction between Nck and p21-activated kinase**. *J Biol Chem* 2001, **276**:14541-14544.
86. Simm A, Nestler M, Hoppe V: **PDGF-AA, a potent mitogen for cardiac fibroblasts from adult rats**. *J Mol Cell Cardiol* 1997, **29**:357-368.
87. Laemmli UK: **Cleavage of structural proteins during the assembly of the head of bacteriophage T4**. *Nature* 1970, **227**:680-685.
88. Benard V, Bohl BP, Bokoch GM: **Characterization of rac and cdc42 activation in chemoattractant- stimulated human neutrophils using a novel assay for active GTPases**. *J Biol Chem* 1999, **274**:13198-13204.
89. Dharmawardhane S, Sanders LC, Martin SS, Daniels RH, Bokoch GM: **Localization of p21-activated kinase 1 (PAK1) to pinocytic vesicles and cortical actin structures in stimulated cells**. *J Cell Biol* 1997, **138**:1265-1278.
90. Catalfamo J, Dodds WJ: **Isolation of Platelets from Laboratory Animals**. *Methods Enzymol* 1989, **169**:27- 34.
91. Massberg S, Enders G, Leiderer R, Eisenmenger S, Vestweber D, Krombach F, Messmer K: **Platelet-endothelial cell interactions during ischemia/reperfusion: the role of P-selectin**. *Blood* 1998, **92**:507-515.
92. Campisi J: **Replicative senescence: an old lives' tale?** *Cell* 1996, **84**:497-500.
93. Campisi J: **The biology of replicative senescence**. *Eur J Cancer* 1997, **33**:703-709.
94. Price CJ, Brindle NP: **Vasodilator-stimulated phosphoprotein is involved in stress-fiber and membrane ruffle formation in endothelial cells**. *Arterioscler Thromb Vasc Biol* 2000, **20**:2051-2056.
95. Machesky LM, Hall A: **Role of actin polymerization and adhesion to extracellular matrix in Rac- and Rho-induced cytoskeletal reorganization**. *J Cell Biol* 1997, **138**:913-926.
96. Fukata M, Nakagawa M, Kuroda S, Kaibuchi K: **Cell adhesion and Rho small GTPases**. *J Cell Sci* 1999, **112**:4491-4500.
97. Galler AB, Garcia Arguinzonis MI, Baumgartner W, Smolenski A, Walter U, Drenckhahn D, Simm A, Reinhard M: **VASP-dependent regulation of cell adhesion, detachment and actin cytoskeleton rigidity**. 2003.
98. Smolenski A, Poller W, Walter U, Lohmann SM: **Regulation of Human Endothelial Cell Focal Adhesion Sites and Migration by cGMP-dependent Protein Kinase I**. *J Biol Chem* 2000, **275**:25723-25732.
99. Lawrence DW, Pryzwansky KB: **The vasodilator-stimulated phosphoprotein is regulated by cyclic GMP- dependent protein kinase during neutrophil spreading**. *J Immunol* 2001, **166**:5550-5556.
100. Lauffenburger DA, Horwitz AF: **Cell migration: a physically integrated molecular process**. *Cell* 1996, **84**:359-369.
101. Price LS, Leng J, Schwartz MA, Bokoch GM: **Activation of Rac and Cdc42 by integrins mediates cell spreading**. *Mol Biol Cell* 1998, **9**:1863-1871.
102. Schmitz AA, Govek EE, Bottner B, Van Aelst L: **Rho GTPases: signaling, migration, and invasion**. *Exp Cell Res* 2000, **261**:1-12.
103. Obermeier A, Ahmed S, Manser E, Yen SC, Hall C, Lim L: **PAK promotes morphological changes by acting upstream of Rac**. *Embo J* 1998, **17**:4328-4339.
104. Chong C, Tan L, Lim L, Manser E: **The mechanism of PAK activation. Autophosphorylation events in both regulatory and kinase domains control activity**. *J Biol Chem* 2001, **276**:17347-17353.
105. Lloyd-Jones DM, Bloch KD: **The vascular biology of nitric oxide and its role in atherogenesis**. *Annu Rev Med* 1996, **47**:365-375.
106. Radomski MW, Palmer RM, Moncada S: **Comparative pharmacology of endothelium-derived relaxing factor, nitric oxide and prostacyclin in platelets**. *Br J Pharmacol* 1987, **92**:181-187.

107. Reinhard M, Halbrügge M, Scheer U, Wiegand C, Jockusch BM, Walter U: **The 46/50 kDa phosphoprotein VASP purified from human platelets is a novel protein associated with actin filaments and focal contacts**. *Embo J* 1992, **11**:2063-2070.
108. Burack WR, Shaw AS: **Signal transduction: hanging on a scaffold**. *Curr Opin Cell Biol* 2000, **12**:211-216.
109. Levchenko A, Bruck J, Sternberg PW: **Scaffold proteins may biphasically affect the levels of mitogen- activated protein kinase signaling and reduce its threshold properties**. *Proc Natl Acad Sci U S A* 2000, **97**:5818-5823.
110. Raucher D, Sheetz MP: **Cell spreading and lamellipodial extension rate is regulated by membrane tension**. *J Cell Biol* 2000, **148**:127-136.
111. Kidd T, Brose K, Mitchell KJ, Fetter RD, Tessier-Lavigne M, Goodman CS, Tear G: **Roundabout controls axon crossing of the CNS midline and defines a novel subfamily of evolutionarily conserved guidance receptors**. *Cell* 1998, **92**:205-215.
112. Ball LJ, Jarchau T, Oschkinat H, Walter U: **EVH1 domains: structure, function and interactions**. *FEBS Lett* 2002, **513**:45-52.
113. Yuan W, Zhou L, Chen JH, Wu JY, Rao Y, Ornitz DM: **The mouse SLIT family: secreted ligands for ROBO expressed in patterns that suggest a role in morphogenesis and axon guidance**. *Dev Biol* 1999, **212**:290-306.
114. Brose K, Bland KS, Wang KH, Arnott D, Henzel W, Goodman CS, Tessier-Lavigne M, Kidd T: **Slit proteins bind Robo receptors and have an evolutionarily conserved role in repulsive axon guidance**. *Cell* 1999, **96**:795-806.
115. Clark K, Hammond E, Rabbitts P: **Temporal and spatial expression of two isoforms of the Dutt1/Robo1 gene in mouse development**. *FEBS Lett* 2002, **523**:12-16.
116. Nobes CD, Hall A: **Rho GTPases control polarity, protrusion, and adhesion during cell movement**. *J Cell Biol* 1999, **144**:1235-1244.
117. Kiosses WB, Daniels RH, Otey C, Bokoch GM, Schwartz MA: **A role for p21-activated kinase in endothelial cell migration**. *J Cell Biol* 1999, **147**:831-844.
118. Machesky LM: **Putting on the brakes: a negative regulatory function for Ena/VASP proteins in cell migration**. *Cell* 2000, **101**:685-688.
119. Mullins RD: **How WASP-family proteins and the Arp2/3 complex convert intracellular signals into cytoskeletal structures**. *Curr Opin Cell Biol* 2000, **12**:91-96.
120. Machesky LM, Insall RH: **Signaling to actin dynamics**. *J Cell Biol* 1999, **146**:267-272.
121. Nobes CD, Hall A: **Rho, rac and cdc42 GTPases: regulators of actin structures, cell adhesion and motility**. *Biochem Soc Trans* 1995, **23**:456-459.
122. Mackay DJ, Esch F, Furthmayr H, Hall A: **Rho- and rac-dependent assembly of focal adhesion complexes and actin filaments in permeabilized fibroblasts: an essential role for ezrin/radixin/moesin proteins**. *J Cell Biol* 1997, **138**:927-938.
123. Azuma T, Witke W, Stossel TP, Hartwig JH, Kwiatkowski DJ: **Gelsolin is a downstream effector of rac for fibroblast motility**. *Embo J* 1998, **17**:1362-1370.
124. del Pozo MA, Kiosses WB, Alderson NB, Meller N, Hahn KM, Schwartz MA: **Integrins regulate GTP-Rac localized effector interactions through dissociation of Rho-GDI**. *Nat Cell Biol* 2002, **4**:232-239.
125. Manser E, Loo TH, Koh CG, Zhao ZS, Chen XQ, Tan L, Tan I, Leung T, Lim L: **PAK kinases are directly coupled to the PIX family of nucleotide exchange factors**. *Mol Cell* 1998, **1**:183-192.
126. Turner CE, Brown MC, Perrotta JA, Riedy MC, Nikolopoulos SN, McDonald AR, Bagrodia S, Thomas S, Leventhal PS: **Paxillin LD4 motif binds PAK and PIX**

through a novel 95-kD ankyrin repeat, ARF-GAP protein: A role in cytoskeletal remodeling. *J Cell Biol* 1999, **145**:851-863.
127. West KA, Zhang H, Brown MC, Nikolopoulos SN, Riedy MC, Horwitz AF, Turner CE: **The LD4 motif of paxillin regulates cell spreading and motility through an interaction with paxillin kinase linker (PKL)**. *J Cell Biol* 2001, **154**:161-176.
128. Hobert O, Schilling JW, Beckerle MC, Ullrich A, Jallal B: **SH3 domain-dependent interaction of the proto-oncogene product Vav with the focal contact protein zyxin**. *Oncogene* 1996, **12**:1577-1581.
129. Newsome TP, Schmidt S, Dietzl G, Keleman K, Asling B, Debant A, Dickson BJ: **Trio combines with dock to regulate Pak activity during photoreceptor axon pathfinding in Drosophila**. *Cell* 2000, **101**:283-294.
130. Seipel K, O'Brien SP, Iannotti E, Medley QG, Streuli M: **Tara, a novel F-actin binding protein, associates with the Trio guanine nucleotide exchange factor and regulates actin cytoskeletal organization**. *J Cell Sci* 2001, **114**:389-399.
131. Bar-Sagi D, Hall A: **Ras and Rho GTPases: a family reunion**. *Cell* 2000, **103**:227-238.
132. Ruggeri ZM: **Platelets in atherothrombosis**. *Nat Med* 2002, **8**:1227-1234.
133. Massberg S, Sausbier M, Klatt P, Bauer M, Pfeifer A, Siess W, Fassler R, Ruth P, Krombach F, Hofmann F: **Increased adhesion and aggregation of platelets lacking cyclic guanosine 3',5'-monophosphate kinase I**. *J Exp Med* 1999, **189**:1255-1264.
134. Conran N, Ferreira HH, Lorand-Metze I, Thomazzi SM, Antunes E, de Nucci G: **Nitric oxide regulates human eosinophil adhesion mechanisms in vitro by changing integrin expression and activity on the eosinophil cell surface**. *Br J Pharmacol* 2001, **134**:632-638.
135. Lelamali K, Wang W, Gengaro P, Edelstein C, Schrier RW: **Effects of nitric oxide and peroxynitrite on endotoxin-induced leukocyte adhesion to endothelium**. *J Cell Physiol* 2001, **188**:337-342.
136. Fischer TA, Palmetshofer A, Gambaryan S, Butt E, Jassoy C, Walter U, Sopper S, Lohmann SM: **Activation of cGMP-dependent protein kinase Ibeta inhibits interleukin 2 release and proliferation of T cell receptor-stimulated human peripheral T cells**. *J Biol Chem* 2001, **276**:5967-5974.
137. Enserink JM, Christensen AE, de Rooij J, van Triest M, Schwede F, Genieser HG, Doskeland SO, Blank JL, Bos JL: **A novel Epac-specific cAMP analogue demonstrates independent regulation of Rap1 and ERK**. *Nat Cell Biol* 2002, **4**:901-906.
138. de Rooij J, Rehmann H, van Triest M, Cool RH, Wittinghofer A, Bos JL: **Mechanism of regulation of the Epac family of cAMP-dependent RapGEFs**. *J Biol Chem* 2000, **275**:20829-20836.
139. Bertoni A, Tadokoro S, Eto K, Pampori N, Parise LV, White GC, Shattil SJ: **Relationships between Rap1b, affinity modulation of integrin alpha IIbbeta 3, and the actin cytoskeleton**. *J Biol Chem* 2002, **277**:25715-25721.
140. Tsukamoto N, Hattori M, Yang H, Bos JL, Minato N: **Rap1 GTPase-activating protein SPA-1 negatively regulates cell adhesion**. *J Biol Chem* 1999, **274**:18463-18469.
141. Bos JL, de Rooij J, Reedquist KA: **Rap1 signalling: adhering to new models**. *Nat Rev Mol Cell Biol* 2001, **2**:369-377.

8. Abbreviations

8pCPT-cGMP	**8-(para-Chlorophenylthio)guanosine-3',5'-cyclic monoposphate**
Abl	**Ableson tyrosine kinase**
AC	**Adenylate cyclase**
ADF	**Actin depolymerization factor**
APS	**Amonium persulfate**
Arp 2/3	**Actin related protein 2/3 complex**
ATP	**Adenosine triphosphate**
BSA	**Bovine serum albumine**
cAK	**cAMP- dependent protein kinase**
cAMP	**Cyclic adenosine-3',5'- monophosphate**
cBIMPS-cAMP	**5,6-Dichloro-1-β-D-ribofuranosylbenzimidazol-3',5'-cyclic monophosphorothioate,Sp-isomer-cAMP**
CCD	**Citrate citric acid dextrose buffer**
cGK	**cGMP- dependent protein kinase**
cGMP	**Cyclic guanosine-3',5'- monophosphate**
DIG	**Digoxigenin**
DMEM	**Dulbecco's Modified Eagle Medium**
dNTP	**Deoxyribonucleotides**
DTT	**Dithiotreitol**
ECL	**Enhanced chemoluminiscence**
ECM	**Extracellular matrix**
EDTA	**Ethylendiamine tetraacetic acid**
EGF	**Epithelial growth factor**
EGTA	**Ethylene glycol-bis(2-aminoethylether)-N,N,N',N'-tetraacetic acid**
Epac	**Exchange protein directly activated by cAMP**
EtBr	**Ethidium bromide**
EtOH	**Ethanol**
F-actin	**Filamentous actin**
Fyb/SLAP	**Fyn binding protein/SLP76 associated protein**
G-actin	**Globular actin (monomeric actin)**
GAP	**GTPase activating protein**
GC	**Guanylate cyclase**
GDP	**Guanine 5'-diphosphate**
GEF	**GTP exchange factor**
GST-PBD	**Glutathione-S-transferase – Pak binding domain**
GTP-γ-S	**Guanosine 5'-[γ thio] triphosphate**
HEPES	**N-2-Hydroxyethylpiperazin-N'-ethansulfonacid**
IP3	**Inositol-1,4,5-triphosphate**
IPTG	**Isopropyl-β-D-Thiogalacto(pyrano)side**
IRSp53	**Insulin receptor protein kinase substrate**
LB	**Luria Bertani medium**
LPA	**Lysophosphatidic acid**
LPP	**Lipoma preferred partner**
MCFB	**Mouse cardiac fibroblast**
MeOH	**Methanol**
MLC	**Myosin light chain**
MLCK	**Myosin light chain kinase**
Pak	**p21-activated kinase**
PBS	**Phosphate buffered saline**
PCR	**Polymerase chain reaction**
PDGF	**Platelet derived growth factor**
PGE_1	**Prostaglandin E_1**
PGi_2	**Prostaglandin I_2 (Prostacyclin)**
PIP2	**Phosphatidylinositol-4,5-biphosphate**

PIP5K	**Phosphatidylinositol-4-phosphate-5-kinase**
PIX	**Pak interacting exchange factor**
Robo	**Roundabout**
RT-PCR	**Reverse Transcriptase- polymerase chain reaction**
SCAR/WAVE	**Supressor of cAMP receptor/ WASP family verprolin homologous protein**
SDS	**Sodium dodecyl sulfate**
SH3	**Src homology domain 3**
SLP 76	**SH2 domain containing leukocyte protein of 76kDa**
TBS-T	**Tris buffered saline-with Tween-20**
TCA	**Trichloroacetic acid**
TEMED	**N,N,N',N'-tetramethylendiamine**
TxA_2	**Thromboxane A2**
VASP	**Vasodilator Stimulated phosphoprotein**
WASP	**Wiskott Aldrich Syndrom protein**

9. Curriculum Vitae

Name	Maísa Inés García Arguinzonis
Nationality	Argentinean
Date and Place of birth	November 16th, 1973 – Buenos Aires
Marital Status	Married

1991	**Diplôme du Baccalauréat de l'enseignement du Second Degré.** en Mathématiques et Sciences de la Nature Lycée Franco-Argentin "Jean Mermoz" (Académie de Poitiers) 1991
1997	Licenciatura en Ciencias Biológicas Universidad de Buenos Aires (Grade in Molecular Biology (six years Course))

Research Experience

September 1996 / December 1997	*"Stable Expression of the highly active human plasma membrane Ca^{2+} pump mutant hPMCA4b(ct120) in CHO cells"* (Grade Thesis) Director: Dr. Hugo P. Adamo. Institution: IQUIFIB - Dept. Biological Chemistry - Facultad de Farmacia y Bioquímica - UBA.
December 1997 / December 1998	*"Expression and study of human plasma membrane Ca^{2+} pump mutants in CHO cells."* Director: Dr. Hugo P. Adamo. Institution: IQUIFIB - Dept. Biological Chemistry - Facultad de Farmacia y Bioquímica - UBA.
Since January 1999	*„Analysis of signal transduction pathways and the cytoskeleton in VASP-deficient cell lines and mouse models"* Thesis Advisor: Prof. Dr.med. Ulrich Walter Institution: Institut für Klinische Biochemie und Pathobiochemie – Universität Würzburg – Germany

10. List of Publications

Hugo P. Adamo, Mirta E. Grimaldi, and **Maísa I. García Arguinzonis** (2000) Deletions in the N-Terminal Segment of the Plasma Membrane Ca 2+ Pump Impair the Expression of a Correctly Folded Functional Enzyme ***Biochemistry*****,** 39, 14893-14899

Publications resulting from this work:

Maísa I. García Arguinzonis, Annette B. Galler, Ulrich Walter, Andreas Simm and Matthias Reinhard (2002) Increasing Spreading, Rac/Pak activity and Compromised Cell Motility in VASP-deficient Cells. ***J. Biol. Chem***, 277: 4504-45610

Steffen Massberg, Sabine Grüner, Ildiko Konrad, **Maísa I. García Arguinzonis**, Martín Eigenthaler, Karin Hemler, Julia Kersting, Christian Schulz, Iris Müller, Ulrich Heinzmann, Ulrich Walter and Meinrad Gawaz (2003) Enhanced in vivo platelet adhesión in vasodilator-stimulated phosphoprotein (VASP)-deficient mice. **Blood in revisión**

Annette B. Galler, **Maísa I. García Arguinzonis**, Werner Baumgartner, Albert Smolenski, Ulrich Walter, Detlev Drenckhahn, Andreas Simm and Matthias Reinhard (2003) VASP-dependent regulation of cell ahesion and actin cytoskeleton rigidity. **Manuscript in preparation**